THE
PHYSICAL REVIEW
A Journal of Experimental and Theoretical Physics
VOL. 46, NO. 3 AUGUST 1, 1934 SECOND SERIES

The Absorption of Monochromatic X-Rays of Short Wave-Length

T. M. HAHN, *University of Chicago*
(Received June 7, 1934)

With a Société Genevoise double crystal spectrometer, the mass absorption coefficients of eight different elements extending from hydrogen (from paraffin and carbon) to lead were determined for a wave-length of 208.6 x-units. An attempt to make a similar series of measurements on the $K\beta_1$ line of tungsten failed because of the low intensity of the x-rays. With the same instrument but with the first crystal removed as a single crystal spectrometer, measurements were extended down to 138 x-units. The atomic absorption coefficients determined from these measurements were found to be given accurately by the equation $(\mu_a/Z)=C_kZ^{3.18}\lambda^q+(\sigma/\sigma_0)\sigma_0$, where σ/σ_0 is given by the Klein-Nishina formula rather than the Breit and Dirac or Compton formulas for scattering. In the case of hydrogen however the atomic absorption coefficient (calculated from the difference between measurements on paraffin and carbon) was within experimental error equal to the Thomson scattering for the range of wave-lengths used. The constant q appears to have the value 2.50 for this region, and C_k the value 5.81×10^{-7}, if λ is measured in centimeters. In general the absorption coefficients agree fairly well with those of other observers except for a slight discrepancy in the case of copper; a peculiarity is pointed out in the case of silver.

INTRODUCTION

IT is generally recognized that an accurate measurement of the x-ray absorption coefficients in the region of wave-lengths shorter than 0.250 Angstrom would be of considerable value, both in checking the validity of the empirical formula

$$\mu_a=C_kZ^p\lambda^q+K_1Z\sigma_0 \qquad (1)$$

for the total absorption and in giving additional information as to the proper values of the exponents p and q, but more especially since it is only for short wave-lengths that the last term representing the scattering is an appreciable part of the total absorption. The most direct test of the various formulas for the intensity of scattered x-rays as derived by A. H. Compton,[1] Breit[2] and Dirac,[3] and Klein and Nishina[4] is a comparison with the experimental values of the intensity I_ϕ scattered at any given angle ϕ. Unfortunately it is very difficult to obtain experimental values of I_ϕ which are sufficiently reliable for this test, particularly since the formula of Breit and Dirac and the Klein-Nishina formula give nearly the same result for the scattering at a given angle ϕ. On the other hand, when the above formulas are applied to give the total scattering, the formulas of Compton and Breit and Dirac give about the same result, but the result given by the Klein-Nishina formula differs quite appreciably.

Unfortunately accurate absorption measurements are also difficult to make in this region. Hewlett,[5] Richtmyer,[6] Allen[7] and others have made such measurements, but there is considerable divergence in their results. One of the major difficulties in making absorption measurements

[1] A. H. Compton, Phys. Rev. **21**, 483 (1923).
[2] G. Breit, Phys. Rev. **27**, 242 (1926).
[3] P. A. M. Dirac, Proc. Roy. Soc. **A111**, 405 (1927).
[4] Klein and Nishina, Zeits. f. Physik **52**, 853 (1928).
[5] C. W. Hewlett, Phys. Rev. **17**, 284 (1921).
[6] F. K. Richtmyer, Phys. Rev. **18**, 13 (1921).
[7] S. J. M. Allen, Phys. Rev. **27**, 266 (1926).

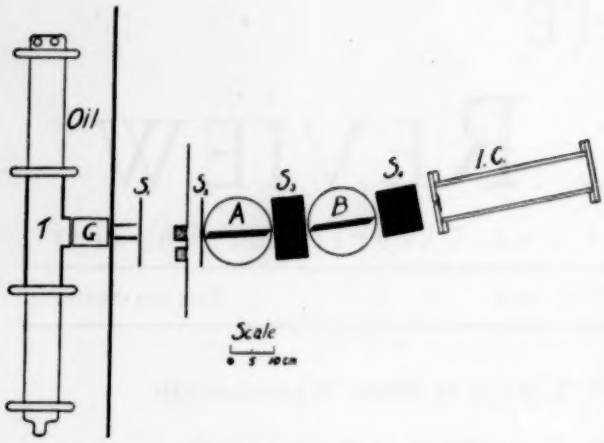

FIG. 1. Schematic diagram of apparatus.

for wave-lengths of 250 x-units and less is that in order to obtain sufficient intensity to make reliable measurements, the slit system must be so wide that $\Delta\lambda$ is a large fraction of λ and the uncertainty in the effective wave-length is large. For this reason this investigation was undertaken to determine the feasibility of employing a double crystal spectrometer in the measure of absorption coefficients in this region.

APPARATUS

The instrument used was made by the Société Genevoise, and has been previously described by A. H. Compton.[8] A 140-kilovolt line-focus tube T (see Fig. 1) with a tungsten target was used as a source of x-rays. This tube was immersed in oil in a lead box mounted upon a lathe bed to permit the adjustment required with the Compton type of double crystal spectrometer. A short piece of glass tubing G covered at the ends with celluloid provided an air path for the x-rays in the box. The tube-target was cooled with kerosene circulated by a pump through a copper cooling coil immersed in running water. The high voltage was supplied by a transformer, rectified by 250 kilovolt valves and smoothed by condensers. The voltage was kept constant with the aid of a pre-reading voltmeter in the primary circuit and manually controlled rheostats. The tube current was read on a milliammeter in the aerial system reflecting a beam of light on a wall nine feet away. This current was kept constant by a voltage stabilizer in the primary of the filament transformer circuit and an additional manually operated rheostat.

Two very large calcite crystals were used in the (1, 1) position according to the notation of Allison[9] to reflect the $K\alpha_1$ line of tungsten into a large copper ionization chamber containing air at a pressure of thirty atmospheres. The ionization current was measured with a Compton electrometer operated at a sensitivity of about 3000 mm per volt. Especial care was taken to shield this electrical system from scattered x-rays, and dry air was passed slowly through the shields about the electrometer to ionization chamber connection. Various tests were made to insure that the x-radiation entering the ionization chamber was entirely the twice reflected $K\alpha_1$ radiation. The materials investigated were all mounted upon a large disk between the first two spectrometer slits; by rotating this disk through a small angle a sample could be removed, and by an additional small rotation another substituted.

RESULTS

The materials investigated were paraffin, graphite, aluminum, copper, silver, tantalum, tungsten and lead. The paraffin was later analyzed for its carbon and hydrogen content, and the graphite and aluminum for small impurities. The other elements used were believed to be of a high degree of purity. The values obtained for the mass absorption coefficients of

TABLE I. *Mass absorption coefficients for $K\alpha'$ line of tungsten ($\lambda = 208.6x$), with double crystal spectrometer.*

Substance	No. Obs.	μ_m	Prob. error
Lead	13	5.07	0.04
Tungsten	10	3.81	0.03
Tantalum	12	3.62	0.02
Silver	12	5.99	0.09
Copper	26	1.617	0.012
Aluminum	21	0.278	0.002
Carbon I	23	0.177	0.002
Carbon II	15	0.174	0.003
Paraffin	14	0.209	0.002
Hydrogen (calculated[1])		0.40	

[1] Value for hydrogen calculated from difference between measurements on carbon and paraffin.

[8] A. H. Compton, R. S. I. **2**, 365 (1931).

[9] S. K. Allison and J. H. Williams, Phys. Rev. **35**, 149 (1930).

the materials used are given in Table I. Each individual measurement consisted of three values of (I_0+I_b), three values of $(I+I_b)$, and then three more values of (I_0+I_b), where I and I_0 are, respectively, the ionization currents due to the twice reflected x-ray beam with the absorber in the path and removed. I_b, the residual ionization current due to cosmic rays and local gamma radiation, was determined from an average of three or more readings taken at about two hour intervals. No ionization current determination was discarded unless an obvious experimental error had occurred during its reading.

Following this series of measurements the spectrometer was set on the $K\beta_1$ line of tungsten and a few measurements taken. However, the intensity which could be obtained with this line was small in comparison with the residual ionization, and for this reason it was decided that it would be preferable to remove the first crystal and use the instrument as a single crystal spectrometer. There is, though, one interesting feature in connection with the measurements made with the two crystals set on this line. The wave-length of the $K\beta_1$ line of tungsten is according to J. H. Williams[10] 184.0 x-units, while the K absorption edge of tantalum has been reported to be 183.6 x-units. The value obtained for the absorption coefficient of tantalum was 3.00 ± 0.09, a value which in spite of the rather large probable error seems to be somewhat too high to be on the long wave-length side of the K edge, and much too low to be on the short wave-length side.

With the instrument as a single crystal spectrometer the slit system was adjusted so that $\Delta\lambda$ was 5 x-units. Absorption measurements were then carried down to 138 x-units. The results are shown in Fig. 2, where the solid lines represent the best average values of μ_m from 0.140A up to 0.230A. The dotted lines represent extensions to fit the average values of other observers.

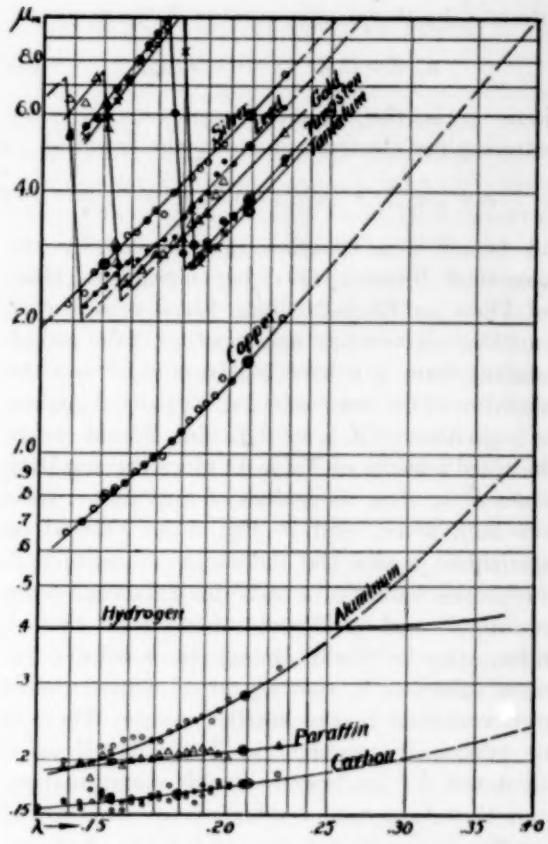

FIG. 2. Mass absorption curves for elements studied. Double circles at 0.2086A and 0.184A for tantalum represent measurements with double crystal spectrometer. Large circles with cross on carbon curve Hewlett's values for this region. Heavy circle at 0.151A for silver mean of fifteen separate readings with single crystal.

TABLE II. *Mass absorption and atomic absorption* ($\times 10^{25}$) *coefficients.*

	λ=208.6x			λ=170x			λ=140x		
Z	μ_m	μ_a/Z	τ_a/Z	μ_m	μ_a/Z	τ_a/Z	μ_m	μ_a/Z	τ_a/Z
82	5.07	211.5	206.0						
74	3.81	156.3	150.8	9.36	384.0	378.8			
73	3.62	148.5	143.0	8.83	352.0	346.8			
47	5.99	229.0	223.5	3.62	138.4	133.1	2.26	86.3	81.2
29	1.617	58.4	52.9	0.992	35.8	30.5	0.658	23.8	18.7
13	0.278	9.51	4.06	0.222	7.60	2.35	0.192	6.57	1.51
6	0.176	5.80	0.35	0.165	5.57	0.20	0.157	5.18	0.13
1	0.40[1]	6.65	0.001[2]	0.40[1]	6.65	0.001[2]	0.40[1]	6.65	0.001[2]
		$\sigma=5.45$			$\sigma=5.24$			$\sigma=5.05$	

[1] Calculated from carbon and paraffin.
[2] Obtained by an extension of straight lines of Fig. 3.

[10] John H. Williams, Phys. Rev. **40**, 791 (1932).

DISCUSSION OF RESULTS

The values of μ_m as measured at 208.6 x-units with the double crystal spectrometer, and taken from Fig. 2 at 170 and 140 x-units are given in Table II. In the second column is given the corresponding value of the atomic absorption coefficient divided by the atomic number of the element, and multiplied by a factor of 10^{25}.

If the usual absorption equation

$$\mu_a = C_k Z^p \lambda^q + (\sigma/\sigma_0) Z \sigma_0 \quad \cdot \quad (2)$$

is divided by the atomic number Z, there results

$$\mu_a/Z = C_k Z^{p-1}\lambda^q + (\sigma/\sigma_0)\sigma_0, \quad (3)$$

where σ_0 is the classical expression for the scattering per electron, given by the equation

$$\sigma_0 = (8\pi/3)(e^4/m^2c^4) = 6.58\times10^{-25}\ \text{cm}^2 \quad (4)$$

and (σ/σ_0) is a function of λ, given by the theoretical formula of either Compton, Breit and Dirac or Klein-Nishina. Since σ/σ_0 is constant[11] for a given λ, it appears that if the proper constant term is subtracted from μ_a/Z and the logarithm of the remainder, τ_a/Z, plotted against the logarithm of Z, a straight line should result. The third column of Table II gives the resulting values of τ_a after the values of σ as shown have been subtracted, and in Fig. 3 are plotted on logarithmic scales the values of τ_a against Z. The proper values of σ to be used for each λ are accurately and easily obtained from such a graph, since a slight change in σ affects the larger values of τ_a scarcely at all, but causes a large variation in the smaller values. There is one glaring discrepancy in Table II; if μ_m is calculated for hydrogen in the usual manner from the absorption coefficients of carbon and paraffin, a constant value of 0.40 is obtained, giving a value of 6.65×10^{-25} cm^2 for μ_a/Z, which in spite of the large probable error is almost exactly σ_0. The value of τ_a for hydrogen is obtained by extending the straight lines of Fig. 3. There is another peculiarity which should be mentioned; the points for silver in each case fall just slightly under the straight lines, while the points for tantalum and tungsten for 170 x-units are considerably below. The slope of the lines is 3.18 except for the portion of the 208.6 line beyond the K absorption edge, which has a slope of 3.10.

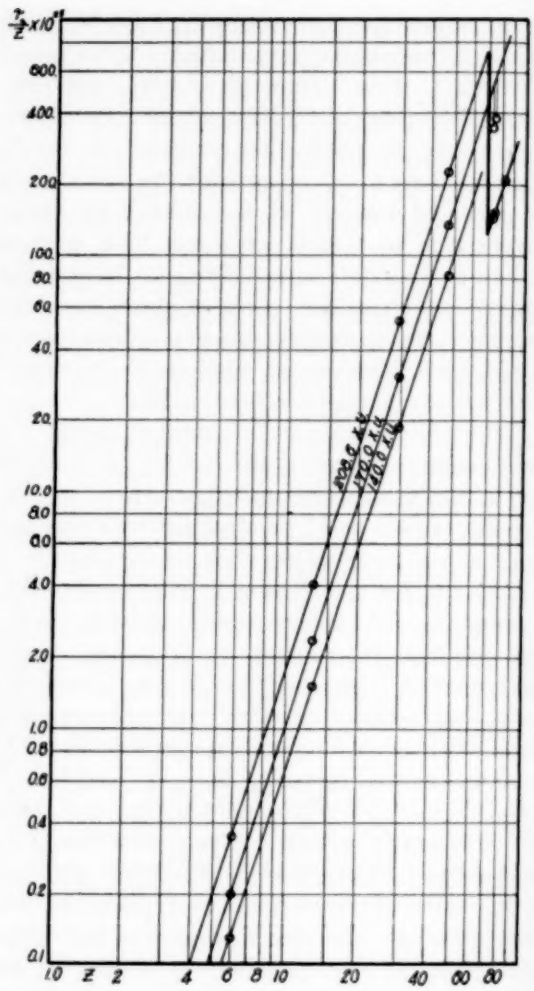

FIG. 3. τ_a/Z plotted against Z for three wave-lengths.

In Table III the experimental values of σ/σ_0 are compared to the theoretical values. The agreement with the values calculated from the Klein-Nishina formula is seen to be exceptionally good. It is believed that this is really a significant test of these theories, since the difference between the predictions of the various theories seems to be greater than the experimental error. The exponent of λ indicated by these values of τ_a is

TABLE III. *Comparison of experimental and theoretical values of scattering per electron.*

λ	σ/σ_0	Compton	Breit, Dirac	Klein-Nishina
208.6	0.828	0.811	0.813	0.825
170.0	0.796	0.778	0.782	0.794
140.0	0.768	0.743	0.746	0.768

$\sigma_0 = 6.58\times10^{-25}$ cm^2

[11] On both classical and quantum theories, this statement is valid only when there occurs no interference between the rays from the different electrons in the atoms, i.e., when no "excess scattering" occurs. The relation is thus more strictly valid for the light elements.

TABLE IV. *Exponent of λ in atomic absorption equation.*

Pb	(Ta,W)[1]	(Ta,W)[2]	Ag	Cu	Al	(C)[3]
2.56	2.6	3.3	2.54	2.54	2.47	2.43

[1] Long wave-length side of K absorption edge.
[2] Short wave-length side of K absorption edge.
[3] Large probable error, since τ_a is very small.

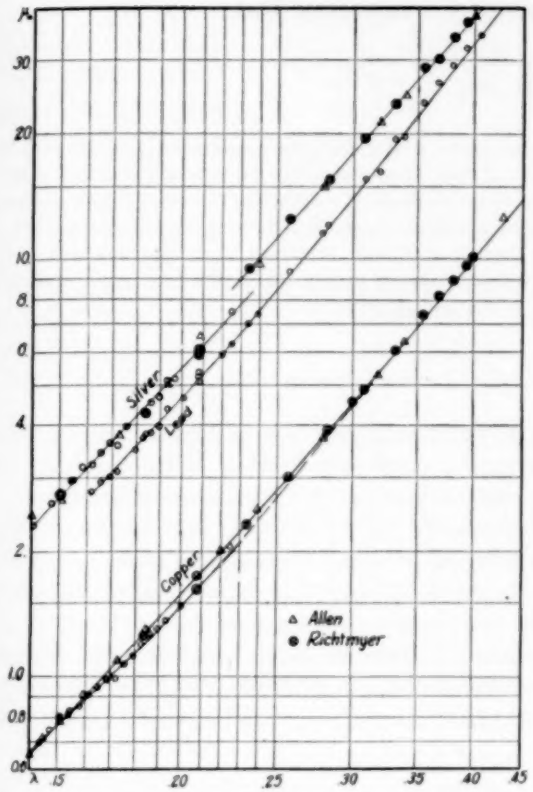

FIG. 4. Comparison of values of μ_m for silver and copper with those of Richtmyer and Allen.

(for the four elements far removed from their K absorption edges) 2.50, with a large probable error.

Referring again to Fig. 2, it may be mentioned that the values of the K absorption discontinuities agree with the published values of other observers. It will be noticed that in the case of lead and gold the values of μ_m on the long wave-length side of the K discontinuity may be interpreted as lying on a curve parallel to the main absorption curve but somewhat above it, up to a wave-length corresponding to an energy sufficient to remove an electron from the K to the L energy level. However, such a condition does not appear in the values obtained for tantalum and tungsten. Also the fit will be nearly as good for lead and gold if the absorption curve is given an increased curvature in this region.

For the most part the values of μ_m obtained agree fairly well with those of other observers. There are though two cases for which this is not true. In Fig. 4 the author's values are shown plotted with those of Allen[7] and Richtmyer[6] for silver, lead and copper. In the case of silver, all values agree quite well up to about 230 x-units. For longer wave-lengths than this their values lie on a higher curve as indicated. For the case of lead no such anomaly occurs, and all values lie on a smooth curve; this curve was included for comparison with that of silver. In the case of copper the author's values diverge considerably from those of others in this wave-length region.

With a value of 2.50 for the exponent of λ, the constant C_k in Eq. (3) has a value of 5.8×10^{-7}. It should be noted however that a very small variation in the exponent of λ will produce large changes in the constant C_k, since λ in this equation is to be measured in centimeters. The fact that the range of wave-lengths used was rather limited together with the fact that λ is small prohibits a really good test of the dependence of τ_a on λ. Nevertheless the values shown in Table IV, with the exception of the high value for tungsten and tantalum on the short wave-length side of the K absorption edge, seem to indicate a value of the exponent of λ considerably smaller than previously reported for this region. It is perhaps interesting to compare this value with Messner's[12] recently reported value of 2.50 for the extremely long wave-length region, and the value of 2.56 obtained by Patten[13] in the study of the L absorption edges of the heavy elements.

It is a great pleasure to express my appreciation to Professor A. H. Compton for help and encouragement throughout the course of this work.

[12] R. H. Messner, Zeits. f. Physik **85**, 727 (1933).
[13] C. G. Patten, Phys. Rev. **45**, 662 (1934).

On the Mathematical Analysis of Cosmic-Ray Data

LOUIS V. KING, *Macdonald Physics Laboratory, McGill University, Montreal, Quebec*

(Received May 29, 1934)

In connection with cosmic-ray calculations, attention is drawn to the existence of extensive tables by Miller and Rosebrugh of the integral $\int_x^\infty e^{-u}u^n du$ for integral values of n from -2 to $+2$. Cosmic-ray data may be analyzed by a procedure which ultimately depends on Prony's method of analyzing a curve into a finite number of exponential constituents. By the use of interpolation theorems and the methods of the calculus of finite differences, observational data for exponential analysis may be derived free from the uncertainties of graphical differentiation. Methods of calculating the effect of self-scattering by the atmosphere are indicated. The exact calculation of the effect of wall thickness in a spherical ionization chamber is shown to depend on the functions tabulated by Miller and Rosebrugh.

§1. INTRODUCTION

THE principal object of this brief note is to draw attention to extensive and convenient tables by W. Lash Miller and T. R. Rosebrugh[1] of integrals of the type

$$I_n(x)=\int_x^\infty e^{-u}u^n du. \tag{1}$$

For negative values of n, these integrals may ultimately be reduced to depend on the exponential integral. The integrals $I_{-2}(x)$, $I_{-1}(x)$, $I_0(x)$, $I_1(x)$ and $I_2(x)$ are, however, tabulated directly to 9 significant figures at intervals of 0.001 between $x=0$ and $x=1$, and at intervals of 0.01 between $x=1$ and $x=2$.

In terms of the integral

$$G(x)=\int_1^\infty u^{-2}e^{-xu}du, \tag{2}$$

which plays an important part in atmospheric radiation problems, we obviously have,

$$G(x)=xI_{-2}(x). \tag{3}$$

A short table of $G(x)$ is given by E. Gold[2] to 5 significant figures at intervals of 0.01 between $x=0$ and $x=1$; 0.05 between 0.1 and 1.0; 0.1 between 1 and 2; 0.2 between 2 and 3; 0.5 between 3 and 6. Enlarged tables of the integral have been computed by L. D. Weld,[3] but apparently have not been published: this is now perhaps unnecessary in view of the existence of the Miller-Rosebrugh tables referred to above.

Obviously $I_{-1}(x)=Ei(-x)$ and $I_0(x)=e^{-x}$, for which well-known tables are available.

In the following sections we deal briefly with two problems connected with the analysis of cosmic-ray data in regard to which the Miller-Rosebrugh tables are likely to prove extremely convenient, and deserve to be better known.

§2. EXPONENTIAL ANALYSIS OF COSMIC-RAY DATA

The mathematical problem of analyzing the radiation from sun and sky has many points in common with the corresponding problem relating to cosmic-rays.

If $E_0(\zeta)$ is the intensity per unit solid angle outside the earth's atmosphere, the corresponding intensity $E(\zeta, z)$ at height z above sea level is easily seen to be[4]

$$E(\zeta, z)=E_0(\zeta)e^{-\mu_0(H-Z)\sec\zeta}. \tag{4}$$

The coefficient of attenuation is assumed to be proportional to the density, and μ_0 is its value at standard density ρ_0.

In the above formula, which is valid for any law of variation of atmospheric density with height, the curvature of the earth is neglected, and

$$Z=\int_0^z \rho/\rho_0\, dz \quad \text{and} \quad H=\int_0^\infty \rho/\rho_0\, dz. \tag{5}$$

[1] W. Lash Miller and T. R. Rosebrugh, Trans. Roy. Soc. Canada [2] **9**, 73–107, 1903, Sect. III, University of Toronto Studies, No. 43 (Published by the Librarian, University of Toronto).

[2] E. Gold, Proc. Roy. Soc. London **A82**, 62 (1909).

[3] L. D. Weld, Phys. Rev. **40**, 713 (1932).

[4] L. V. King, Trans. Roy. Soc. London **A212**, 392 (1912).

Obviously H is the height of the "homogeneous atmosphere," and in terms of the barometric pressure p at height z, and the standard pressure p_0 at sea level we have, $(H-Z)/Z=p/p_0$, so that we may write (4) in the form

$$E(\zeta, z)=E_0(\zeta)\exp\left[-(\mu_0 H_0/p_0)\cdot p\sec\zeta\right]. \quad (6)$$

If it is assumed that the ionization produced in a spherically symmetrical ionization chamber is proportional to $E(\zeta, z)$, the total ionization at height z from all direction is given by

$$I(z)=k\int E(\zeta, z)d\omega, \quad (7)$$

where k is a constant of proportionality depending on the structure of the ionization vessel.

If it is further assumed that outside the earth's atmosphere $E_0(\zeta)$ is independent of zenith distance and azimuth, we have from (6) and (7), writing $d\omega=2\pi\sin\zeta\, d\zeta$, measuring height in terms of barometric pressure p, and denoting $\lambda_0=\mu_0 H_0/p_0$,

$$I(p)=2\pi kE_0\int_0^{\frac{1}{2}\pi} e^{-\lambda_0 p\sec\zeta}\sin\zeta\, d\zeta. \quad (8)$$

We readily find, in the notation of §1 that

$$I(p)=2\pi kE_0\lambda_0 pI_{-2}(\lambda_0 p), \quad (9)$$

and hence that

$$\psi=-p^2\frac{d}{dp}\left(\frac{I}{p}\right)=2\pi kE_0 e^{-\lambda_0 p}. \quad (10)$$

If the incident radiation consists of several constituents having different coefficients of attenuation μ_{0n}, and ionization-chamber constants k_n, the ionization is additive, and we replace (9) by[5]

$$\psi=-p^2\frac{d}{dp}\left(\frac{I}{p}\right)=2\pi\sum(n)k_n E_{0n}e^{-\lambda_{0n}p}. \quad (11)$$

It will be noticed that the left-hand side contains only observed quantities I and p, while the exponential form of the right-hand side makes it possible to utilize Prony's method of exponential analysis[6] to determine whether curves obtained from balloon or aeroplane observations can be analyzed into a finite number of exponential constituents. Records of the variation of ionization with height (or recorded barometric pressure) give I as a function of p, from which a graph of I/p at *equal* intervals of p may be determined. If a series of observations for unequal intervals of p is to be analyzed, interpolations for equal intervals may be calculated by the use of Newton's formula.[7] Utilizing well-known theorems in the calculus of finite differences, the slopes $d(I/p)/dp$ may be readily computed, so that the left-hand side of (9) may be tabulated at equal intervals independently of the uncertainties of graphical differentiation. The observational material is now ready for the application of Prony's method which enables $2\pi k_n E_{0n}$ and λ_{0n} to be evaluated. Computation should be carried out successively for two, three, or more exponential terms, the constants $2\pi k_n E_{0n}$ and λ_{0n} so determined being utilized, in each case, with the use of the Miller-Rosebrugh tables, to re-synthesize the original ionization curve,

$$I(p)=2\pi\sum_n k_n E_{0n}(\lambda_{0n}p)I_{-2}(\lambda_{0n}p) \quad (12)$$

until a satisfactory fit has been obtained. Should this not prove to be possible for a reasonably small number of exponential terms, it must be concluded that the extra-atmospheric spectrum of the incident radiation is, at least in part, continuous, the problem then resolving into the more difficult one of solving from observational data an equation of the type

$$\psi(p)=-p^2\frac{d}{dp}\left(\frac{I}{p}\right)=2\pi\sum_n k_n E_{0n}e^{-\lambda_{0n}p}+\int_0^\infty 2\pi kE(\lambda)e^{-\lambda p}d\lambda. \quad (13)$$

The procedure outlined in this section supplies

[5] The left-hand side of (11) is identical with $\psi(p)=I-pdI/dp$ introduced by B. Gross (Zeits. f. Physik **83**, 217 (1933)), and now utilized in plotting experimental data.

[6] Whittaker and Robinson, *Calculus of Observations*, §180, p. 369 (Blackie and Son, London, 1924).

[7] Reference 6, p. 35.

in part the need expressed by K. K. Darrow[8] for a convenient method of analyzing cosmic-ray data analogous to the use of Fourier's theorem in the analysis of periodic effects. It is suggested as a procedure supplementary to that utilized by L. D. Weld, and may show some advantage as regards ease of computation. Although either method is likely to be somewhat laborious, records of variation of ionization with barometric pressure are now becoming more numerous and accurate, and better adapted to analysis.[9]

The reader will find no difficulty in adapting the method of computation just outlined to the analysis of under-water ionization curves.

The effect of scattered atmospheric radiation, if appreciable, complicates the analysis. If a law of scattering by air is known, the methods developed by the writer for dealing with the somewhat similar problem of scattering of light in the atmosphere may prove serviceable. In this problem self-illumination of the atmosphere contributes a term $\Phi(Z, \zeta)$ to the right-hand side of Eq. (4). This function is determined from the approximate solution of an integral equation. It is shown[10] to have a maximum value at $Z=\frac{1}{2}H$ or $p=\frac{1}{2}p_0$. When the complete expression for $E(Z, \zeta)$ is integrated for radiation from all directions, the part due to self-illumination or self-scattering will have its maximum shifted to a higher altitude depending on the coefficient of attenuation. The detailed examination of the problem as applied to cosmic radiation must, however, be deferred to a future investigation. It would appear, however, that the criterion $d^2(\log \psi)/dp^2>0$, easily seen from (13) to be necessary if primary constituents of an exponential type alone are considered, may require modification when the additional terms due to atmospheric self-scattering (assumed to have the same coefficient of attenuation as the primary radiation) are taken into account. This latter factor may, in fact, give an adequate explanation of the points of inflection observed in the more recent graphs of $\log \psi$ plotted against p.[11]

[8] K. K. Darrow, *Data and Nature of Cosmic Rays*, Bell Syst. Tech. J. **9**, 165 (1932).

[9] A. H. Compton and R. J. Stephenson, *Cosmic-Ray Ionization at High Altitudes*, Phys. Rev. **45**, 441 (1934).

[10] L. V. King, Trans. Roy. Soc. London **A212** (1912), Eq. (36).

[11] A. H. Compton and R. J. Stephenson, *Cosmic-Ray Ionization at High Altitudes*, Phys. Rev. **45**, 446 (1934).

§3. Effect of Wall Thickness in a Spherical Ionization Chamber

In a recent paper, C. Eckart[12] has examined the absorption of a homogeneous beam of radiation by the walls of a spherical ionization chamber of internal radius r, external radius R, the material having a coefficient of attenuation κ. The average ionization per unit volume is shown to be proportional to

$$H=\xi\int_0^1 e^{-\kappa\xi}z^2dz, \tag{14}$$

where

$$\xi=(t^2+r^2z^2)^{\frac{1}{2}}-rz, \quad \text{and} \quad t^2=R^2-r^2. \tag{15}$$

The integral in (14) may be evaluated without approximation in terms of the functions tabulated by Miller and Rosebrugh. From the first equation in (15) we have $2rz=(t^2/\xi)-\xi$, so that in terms of ξ,

$$H=-\left(\frac{3}{8r^3}\right)\int_{\xi_0}^{\xi_1} e^{-\kappa\xi}\left(\frac{t^6}{\xi^4}-\frac{t^4}{\xi^2}-t^2+\xi^2\right)d\xi. \tag{16}$$

Introducing the dimensionless variables, $x=\kappa\xi$, $\tau=\kappa t$, $\rho=\kappa r$, $\tau'=(\tau^2+\rho^2)^{\frac{1}{2}}-\rho$, Eq. (16) may be written

$$H=\tfrac{3}{8}\rho^{-3}\left[\tau^6 I_{-4}(x)-\tau^4 I_{-2}(x) - \tau^2 I_0(x)+I_2(x)\right]_\tau^{\tau'}. \tag{17}$$

The last three integrals are directly tabulated, while

$$I_{-4}(x)=\tfrac{1}{3}e^{-x}/x^3-\tfrac{1}{6}e^{-x}/x^2+\tfrac{1}{6}I_{-2}(x). \tag{18}$$

The use of the exact formula (17) makes the computation of H a comparatively easy matter, so much so that experiments for analyzing cosmic radiation at any one locality by varying t is suggested. It should be possible, as in Section 2, to transform Eq. (17) in such a way that we have in the left-hand side a function of H, $\partial H/\partial t$, etc., and on the right a number of exponential terms, so that Prony's method of analysis may be utilized. The correction to be applied for self-scattering by the spherical walls is likely to prove difficult and its calculation only to be attempted if experiments of high precision of the type considered were seriously considered.[13]

[12] C. Eckart, Phys. Rev. **45**, 451 (1934).

[13] The problem of scattering of solar radiation by a spherically curved atmosphere has recently been considered by C. L. Pekeris, Skrifter utgitt av Det Norske Videnskaps, Akademi i Oslo, 1934, p. 12.

The Magnetic Moment of the Proton

I. I. Rabi, J. M. B. Kellogg and J. R. Zacharias, *Columbia University*

(Received June 15, 1934)

The magnetic moment of the proton has been measured by a method depending on the deflection of a beam of neutral hydrogen atoms in weak magnetic fields of sufficient inhomogeneity. When the field is of such magnitude that the nuclear spin is only partially decoupled from the electron spin the nuclear moment can be evaluated by measuring the atomic magnetic moments of the magnetic levels. Detection was effected on a molybdenum oxide coated plate and the results evaluated by the measurement of the widths and separation of the traces produced. A novel method of great convenience and simplicity for producing the proper magnetic field is described. The value of the proton moment obtained is 3.25±10 percent.

THE discovery of the intrinsic magnetic moment of the electron was of first importance in obtaining an understanding of atomic structure. It may likewise be expected that a knowledge of the magnetic moment of the proton will play a similar rôle in the field of nuclear structure. Nuclear magnetic moments have been obtained principally from an investigation of the hyperfine structure of spectral lines. From the intervals between the hyperfine levels one can calculate the magnetic moment of the nucleus if sufficient knowledge of the wave functions is available. For hydrogen this optical method is inadequate. The Lyman lines are in the far ultraviolet and the h.f.s. has never been detected. However a more powerful method based on the use of molecular beams and proposed originally[1] for measuring nuclear spins may be modified to apply to such cases.

The experiments to be described consist in deflecting a narrow beam of neutral hydrogen atoms in the normal $^2S_1$ state by a weak magnetic field of sufficient inhomogeneity. When a hydrogen atom is in a magnetic field the electronic moment is under the influence of both the external field and the magnetic field due to the nuclear moment. Instead of taking on just the two orientations characterized by $m_s=+\frac{1}{2}, -\frac{1}{2}$ it takes four orientations since the nuclear spin is $\frac{1}{2}$. These four magnetic levels arise from

$$(m_s, m_i)=(\tfrac{1}{2}, \tfrac{1}{2}), (\tfrac{1}{2}, -\tfrac{1}{2}), (-\tfrac{1}{2}, \tfrac{1}{2}), (-\tfrac{1}{2}, -\tfrac{1}{2}).$$

In these levels the component of the magnetic moment of the atom in the direction of the field is given by

$$f_1=1, \quad f_2=x/(1+x^2)^{\frac{1}{2}},$$
$$f_3=-x/(1+x^2)^{\frac{1}{2}}, \quad f_4=-1, \quad (1)$$

in units of the Bohr magneton. The parameter x is defined by

$$x=2\mu_0 H/hc\Delta\nu, \quad (2)$$

where H is the value of the magnetic field, and $\Delta\nu$ is the separation in wave numbers of the hyperfine levels $F=1$ and $F=0$ corresponding to the electron spin and the nuclear spin parallel and anti-parallel. Due to the precession the other components average out to zero and do not contribute to the force on the atom. The contribution of the magnetic moment of the nucleus to the total magnetic moment of the atom may be neglected to this approximation; its effect is only on the average orientation of the electron moment with respect to the field.

Our deflection experiment has as its object the measurement of f_2 and f_3, and hence of the unknown $\Delta\nu$. Our method therefore measures the same quantity as does the h.f.s. method when available. The quantity $\Delta\nu$ is related to the nuclear moment by[2]

$$\Delta\nu=(32\pi/3hc)\mu_P\mu_0|\psi^2(0), \quad (3)$$

where μ_P is the unknown magnetic moment of the proton and $\psi(0)$ is the value of the Schrödinger wave function at the nucleus which is known exactly for hydrogen. The other symbols possess their usual meanings. If μ_P is expressed in units of $\mu_0/1838$[3] we have, putting in numerical values,

$$\mu_P=\Delta\nu/0.0169. \quad (4)$$

[1] Breit and Rabi, Phys. Rev. **38**, 2082 (1931); Rabi, Phys. Rev. **39**, 864 (1932); Rabi and Cohen, Phys. Rev. **43**, 582 (1933).

[2] Fermi, Zeits. f. Physik **60**, 320 (1930).

[3] A convenient unit of nuclear magnetic moment for which we propose the symbol μ_n.

In Fig. 1 is plotted the variation of the effective atomic moments f (in units of μ_0) with x. Measurements of the values of f at different fields yield independent relations for the calculation of $\Delta\nu$. For a given value of x a beam of atoms of homogeneous velocity will give a deflection pattern consisting of four lines corresponding to the four values of f in Eq. (1). For $x=0.354$ the four lines will be equidistant, and if $\mu_P=\mu_e$ (i.e., $\Delta\nu=0.0169$), the value of H will be 64.5 gauss. For larger values of μ_P the field will be proportionally larger.

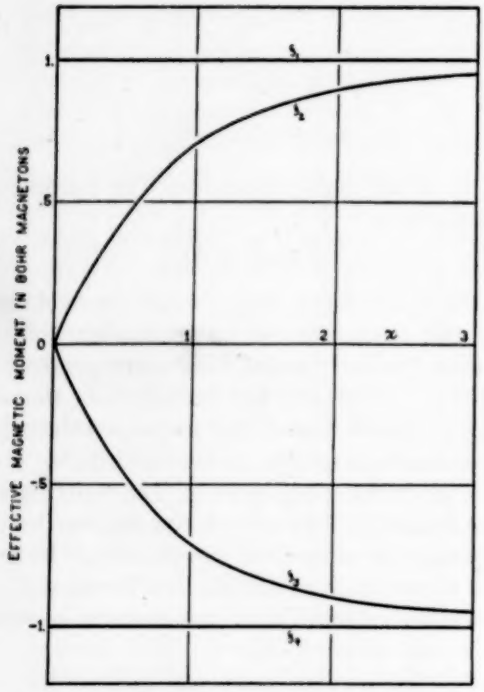

FIG. 1. Variation of the moments of the magnetic levels with magnetic field.

In these experiments no source of hydrogen atoms homogeneous in velocity was available; consequently these considerations have to be modified to take account of the Maxwellian distribution of velocities. Although all the atoms in a given magnetic level are under the influence of the same force, the fast atoms are deflected less than the slow. Each level thus gives rise to a band instead of a line. Since each level is equally probable the areas under the component bands are equal. The superposition of these bands yields instead of lines a deflection pattern as shown in Fig. 2. However a measurement of this pattern can still give results of sufficient precision under proper conditions.

APPARATUS

The hydrogen atoms are formed in a long (5 meter) Wood discharge tube. The pressure in this tube is maintained by a continuous circulation of moist hydrogen at 0.2 to 0.3 mm of mercury. Examination of the discharge with a spectroscope shows very little background to the Balmer lines. A side arm of 6 mm Pyrex tubing 20 cm long and cooled for part of its length leads from the middle of the discharge tube to the source slit S_1', Fig. 3. This slit, in reality a canal 0.02 mm wide and 4 mm high is made by sawing a 0.1 mm slot in the end of a closed Pyrex tube. The jaws of this slot are then collapsed on a thin copper foil which is subsequently dissolved out. The source

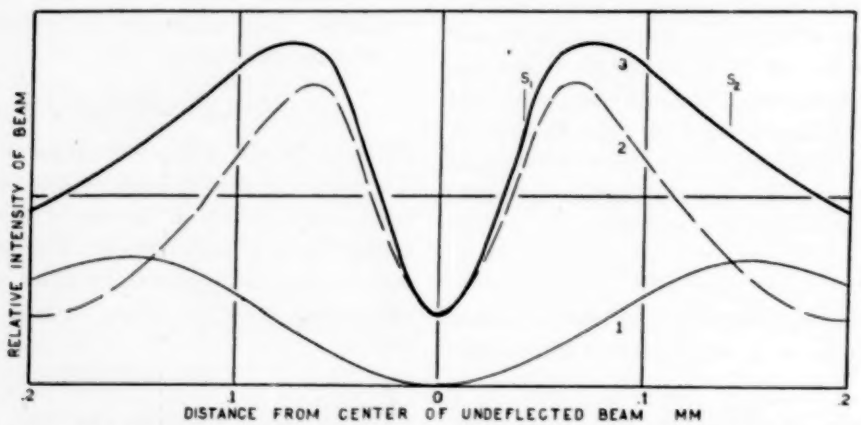

FIG. 2. Deflection pattern with $T=300$, $l_1^2+2l_1l_2=303$, $H=244$, $\partial H/\partial y=1980$, and an assumed proton moment of 2.6 units.

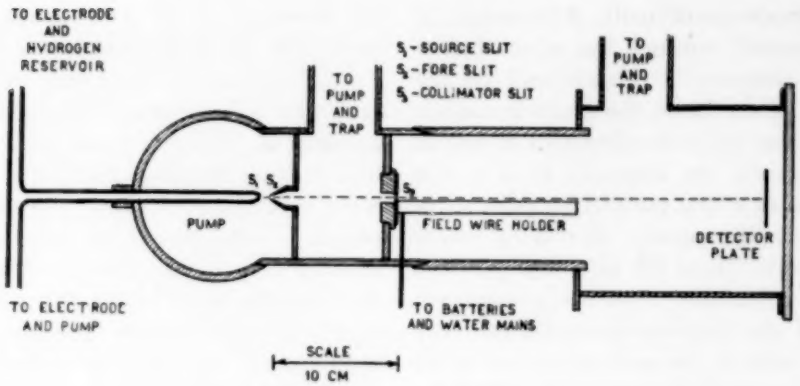

FIG. 3. Diagram of apparatus.

slit projects into the inlet of a high speed oil diffusion pump which maintains a pressure of 3×10^{-5} mm in the source chamber *S.C.* To obtain high vacuum for the greater part of the beam path the source chamber is isolated by an adjustable steel fore slit S_2, 0.1 mm wide and 7 mm from S_1. A fast oil diffusion pump[4] with a liquid air trap maintains a pressure of 10^{-6} mm in the space between S_2 and the collimating slit S_3. This slit, formed by adjustable phosphor bronze jaws, is 0.02 mm wide and 2.4 mm high. The remaining beam path is maintained at a pressure of 5×10^{-7} mm by another fast oil pump with a liquid-air trap. This pressure is measured with an ionization gauge whereas all the others are measured with a McLeod.

Detection of the beam is effected on a layer of molybdenum oxide soot[5] deposited on a glass plate. This yellow oxide is reduced by the atomic hydrogen to the so-called "blue" oxide of molybdenum. The plate is carried on a slide which may be moved across the beam by a magnetic control. In addition the distance of the plate from the end of the field may also be varied. The detector is so sensitive that the trace of an undeflected beam 40 cm long appears after four minutes of exposure.

The three slits cannot be aligned by optical means alone. Since the source slit is a canal the atoms do not emerge according to the cosine law but are so strongly concentrated in the forward direction that a fairly sharp trace is obtained on a detecting plate placed between S_1 and S_2. The fore slit is set in the line of the beam with the aid of this trace. This precaution is very important if maximum intensity is to be obtained. A shift in the position of the fore slit of 0.1 mm would cause a reduction of intensity at the receiving end of 90 percent although optically the line up could still appear perfect.

A novel feature of this apparatus is the production of the magnetic field without the use of iron. The field must meet exacting requirements. As will be evident in the discussion of procedure, the magnetic field must be small (100 to 400 gauss), the gradient of the field must be sufficiently large to produce easily measurable deflections, both the magnitude of the field and the gradient must be constant over the height of the beam, and both must be accurately known. These conditions

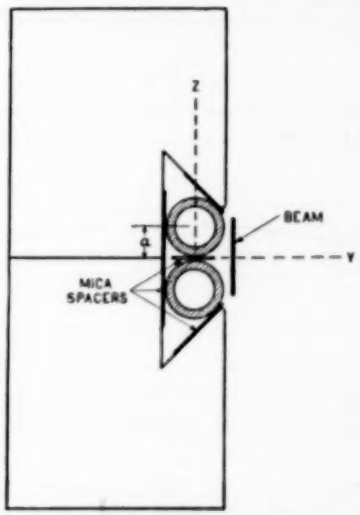

FIG. 4. Cross section showing field wire holder and field wires. The direction of the beam is perpendicular to the plane of the paper.

[4] After a design kindly sent us by Dr. R. M. Zabel.
[5] Phipps and Taylor, Phys. Rev. **29**, 309 (1927).

introduce only moderate difficulty if the height of the beam be severely limited, but since the intensity at the detector is proportional to the effective height of the beam the problem cannot be met in this way with the detectors in use at present. Fortunately the magnetic field in the neighborhood of two long parallel straight wires carrying currents in opposite directions meets these requirements. Since the field and gradient are completely calculable from the geometrical arrangement of the currents we avoid the very difficult and tedious measurement of these quantities. Fig. 4 shows in cross section the relation of such a pair of wires to the beam and to a set of coordinate axes yz. Graphs of the magnitude of the magnetic field and of the gradient are shown in Figs. 5 and 6. If $2a$ is the distance between the centers of the wires, then it is evident from these curves that for $y=1.2a$ both field and gradient are nearly constant over the region between $z=-0.7a$ and $z=+0.7a$. The relations giving the field and gradient at any point are

$$H=2I\frac{2a}{r_1r_2}, \quad \frac{\partial H}{\partial y}=-2I\frac{2a}{r_1^3r_2^3}(r_1^2+r_2^2)y,$$

where I is the current in amperes/10 and r_1 and r_2 the distances of the point in question from the centers of the two wires. In our apparatus with $a=1.23$ mm and $z=0$, a current of 100 amp. in each wire will produce a field of 133 gauss and a gradient of 1080 gauss per cm at $y=1.2a$. Such high current densities require the use of hollow water cooled copper tubes instead of wires. These tubes, 15 cm long, 0.241 cm in diameter, and separated by a mica spacer 0.005 cm thick, are held rigidly in an aluminum block. Current is supplied to these tubes by a bank of twelve 160 amp.-hr. storage batteries in parallel. The position of the field wires with respect to the beam is conveniently determined by the beam itself. A detecting plate is mounted with one edge in contact with the wires and a trace is formed. The distance from the edge of the plate to the middle of the trace is then measured with a travelling microscope.

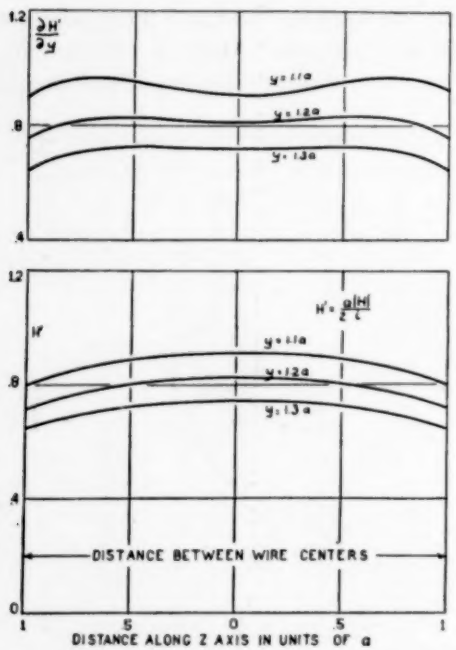

FIGS. 5–6. Plot of the magnetic field and gradient in the region of the beam.

PROCEDURE

The field current is adjusted to a suitable value and the beam turned on. The double trace corresponding to curve III, Fig. 2 appears on the detecting plate usually within 45 minutes, and after 6 to 8 hours is fairly intense. Fig. 7 is a photograph of a typical trace. The plate is then moved a few millimeters to one side and a trace of the direct beam without the field is made. This serves as a check on the width of the beam and on the general constancy of the alignment of the slits. The experimental results are evaluated from a measurement of the separation of the inside edges of the traces and their widths. These distances are measured with a microscope with a micrometer ocular or a micrometer stage. The aim of the measurement is to obtain four points on the traces of presumably equal intensity. As is evident from Fig. 7 the edges of the traces are rather fuzzy and somewhat difficult to measure. The precision of these experiments is limited by these conditions more than by any other factors. However, this method of evaluation first suggested by Stern,[6] has been applied by his school and others to experiments on a variety of atoms including hydrogen at high fields with satisfactory results.

[6] Stern, Zeits. f. Physik **41**, 563 (1927); Rabi, Zeits. f. Physik **54**, 190 (1929).

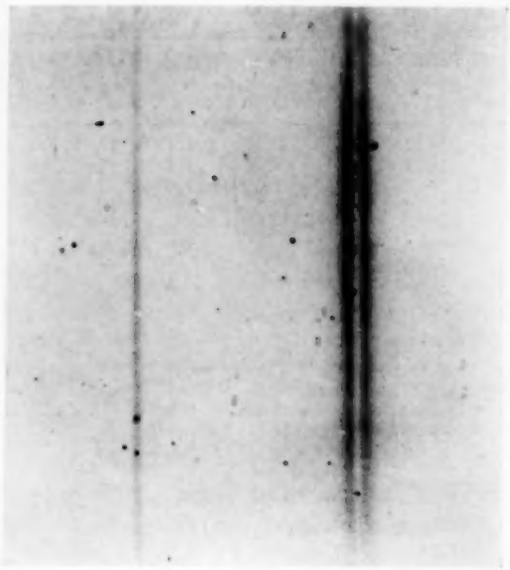

FIG. 7. Photograph of trace. Distance between center of split trace and direct trace is 2.06 mm.

The deflection of an atom in the direction y perpendicular to the beam is given by

$$s=\frac{f_j\mu_0}{4E}\frac{\partial H}{\partial y}(l_1^2+2l_1l_2),$$

where l_1 and l_2 are the distances the atom moves in the field and beyond the field, respectively, E is the kinetic energy of the atom and f_j is the magnetic moment of the atom in a given magnetic level (f_2 and f_3 are functions of H, f_1 and f_4 are independent of H, see Fig. 1). For an atom with kinetic energy $E=E_\alpha=\frac{1}{2}mv_\alpha^2=kT$, s will have the particular value

$$s_\alpha=\frac{f_j\mu_0}{4kT}\frac{\partial H}{\partial y}(l_1^2+2l_1l_2). \tag{5}$$

For atoms with $f_j=\pm 1$, $s_\alpha=\pm s_\alpha{}^0$ may be calculated directly since the quantities in this equation are then all known. For atoms with $f_j=\pm x/(1+x^2)^{\frac{1}{2}}$ (Eq. (1)) experimental evaluation of $s_\alpha=s_\alpha{}^i$ permits calculation of f_2 and f_3 and therefore of $\Delta\nu$ by Eq. (2).

Consider atoms which are deflected from an element du, Fig. 8, in the undeflected beam a distance w to the element ds at s. The form of the undeflected trace is trapezoidal as calculated from the geometry of the apparatus and can be

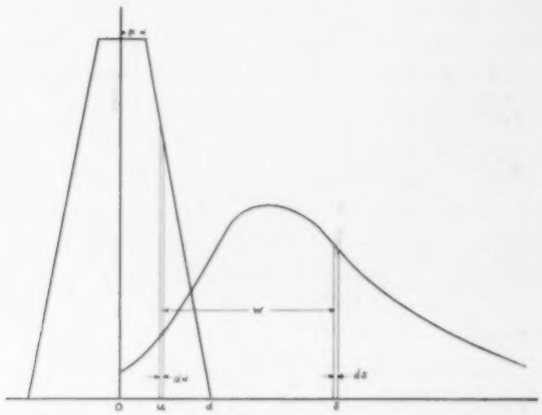

FIG. 8.

represented by the function $I(u)$. The deflection is a function of f_j and E. For atoms in a state with moment f_j and *a priori* probability w_j this number will be

$$dn_j=w_jI(u)du e^{-v_w{}^2/v_\alpha{}^2}(2v_w{}^2/v_\alpha{}^4)dv_w$$
$$=w_jI(u)du e^{-E_w/E_\alpha}(E_w/E_\alpha{}^2)dE_w.$$

Since all magnetic levels are equally probable, $w_j=\frac{1}{4}$. The intensity (number of atoms per unit width) at the position s is

$$dJ=\frac{dn}{ds}=w_jI(u)du e^{-E_w/E_\alpha}\frac{E_w}{E_\alpha{}^2}\frac{dE_w}{ds}$$
$$=w_jI(u)e^{-E_w/E_\alpha}\frac{E_w}{E_\alpha{}^2}dE_w,$$

since $s=u+w$, $ds=dw=-du$. Since w is a function of E only, we can integrate this expression over the undeflected trace and obtain

$$J(s,s\alpha)=\{1/4(d-p)\}\{(s+d)e^{-s\alpha/s+d}$$
$$+|(s-d)|e^{-s\alpha/|(s-d)|}-(s+p)e^{-s\alpha/(s+p)}$$
$$-|(s-p)|e^{-s\alpha/|(s-p)|}\},$$

where the symbol $|\ |$ means that the absolute value of this quantity is used. This gives the relative intensities due to the component to the right of the undeflected trace. The deflection pattern is symmetrical with respect to the center. The total intensity is obtained by summing the two component intensities, $J(s,s_\alpha{}^0)+J(s,s_\alpha{}^i)$. Fig. 2 is a plot of the intensity curve obtained by this means. If s_1 and s_2 denote the position on the

trace of two points of equal intensity, see Fig. 2, then

$$J(s_1, s_a^0)+J(s_1, s_a^i)=J(s_2, s_a^0)+J(s_2, s_a^i).$$

Solution of this equation yields s_a^i and therefore from Eqs. (5, 1, 2, 4) a value of μ_P.

The above procedure has to be somewhat modified to take account of the fact that both the field and the gradient vary by a few percent over the width of the deflected beam. This has been taken into account in the table of results given below.

These considerations tell us how to obtain a moment from a given set of measurements. To obtain maximum precision we should have f_2, f_3 which correspond to curve 2 Fig. 2 as different as possible from f_1, f_4 consistent of course with obtaining sufficient inner separation of the traces to measure comfortably. This circumstance separates to a large extent the contributions to the summation curve of the two sets of moments. It is easily shown that when this is not the case experimental errors (e.g. in T, l_1, l_2, $\partial H/\partial y$) are greatly magnified in the determination of f. A second consideration which is of equal importance is the fact that when x is small (in the region of 0.3) the error in the evaluation of the nuclear moment is practically equal to the error in the determination of f, since $\Delta\mu/\mu=(1+x^2)\Delta f/f$ but when x is large (greater than 1.5) the error in μ_P may become several times the experimental error in f. It is consequently of great advantage to be able to perform these experiments at sufficiently low field intensities.

Results

A tabulation of the results of the various runs is given in Table I. As can be seen the measurements were made under a great variety of conditions. In the different runs the width of the initial beam $2d$, was changed by a factor of 1.5, the field by a factor of 2, l_2 by a factor of 3, and the inside separation of the traces by a factor of 3. In addition the density of the traces themselves was greatly varied. The energy distribution of the atoms emerging from the source slit was taken to be characteristic of the temperature of the walls of the glass tube leading to the slit, i.e., room temperature. The proton moment obtained by averaging the results of the various runs is 3.25 ± 10 percent. The sources of error which enter are chiefly those of measurement of the traces. These we consider as accidental errors in view of the experience of other observers with this type of measurement. Another possible source of error which would operate only toward reduction of the moment lies in the estimation of the temperature of the beam. However in the view of length of the communicating tube, the pressure in the discharge tube, and the fineness of the source slit the hydrogen atoms must have suffered a sufficient number of collisions to take on the temperature of the walls. Errors in the determination of the width of the direct beam which might be brought about by scattering of the beam or by error in the estimation of the slit widths have a very small effect on the calculated values of the moment. An assumed increase of 15 percent in d brings about an increase in the calculated nuclear moment of about 1.5 percent. These considerations and the general consistency of the results as presented in Table I make it seem unlikely that a constant error of any considerable magnitude has entered into the measurement. We consider 10 percent a fairly conservative estimate of the precision.

Table I.

H gauss	$\partial H/\partial y$ gauss/cm	$(l_1^2+2l_1l_2)$ cm^2	d mm	s_1 mm	s_2 mm	f	μ_P
175	1422	652	0.07	0.037	0.152	0.299	3.06
208	1691	652	.07	.048	.195	.347	3.08
210	1709	473	.058	.040	.150	.358	3.00
236	1920	391	.052	.031	.148	.351	3.44
244	1985	303	.047	.028	.122	.367	3.38
272	2215	652	.07	.079	.275	.423	3.20
306	2490	652	.07	.094	.335	.456	3.26
306	2490	652	.07	.090	.303	.429	3.52
306	2490	652	.07	.093	.333	.451	3.32

Because of various corrections the values of s_1 and s_2 recorded are not the values which will lead exactly to the corresponding moment, but are included in order to give an idea of the magnitude of these quantities.

Conclusions

The value we obtain for the proton moment is 3.25 ± 10 percent. This value differs considerably from the value 2.5 ± 10 percent obtained by Stern, Estermann and Frisch[7] who measured the quantity by an entirely different method depend-

[7] Frisch and Stern, Zeits. f. Physik **85**, 4 (1933); Estermann and Stern, Zeits. f. Physik **85**, 17 (1933).

ing on the deflection of hydrogen molecules in a very strongly inhomogeneous field. The deflection in their experiments is due to the force exerted directly on the nuclear moment. The moment is evaluated from these deflections after various corrections are made for the moment due to the rotation of the molecule. At present the substantially fair agreement of the two results must be regarded as more important than the difference. There is as yet no sufficient theoretical basis to discuss the far reaching implications of this value of the proton moment. However it can be taken as certain that the proton is not describable by the simple type of Dirac wave equation which describes the electron. An important consequence of these experiments is that we can compare for the first time a measurement made on a nuclear moment directly and one which is fundamentally analogous to the h.f.s. method. The result establishes the h.f.s. method of measuring nuclear moments on firm experimental ground. When both methods are brought to a greater degree of precision we may hope to obtain further tests of the Dirac equation for the electron and perhaps detect other modes of interaction between electron spin and the proton.

The Magnetic Moment of the Deuton[1]

I. I. Rabi, J. M. B. Kellogg and J. R. Zacharias, *Columbia University*

(Received June 15, 1934)

The magnetic moment of the deuton was measured by the deflection of a beam of neutral deuterium atoms. The magnetic moment of the deuton is found to be 0.75 ± 0.2 nuclear units.

THE deuton as the simplest atomic nucleus next to the proton is of particular interest in nuclear investigations. In view of the extreme likelihood that the deuton consists of a proton and a neutron, an evaluation of the magnetic moment of the deuton must yield important information with regard to the magnetic moment of the neutron.

In the experiments to be described the magnetic moment of the deuton was measured by the same method and in the same apparatus which we used for the measurement of the proton moment.[2] A narrow beam of neutral deuterium atoms from a Wood discharge tube is sent through a magnetic field weak enough not to decouple entirely the deuton spin from the electron spin. The field must be sufficiently inhomogeneous to produce easily measurable deflections. As with the H^1 detection was effected on a molybdenum oxide plate. It turned out that the chemical properties of deuterium are not sufficiently different to affect this reaction to any appreciable extent. The traces were measured in the same way as the traces produced by H^1.

The deuton is known to have a spin of 1,[3] consequently there are six magnetic levels corresponding to

$$(m_i, m_s) = (1, \tfrac{1}{2}),\ (-1, -\tfrac{1}{2}),\ (0, \tfrac{1}{2}),$$
$$(0, -\tfrac{1}{2}),\ (-1, \tfrac{1}{2}),\ (1, -\tfrac{1}{2}), \quad (1)$$

which have effective magnetic moments of

$$f_1 = \pm 1, \qquad f_2 = \pm x + \tfrac{1}{2}/(1 + \tfrac{3}{4}x + x^2)^{\frac{1}{2}},$$
$$f_3 = \pm x - \tfrac{1}{2}/(1 - \tfrac{3}{4}x + x^2)^{\frac{1}{2}} \quad (2)$$

and x is defined by

$$x = \mu_0 H / hc\Delta\nu. \quad (3)$$

---

[1] Estermann and Stern, Phys. Rev. **45**, 761 (1934); Rabi, Kellogg and Zacharias, Phys. Rev. **45**, 769 (1934).

[2] See preceding paper, *The Magnetic Moment of the Proton*, page 157. The deuterium gas as well as a sufficient quantity of heavy water to poison the walls of our discharge tube was generously supplied to us by Professor H. C. Urey.

[3] Murphy and Johnston, Phys. Rev. **45**, 761 (1934).

The quantity $\Delta\nu$ is the energy separation in wave numbers between the state $F=3$ where the electron and deuton spin are parallel and $F=\frac{1}{2}$ where they are opposed. In Fig. 1 is plotted the relation between the values of f and of x. The deuton moment is involved in $\Delta\nu$ through the relation

$$\Delta\nu=\tfrac{3}{4}\cdot(32\pi/3hc)\mu_d\mu_0\psi^2(0), \qquad (4)$$

where μ_d is the magnetic moment of the deuton, and $\psi(0)$ the value of the Schrödinger eigenfunction of the normal state at the nucleus, and μ_0 is the Bohr magneton. Expressing μ_d in the customary units of $\mu_0/1838$ we have

$$\mu_d=\Delta\nu/0.0127. \qquad (5)$$

The numerical factor in Eq. (5) is different from that for H^1 because of the difference in nuclear spin.

The type of deflection pattern to be expected for deuterium is shown in Fig. 2. The observed traces result from the superposition of 3 patterns, one from each set of moments given in Eq. (2). As with H^1 the images formed on the detector consist of two traces. The moment is evaluated from a measurement of the width and inner

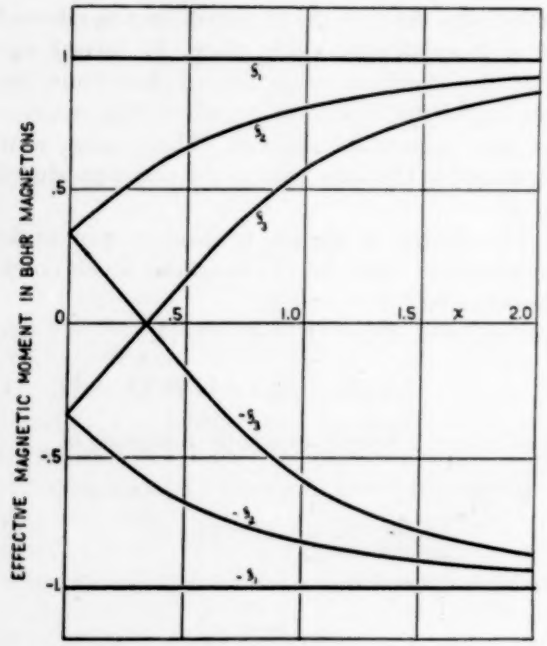

FIG. 1. Variation of the moments of the magnetic levels with magnetic field.

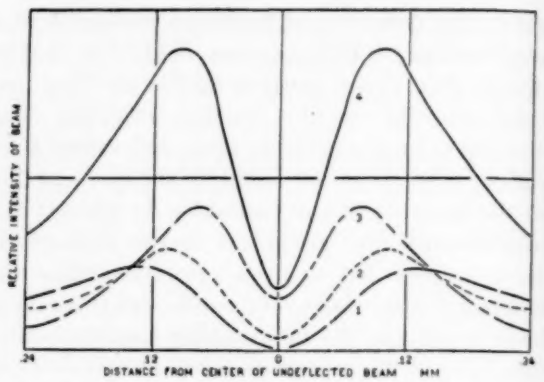

FIG. 2. Deflection pattern with $T=300$, $l_1^3+2l_1l_2=652$, $H=121$, $\partial H/\partial y=984$, and an assumed deuton moment of 1.

separation of these traces. Fig. 3 is a photograph of a typical trace. The theory on which the evaluation of the experimental results is based is the same as with H^1 modified to take account of the fact that there are six magnetic levels of equal *a priori* probability instead of four. The relationship which yields the value of f from which x can be calculated is

$$J(s_1, s_a')+J(s_1, s_a'')+J(s_1, s_a''') = J(s_2, s_a')+J(s_2, s_a'')+J(s_2, s_a'''), \qquad (6)$$

where s_a', s_a'' and s_a''' correspond to f_1, f_2 and f_3. By Eq. (2), s_a'' is a function of s_a''' which is therefore determined by Eq. (6).

The conditions for optimum precision are more difficult to attain with H^2 than with H^1 due to the fact that not only is the moment very much smaller, but for a given moment the $\Delta\nu$ is less and the value of x is therefore greater. This necessitates performing the experiment at much lower values of the magnetic field with the consequent small gradients and deflections. Another source of error is due to the fact that however pure the deuterium used may be originally, it is contaminated by H^1 from the electrodes in the discharge tube. It is a matter of common experience that this difficulty is not entirely eliminated even by prolonged flushing of the discharge tube with He and with deuterium. To reduce the effect of protium contamination the discharge tube was run for about an hour and then pumped down to high vacuum. Fresh deuterium was then admitted and the process repeated.

FIG. 3. Photograph of trace. Distance between center of split trace and direct trace is 2.15 mm.

The results of the various runs are given in Table I. The value of the deuton moment is found to be 0.77 ± 0.2. The effect of the protium correction is such that a 5 percent correction results in a moment change of 0.2 of a unit.

TABLE I.

$l_1^2+2l_1l_2=652$ cm^2				$d=0.07$ mm			
H Gauss	$\partial H/\partial y$ Gauss/cm	s_1 mm	s_2 mm	f_2	f_1	μ_d	Estimated H^1 content
98	796	0.03	0.147	0.536	0.802	0.77	5%
121	984	.05	.190	.656	.844	.77	5%
121	984	.045	.190	.683	.855	.73	10%
179	1455	.082	.295	.800	.898	.82	10%

The corrections we have made for H^1 are more likely to be too small than too great.

It should be emphasized that our measurement cannot distinguish the sign of the nuclear moment.[4] It is thus within the realm of possibility that the proton and deuton moments may both or either be negative. On this basis if we assume the deuton to consist of a proton and a neutron which retain their identities in the deuton, and if we further assume no rotational moment, then the magnetic moment of the neutron would be about ± 2.5 or ± 4.0 units.

[4] This is also true in the experiments of Stern, Estermann and Frisch.

The Emission of Ions and Electrons from Heated Sources

A. J. DEMPSTER, *University of Chicago*

(Received June 8, 1934)

It is found that pin-hole photographs may be made of ions or electrons emitted by a heated source. The crossed paths of the charged particles is explained by the space charges in the immediate neighborhood of the emitting points on the source, which distort the lines of force and allow of accelerations in various directions. Part of the electron emission from an oxide coated filament and the positive ion emission from spodumene is thus found to be concentrated at definite points on the surface.

BY means of electric or magnetic fields the electrons emitted by a hot filament may be focused on a photographic plate.[1] These photographs often reveal a difference in the emissions from various parts of the surface. The experiments described in the present paper show that, in addition to the general emission, there are concentrated point sources where the emission is especially intense.

[1] E. Brüche and H. Johannson, Ann. d. Physik **15**, 145 (1932); E. F. Richter, Zeits. f. Physik **86**, 697 (1933); E. Ruska, Zeits. f. Physik **87**, 580 (1934); V. K. Zworykin, J. Frank. Inst. **215**, 535 (1933); C. J. Calbick and C. J. Davisson, Phys. Rev. **45**, 764 (1934).

The source of electrons was a heated Western Electric coated filament F, Fig. 1. The source of positive lithium ions was a strip of platinum on which a small crystal of spodumene had been melted. The source was placed 12 mm in front of the slit S_1, the second slit S_2 was 6 cm from S_1 and the photographic plate P was 22 cm from S_2. Constant accelerating potentials of 10,000 to 20,000 volts were applied between F and the slit system. With $S_1=0.5$ mm in width and $S_2=0.02$ mm it was noticed with the positive ions that the image on P was not a single line, as was to be expected, but consisted of four lines.

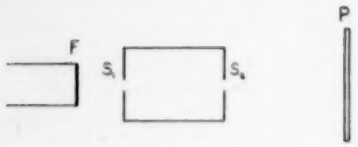

FIG. 1.

When S_1 was widened more lines appeared, and when the front of the metallic cylinder was left completely open, a complex pattern of as many as twenty-five lines appeared. This is illustrated in Fig. 2. With a total current from F of 2×10^{-6} amp. the exposure time with Schumann plates was 45 seconds. The slit S_2 was given a notch at one end, and it is seen that the lines are displaced sideways as well as up and down. The length of the lines agrees with the theory that there are many point sources on F which project images of S_2 on P. S_2 was then removed and a small, irregular hole was inserted between the positions of S_1 and S_2. A great many images of the hole (more than 25) were obtained, each of which showed the irregular form of the hole.

With an oxide coated filament it was found that the electrons gave similar photographs. With a small hole 0.01 mm in diameter in a piece of platinum foil placed 3 cm from F, a group of spots were obtained on P. These differ greatly in intensity and some of them are arranged in straight lines. Four photographs with lithium ions showed the same general arrangement of points is recorded by this method of observation. Around these points, the equipotential surfaces

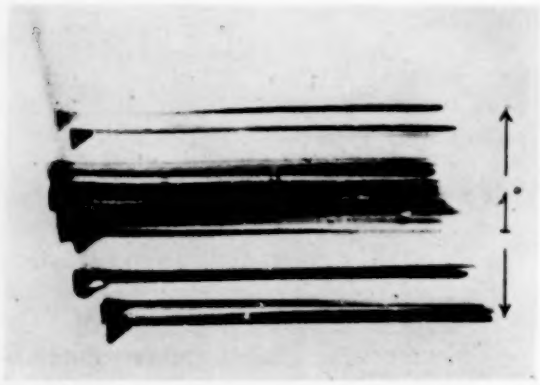

FIG. 2. Images of slit formed by lithium ions.

lines, indicating that the emission remains located at the same points over a considerable time. With 10,000 volts accelerating potential the effect was the same as with 20,000.

The interpretations of the lines and spots as due to point sources of ions or electrons on F seems at first to be untenable, since it would be necessary for the electrons or ions to describe paths that cross at S_2 or at the hole, and that make angles with other paths as large as 1°. We see, however, that this is possible, if we consider the effect of space charge in distorting the field in the immediate neighborhood of emitting points. Only the emission from such are distorted, Fig. 3, so that some of the electrons

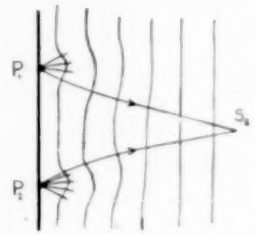

FIG. 3.

leaving P_1, may find their paths crossing the paths of some of the electrons from another point P_2.

We may conclude then that the emission of lithium ions from a heated spodumene crystal, and of electrons from an oxide coated cathode is to a considerable extent concentrated at points on the surface.

The experiments illustrate also a difficulty and possible source of error in dealing with narrow electron or ion bundles in reflection or diffraction experiments. Even with very narrow slits, we do not necessarily have a single beam of uniform intensity issuing from the slit system, but may have a group of several distinct beams making small angles with each other.

Note added in proof: Dr. C. J. Davisson has kindly called an article by H. Seemann to the attention of the author. (Zeits. f. Physik **79**, 742–752 (1932).) In this article tungsten filaments are also shown to emit electrons more strongly from some spots than others. Photographs of the focal spot on an anode first suggested the phenomenon which was later confirmed by direct pin-hole photographs of the cathode.

Correlation Between Variation of Secondary Electron Emission and Atomic Number

PAUL L. COPELAND, *Massachusetts Institute of Technology*

(Received June 9, 1934)

The relative mean variation of the secondary emission as a function of the energy of the primary electrons is found to correlate with the atomic number of the elements bombarded. The evidence suggests that the secondary emission from a given element when bombarded by electrons of high energy may be represented to a first approximation by an equation of the form $R=k/E_p^s$, where R is the ratio of the total secondary current to the incident current and E_p is the energy of the incident beam. k and s are constants characterizing a given curve, and evidence is presented to show that s decreases as the atomic number increases. The significance of the correlation is very briefly discussed.

AS indicated by the work of Petry[1] the general form of the curve obtained when the magnitude of the secondary emission is plotted against the energy of the incident electrons is quite simple. For low primary energies (E_p) the ratio (R) of the return current to the incident current is quite low, but it increases rather rapidly as the primary energy is raised. It approaches a broad maximum at a primary energy of a few hundred volts, and then it decreases as the primary energy is raised still higher. The explanation suggested by Petry for this decline was the deeper penetration of the primaries of high energy.

In comparative studies of the secondary emission from different metals, the writer[2] observed a correlation to exist between the form of the secondary emission curves and the atomic number of the elements bombarded. This correlation was most apparent in the decrease of secondary emission with the increase of primary energy. The curves in which the decline was the most rapid were also the ones showing the highest secondary emission, and to eliminate the suspicion that the observed correlation was due entirely to this cause, the average slope ($\Delta R/\Delta E_p$) obtained from each graph in the region just above the maximum was divided by the magnitude (R) of the secondary emission. The earliest results showed that the relative mean slope ($M=\Delta R/R\Delta E_p$) correlated with atomic number, and that the relation was not far from linear.

Recently the work has been extended to include elements covering a larger range of atomic numbers. At the same time the range of the energies used has been considerably extended. Some of the results are shown in Fig. 1. For elements of low atomic number, the decline of the secondary emission just above the energy

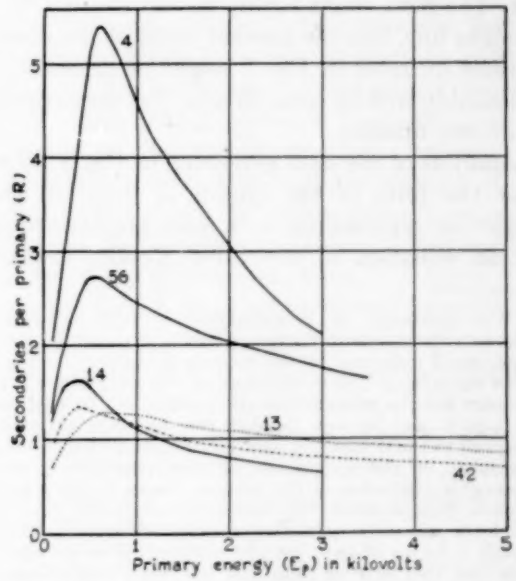

FIG. 1. Secondary electron emission as a function of primary energy. *Erratum:* The curve marked 13 is that obtained for tantalum, atomic number 73.

corresponding to the maximum is very rapid. At higher energies, however, the emission falls off less rapidly, and M is not constant throughout the range. The correlation between the variation of secondary emission and atomic number may be seen by plotting M, the relative mean slope in the first thousand volts above the maximum, against atomic number. Fig. 2 shows the results for sixteen elements examined by the writer.

[1] Petry, Phys. Rev. **26**, 358 (1922).
[2] Copeland, Thesis in the Department of Physics, State University of Iowa, July 1931.

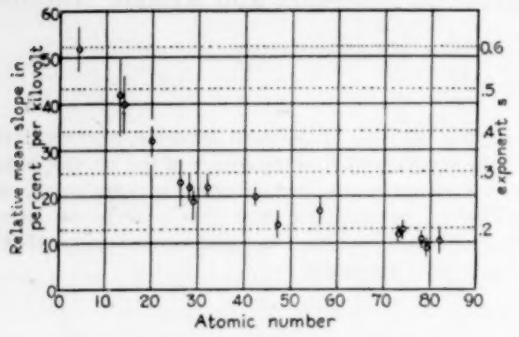

FIG. 2. Mean slope of secondary emission curves as a function of atomic number of target.

The lines indicate the range[3] of the determinations made from the various data. There appears to be a definite correlation between the slopes of the secondary emission curves and atomic number. The data could hardly be represented by a straight line, but the general trend of the observations included in Fig. 2 might be represented reasonably well by some inverse fractional power of atomic number.

Analysis of the data presented in Fig. 1 shows that the form of the curves at high energies might be represented to a first approximation by an equation of the form $R=kE_p^{-s}$ where both k and s vary from element to element. The correlation, noted above, may then be shown as a variation in the value of s required in this equation. This is accomplished by placing the values of s which correspond to chosen values of M at the right of Fig. 2. Thus, while at higher energies, each of the secondary emission curves may be represented as some inverse power of the primary energy, the power required decreases with atomic number. Even for the lightest of the elements examined, however, it is not as high as required by the theory of Frolich[4] who predicts that at high energies the emission should fall off as $E_p^{-1} \ln E_p^{\frac{1}{2}}/W_a$ where W_a is the inner potential of the metal.

These results may be taken as evidence that the decrease in secondary emission at high energies is connected with the deeper penetration of the primary electrons. In the results obtained by the writer, however, a rapid decline is generally preceded by a relatively rapid rise. One can make some progress toward an understanding of secondary emission as a function of primary energy on the basis of primary penetration and secondary diffusion with the sharing of energy. Electrons excited a certain depth, x, below the surface travel on the average a distance x^2 in diffusing back to the surface and probably excite other electrons which may contribute to the secondary current. It seems likely, then, that the secondary electrons resulting from energy lost at a certain depth would increase in number and decrease in energy as a function of the depth. Electrons coming from too great a depth would not have sufficient energy to escape. On this basis many of the observed phenomena may be understood.

[3] The quantity M is essentially a relatively small difference between two measured quantities, and the range of points as indicated by the lengths of the lines in Fig. 2 is not surprising. The consistency of the data seems good evidence for the existence of the correlation. In this connection, it may be well to point out that the writer has observed the first effect of surface contamination to be an alteration in the magnitude of the emission without observable alteration in the relative slopes of the graphs. Thus in the case of beryllium the writer analyzed curves for which the measured secondary emission differed by almost exactly a factor of two, yet the quantity M as computed from the two sets of data did not vary more than is indicated on the graph for atomic number 4. Such stability is evidence for the reliability of the correlation. Notice also that elements as dissimilar in general metallic properties as aluminum and silicon show excellent correlation.

[4] Frolich, Ann. d. Physik **13**, 229 (1932).

Efficiencies of Ionization of Helium and Mercury by Electron Impact at High Voltages

JOHN W. LISKA, *Physical Laboratory, University of Minnesota*

(Received April 10, 1934)

An apparatus which is designed to measure relative efficiences of ionization at high voltages is described. Measurements on helium and mercury vapor are reduced to absolute values by comparison with the data of Smith. The results are given as a function of electron velocities up to 11 kv. The experimental data are compared with theoretical solutions based on classical and quantum mechanics. It is shown that the classical solutions agree fairly well with experiment in form but not in absolute magnitude. The quantum-mechanical solutions agree with experiment over a much larger range of velocities than do the classical solutions. Approximate values for certain constants which appear in the quantum-mechanical solutions yield absolute values for the efficiency of ionization which agree with experiment within a few percent. In both classical and quantum-mechanical solutions, the agreement is good only for electron velocities very much greater than the first ionization potential of the atom.

INTRODUCTION

ALTHOUGH several investigators[1–10] have studied the efficiency of ionization by electron impact in various gases, none of the measurements, with the exception of those by Smith,[10] have been carried out to electron velocities greater than those corresponding to a few hundred volts. Smith, by a method similar to that of Jones,[3] Bleakney,[4] and Hummel,[5] succeeded in measuring this quantity for He, Ne and A as a function of electron velocities up to 4500 volts. In this work the experimental data seemed to be definitely approaching agreement with classical theory,[11] in that at high velocities the efficiency of ionization varied inversely with the energy of the impacting electron.

The problem has been treated theoretically on the basis of quantum mechanics by Ochiai[12] and Bethe,[13] who used Born's approximation method, and by Wetzel,[14] who calculated the effective ionization cross section specifically for helium, employing Born's collision theory (neglecting exchange phenomena). Of these three, only Bethe's work gives a definite formula for the efficiency of ionization as a function of the energy of the impacting electron, the ionization potential of the atom under investigation, and other definitely known or theoretically derived constants. Bethe's results, applicable only to the case of cathode rays having kinetic energies large in comparison with the ionization energy, predicts an inverse relationship between the efficiency of ionization and the energy of the impacting electron, the latter factor multiplied, however, by a logarithmic term involving the energy of the incident electron.

It was found that Bethe's theory agreed quite closely with Smith's results. The data, however, were not carried to high enough voltages to distinguish clearly between the classical and Bethe's theory. It was, hence, considered desirable to design an apparatus especially suited for high velocities and to extend the measurements to as high voltages as possible.

During the course of Smith's investigations on mercury vapor, he observed that for velocities greater than 750 volts, the measured efficiency depended on the magnetic field used to define the electron beam. This effect was peculiar to Hg vapor only and was thought to be due to large angle scattering from the heavy Hg atom; the scattered electrons presumably striking the ion collector plate and emitting secondary electrons or in some other manner affecting the ion current being measured. The ion collector, in the apparatus to be described later, was designed to eliminate this difficulty by making it impossible for the scattered electrons to reach the collector

[1] Compton and Van Voorhis, Phys. Rev. **26**, 436 (1925).
[2] Compton and Van Voorhis, Phys. Rev. **27**, 724 (1926).
[3] T. Jones, Phys. Rev. **29**, 822 (1927).
[4] W. Bleakney, Phys. Rev. **34**, 157 (1929); **35**, 139 (1930).
[5] A. D. Hummel, Thesis, University of Illinois (1928).
[6] A. von Hippel, Ann. d. Physik **87**, 1035 (1928).
[7] W. P. Jesse, Phys. Rev. **26**, 208 (1925).
[8] Hughes and Klein, Phys. Rev. **23**, 450 (1924).
[9] H. Funk, Ann. d. Physik **4**, 149 (1930).
[10] P. T. Smith, Phys. Rev. **36**, 1293 (1930); **37**, 808 (1931).
[11] J. J. Thomson, Phil. Mag. **23**, 449 (1912).
[12] K. Ochiai, Proc. Phys. Math. Soc. Japan **11**, 43 (1929).
[13] H. Bethe, Ann. d. Physik **5**, 325 (1930).
[14] W. W. Wetzel, Phys. Rev. **44**, 25 (1933).

or at any rate to correct for this effect if it persisted.

The object of the present investigation was thus twofold; first, to investigate ionization efficiencies of He at higher velocities than had previously been done, and second, to extend the measurements on Hg vapor to as high velocities as possible.

Apparatus

The apparatus, shown in Fig. 1, was constructed entirely of copper. The parts were baked out in a quartz furnace at approximately 850°C until no further gas emission could be detected. The apparatus was then assembled as shown, and placed in a Pyrex tube having no wax or ground glass joints. Pyrex and mica insulation was used throughout. After sealing the system to a two-stage Hg diffusion pump, the apparatus was again baked out at approximately 425°C until no further gas emission could be detected.

The electron gun

The essential details of the electron gun are shown in Fig. 1. The filament F was made of fine tungsten wire and was placed about 1 mm from the plate P_1. The latter was connected to the shield S and had a hole (S_1) 1 mm in diameter at its center. The holes S_2 and S_3 were about 2 and 3.5 mm in diameter, respectively. The remaining slits S_4–S_{14} were identical with S_3 in diameter. The plates P_2–P_{14}, across which the high potential was to be applied, were separated by pieces of Pyrex tubing (3 mm long) whose ends had been ground and had graphite rubbed over them. The surface of each separator was similarly treated. No attempt was made to insure absolute uniformity of resistance, but since three such separators, chosen at random, were used between each pair of plates, it was found that the resistance between any pair of plates was fairly constant. The total resistance was of the order of 10^9 ohms. A more or less uniform potential gradient from P_2 to P_{14} was thus the result when a high potential was placed across these plates.

The ion collector

Fig. 2 shows a cross section taken through the analyzing region and giving details of the ion collector.

The plates P_L and P_U were supported at their ends by small Pyrex insulators placed in plates P_{14} and P_{15}. The guard "rings" G_1 and G_2 were fastened to P_U and insulated from it by a strip of mica. The collector itself (C_i) was supported by G_1 and G_2 only and was insulated from them by another strip of mica. The slit in the plate P_U was 2 mm wide and about 5 cm long.

The collector was designed to collect only those ions formed in (or very near to) the electron beam. In practice, a small P.D. (3 volts) was placed between P_L and P_U to draw any positive ions formed in the electron beam through the slit in P_U. Another small P.D. (3–4.5 volts) was placed between C_i and P_U, so that any ions which had passed through the slit in P_U would be further attracted toward the ion collector, C_i.

It was realized from the outset that this method would not yield absolute values for the efficiency, but that only relative values could be measured. Since, however, any method for measuring absolute values would leave the ion collector subject to secondary or scattered electron impacts, it was considered best to avoid this and to measure relative values only. By "match-

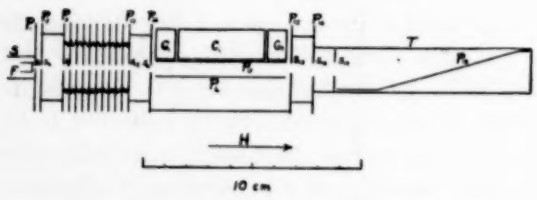

Fig. 1. Diagram of apparatus.

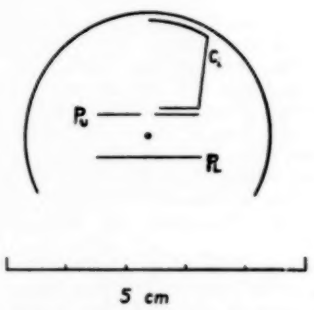

Fig. 2. Details of ion collector.

ing" Smith's curves it would then be possible to obtain absolute values for the efficiency. It was recognized also that this method assumed that the same fraction of the total number of ions produced would be collected at all electron velocities. That this assumption was valid was indicated by the extremely close agreement between Smith's and the writer's data on He (see Fig. 5).

The magnetic field

A solenoid about 40 cm long was used to develop a magnetic field parallel to the axis of the apparatus. The magnetic field aided in separating the ions and electrons and also defined the primary electron beam.

General method of procedure

A complete wiring diagram of the apparatus is given in Fig. 3. The filament battery V_f and the two batteries V_{c_1} and V_{c_2} were placed on an

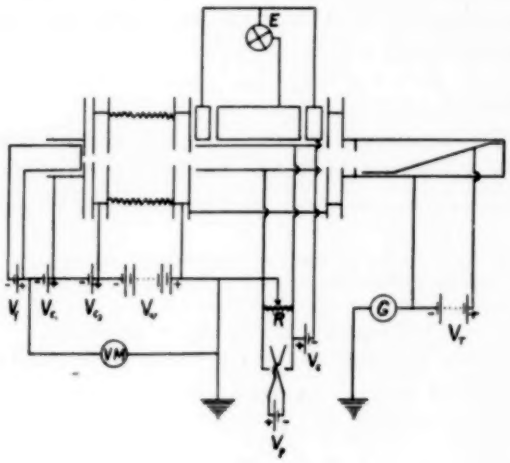

FIG. 3. Wiring diagram.

insulating stand, and once the best working conditions had been found, were left unchanged. The velocity of the electrons was varied by changing V_v. A Weston 750 volt range megohm voltmeter (VM), (with megohm resistors in series) was used to measure the velocity of the electrons over the entire range studied.

Potentials as high as 5500 volts could be obtained from the high potential bank of batteries in this laboratory. For the higher voltages a high tension transformer set, full wave rectified by means of two kenotrons and containing a capacitance of 0.5 microfarad, was built. It was found that below approximately 3 kv, the ripple in the voltage was appreciable, as judged by comparing data obtained with batteries and those obtained with the rectified transformer set. The effect, of course, became more noticeable the lower the voltage. At voltages between 3 kv and 5.5 kv, however, the efficiency measurements were identical, within experimental error, regardless of the source of high potential. It was felt that this check, over a range of 2.5 kv, justified the use of the transformer set in extending the work to higher voltages.

Another feature of the collector which merits description is the manner in which the ion current to C_i can be corrected for scattered or secondary electron effects if they persist. In Fig. 2, if the direction of H (the magnetic field) be taken up out of the plane of the paper, then a positive ion moving from P_L toward P_U will be deflected toward C_i (after passing through the slit in P_U). Only those electrons which are scattered through the slit in P_U and which possess energies of several thousand volts, have any chance whatever of reaching C_i. Those scattered through P_U but having smaller energies will be bent away from C_i, while those scattered in other directions, regardless of their energies, will not reach C_i. If the field between P_U and P_L is reversed, no ions will reach C_i, since they will be drawn toward P_L. The reversal of this small field, however, will have virtually no effect on the paths of the high speed scattered electrons mentioned above. Hence any current to C_i observed with the field thus reversed would give identically the effect of scattered electrons on the measured ion current and, as such, could be subtracted from it as a correction factor.

The electron trap

The only modification introduced in this part of the apparatus, was an increase in the length of the conventional electron collector and the use of higher potentials to draw the electrons toward P_{1s}. In practice, about 700 volts was applied between the plate P_{1s} and the case (T) of the trap.

The ion current was measured by means of a Compton type electrometer (sensitivity 1400 mm per volt). A series of shunts, ranging in resistance from 5×10^7 to 4×10^9 ohms, were used with the electrometer. As a result, the ion currents at almost all voltages could be measured without appreciably altering the electron current density. The electron current to the trap was measured with a galvanometer G having a sensitivity of 13,500 megohms. The potential V_t was furnished by a set of well insulated B batteries.

As was expected, it was found impossible to obtain saturation currents to C_i with reasonable voltages between P_L and P_U. Since, however, the method was designed to give relative values only, it would be sufficient if the relative values, (with reasonable potential differences V_p and V_e), were to agree. Early tests made by varying both V_p and V_e between 3 and 6 volts (all combinations) showed this to be the case. Since $V_p=3$ volts and $V_e=4.5$ volts seemed to give the most consistent results, these values were used in most of the work.

Preliminary tests also showed that, in order to obtain consistent results, especially at the highest electron velocities, V_t had to be approximately 700 volts.

Results

Mercury vapor

The results for mercury vapor at low voltages are shown in Fig. 4. The ordinates ϵ represent the number of positive charges formed per electron per cm length of path per mm pressure at 0°C. Smith's values are also given, the writer's relative measurements being reduced to Smith's absolute values by "matching" the two maximum values for ϵ. The agreement is seen to be close except for voltages below approximately 60 volts. The lack of agreement in this range is not thought to be significant since the present apparatus was not designed for measurements at these low velocities. The results at the higher velocities are shown in Fig. 5.

The results are also tabulated in Table I. In all cases, the results given are the mean of several sets of readings taken at different pressures and different electron current densities. The form of the curve was identical for all conditions, and relative values could be checked at all voltages to within 2 percent. It should also be mentioned that the data were found to be independent of the magnetic field over the entire voltage range investigated.

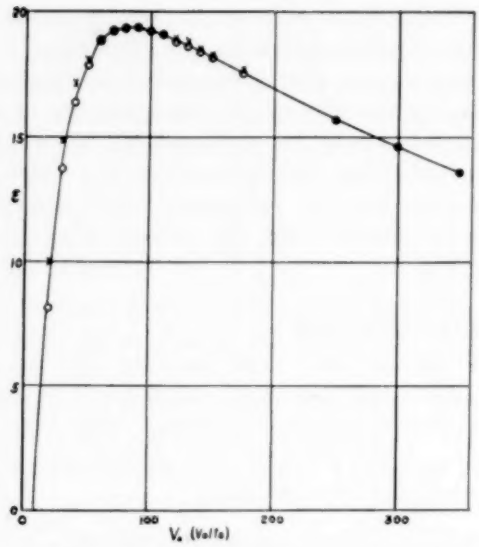

FIG. 4. Efficiency of ionization of mercury vapor plotted as a function of V_a. The circles are Smith's absolute values; crosses are the writer's reduced values.

Helium

The results for helium are given in Fig. 5 and also tabulated in Table I. Since exceptionally close agreement was found between the forms of

TABLE I. *Values of ionization efficiencies in mercury and helium in ions per cm path per mm pressure at 0°C.*

	Mercury Vapor		*Helium*	
V_a	ϵ (Smith)	ϵ (Writer)	ϵ (Smith)	ϵ (Writer)
100	19.25	19.32		
200	16.90	17.00		
300	14.60	14.62		
400	12.55	12.80		
500	11.05	11.29		
600	9.88	10.13		
700	8.90	9.32		
1000		7.30		
1500		5.55		
2000		4.50		
2500		3.80	0.215	0.215
3000		3.35	.183	.181
3500		2.95	.162	.160
4000		2.62	.142	.140
4500		2.37	.127	.128
5000		2.10		.115
6000		1.76		.0945
7000		1.48		.0806
8000		1.28		.0700
9000		1.14		.0624
10000		1.03		.0565
11000		.940		.0520

Smith's and the writer's curves, over the range 2.5 to 4.5 kv, no attempt was made to measure efficiencies below 2.5 kv, as it was felt that Smith's apparatus, which was better suited for study in this range, had furnished all the data necessary.

The data for helium given in Table I and plotted in Fig. 5, represent the mean of several sets of data, taken with different tube conditions. The form of the curve, representing relative values of ϵ was again reproducible within about 2 percent.

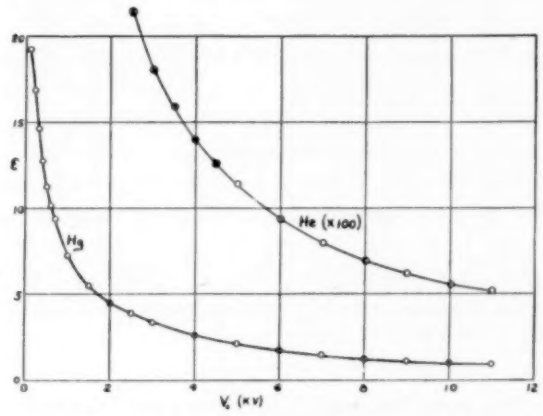

FIG. 5. Efficiency of ionization of He and Hg at high voltages. For Hg, the scale factor was obtained from Fig. 4. For He, the crosses are Smith's absolute values; circles are the writer's reduced values.

DISCUSSION AND COMPARISON WITH THEORY

Several theories for the efficiency of ionization of gases have been advanced. The first of these, developed by J. J. Thomson,[11] and based on classical mechanics, yielded a formula of the form

$$\epsilon_T = [n\pi e^2(300)^2/V_i^2](1-U^{-1})/U, \qquad (1)$$

where

$$U = V/V_i \qquad (2)$$

is the ratio of the tube voltage V to the minimum ionizing voltage V_i (each expressed in volts), e is the electronic charge and n is the number of atoms per cc reduced for the sake of comparison to 1 mm pressure, i.e.,

$$n = (2.7\times10^{19})/760 = 3.55\times10^{16}. \qquad (3)$$

Although the theory predicts an absolute value for the efficiency of ionization, calculation shows that for large values of U, it predicts values considerably smaller than those experimentally determined. Furthermore, the Eq. (1) has its maximum value when $V=2V_i$ or $U=2$. For helium the experimentally determined maximum falls at the point $U=4.5$.

Since the theory is based on the assumption that the electrons in the atom are at rest, the disagreement at low values of U is not unexpected. For large values of U, however, the theory would be expected to give at least the general form of the curve, i.e., relative values. Eq. (1) reduces to

$$\epsilon_T = n\pi e^2(300)^2/V_i^2U \qquad (4)$$

for large values of U. This can be written in the form

$$\epsilon_T = K_{He}/U, \qquad (5)$$

where

$$K_{He} = n\pi e^2(300)^2/(24.5)^2 = 3.81 \qquad (6)$$

for helium.

Fig. 6 shows the experimental data for helium plotted as a function of $1/U$. It can be seen that for large enough values of U the experimental data agree in form with (5), within experimental error. The Thomson formula is thus seen to agree with experiment insofar as relative values are concerned, at least for large values of U. The absolute magnitudes predicted are, however, too small by a factor of about 6 at $U=450$.

N. Bohr[15] modified the Thomson formula somewhat by taking into account the ionization

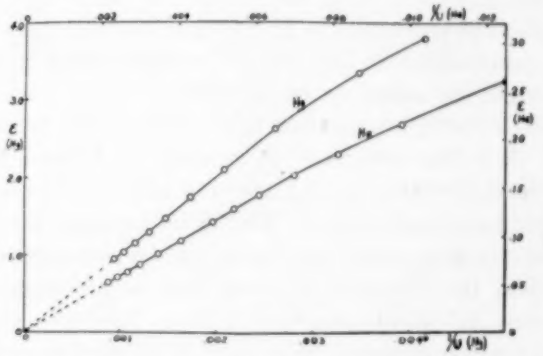

FIG. 6. Efficiency of ionization of He and Hg as a function of $1/U$.

[15] N. Bohr, Phil. Mag. 30, 581 (1915).

produced by the electrons expelled from the atom by the primary ionizing electron. On the assumption that V_i has the same value for all the electrons in the atom, he obtained

$$\epsilon_1 = [n\pi e^2(300)^2/VV_i] \ln V/V_i. \qquad (7)$$

If, however, the different electrons in the atom are assumed to have different ionization potentials, then, for values of V, large compared with any V_i,

$$\epsilon_2 = \frac{n\pi e^2(300)^2}{VV_i} \sum_{r=1}^{m} \ln \frac{V}{(V_i)}. \qquad (8)$$

Bohr pointed out that because of the simplifying assumptions made, the most that could be claimed for Eq. (8) was that it would give an upper limit for the ionization. For an atom with a single shell, such as helium, Eq. (7) is applicable. The results for helium, calculated from Eq. (7) are shown in Fig. 7. It is seen that the data agree very well with experiment, for large values of U. The agreement, moreover, is absolute and not merely relative. This absolute agreement, however, is thought to be only accidental. The lack of agreement at low values of U is undoubtedly due (at least in part) to the fact that the theory takes no account of multiple ionization. No quantitative data are available as to the amount of current carried by doubly charged helium ions, though Bleakney[16, 17] estimates that less than one percent of all the helium ions formed were doubly charged (at electron velocities of several hundred volts). This would account for at most two percent of the disagreement at low values of U. The fact that the theory agrees well with experiment at large values of U might be taken to be an indication that very little multiple ionization takes place in this range.

It is thus seen that the two solutions based on classical theory agree fairly well with experiment for large values of U. The Bohr formula, however, agrees with experiment over a larger range than the Thomson formula and in addition is seen to yield absolute values, whereas the Thomson equation leads only to relative magnitudes.

[16] W. Bleakney, Phys. Rev. **36**, 1303 (1930).
[17] W. Bleakney, Phys. Rev. **35**, 139 (1930).

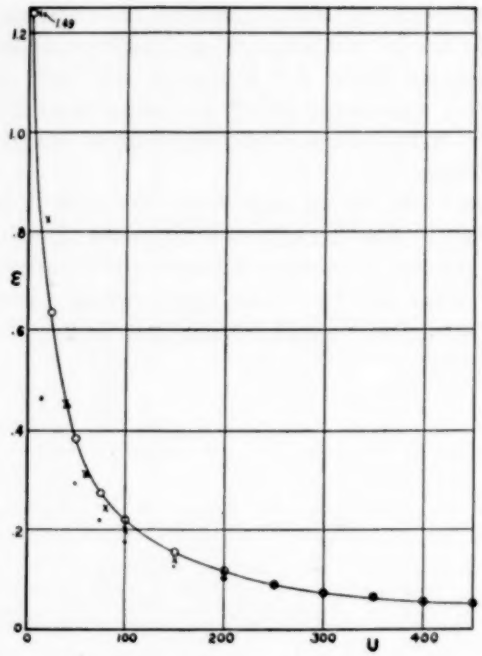

FIG. 7. Comparison of theory with experimental data on He. The circles are experimental values; crosses are values calculated from Bethe's formula; dots are calculated from Bohr's formula.

The most successful theories based on wave-mechanical theory are those by Bethe[13] and Wetzel.[14] Wetzel calculated the effective cross section for ionization of helium. His results checked Smith's values quite closely, in absolute magnitude, for small values of U. For values of $V > 300$ volts, however, the calculated curve fell below the experimental curve. Wetzel's results, which were carried to $V = 500$ volts, were obtained by numerical integration, hence no further comparison with this work is possible.

Bethe's work yielded an equation for hydrogen which can be written

$$\epsilon_B = \frac{n\pi e^2(300)^2}{V_i^2}\left(\frac{2b}{U}\right) \ln \frac{4U}{B}, \qquad (9)$$

where b and B are two constants, approximate theoretical values for which are given. The value 0.048 is given for B for hydrogen while for b the value unity is listed for hydrogen and beryllium. The constant B is further described as being of the order of magnitude of unity for elements in which the K shell is well buried. For more

complicated atoms, Bethe's formula takes the form

$$\epsilon_0=\sum\epsilon_l=\frac{n\pi e^2(300)^2}{V}\sum\frac{C_lZ_l}{(V_i)_l}\ln\frac{4V}{B(V_i)_l}, \quad (10)$$

where

$$\epsilon_l=\frac{n\pi e^2(300)^2}{V}\frac{C_lZ_l}{(V_i)_l}\ln\frac{4V}{B(V_i)_l} \quad (11)$$

is the efficiency of ionization of the lth shell, $(V_i)_l$ is the ionization potential of the electrons in the lth shell, C_l is a constant whose value is a function of the particular shell in question, and Z_l is the number of electrons in the lth shell.

The simple form of Bethe's theory, Eq. (9) can be applied to helium for the same reasons that the simpler Bohr equation was used to calculate results in helium.

Since only approximate values for the constants are given, the most that can reasonably be expected from Eq. (9) is a check on the general form of the curve. Webster, Hansen and Duveneck[18] show curves comparing Smith's data on helium with values calculated from Eq. (9). The writer, using the same values for the constants b and B, is unable to check their results in absolute magnitude. For example, their curve shows $N\Phi_B(U)=\epsilon_B=0.280$ at $U=80$, whereas, substitution in (9) yields $\epsilon_B=0.840$ when $U=80$, $b=1$ and $B=0.048$. If Bethe's values for B and b are used, the calculated values of ϵ_B are too low by about 2 percent at $U=450$. It seems best thus, to use a comparison between (9) and experiment to determine the best values of these constants.

If the hydrogenic value for B (0.048) is used, and relative values are matched at $U=450$, then from (9)

$$b=\frac{\epsilon_BU}{2K_{\text{He}}\ln 4U/0.048},$$

where

$$K_{\text{He}}=\frac{n\pi e^2(300)^2}{(24.5)^2}=3.81$$

or

$$b=\frac{0.052\times450}{2\times3.81\times10.520}=0.291.$$

[18] Webster, Hansen and Duveneck, Phys. Rev. **43**, 839 (1933).

The results obtained by calculating ϵ_B from Eq. (9) with $b=0.291$ and $B=0.048$, are shown in Fig. 7. It is seen that the theory agrees with experiment surprisingly well except for low values of U, where it predicts results much too high. The disagreement for low values of U is not considered a serious defect in the theory, since the approximations made in the theory probably become invalid in this region. It should be noted that an increase in B from 0.048 to 0.500 reduces the values of ϵ_B at low U's, but causes the curve at intermediate U's to dip farther below the experimental curve than does the curve shown in Fig. 7. The "hydrogenic" value for B is hence probably close to the proper value of B for helium.

In Fig. 6 are shown the results in mercury vapor. From the shape of the curve for large values of U, it is seen that the data agree with the Thomson classical theory in form (see Eq. (5)). The numerical disagreement is similar to that found in helium, i.e., predicted results are much too small at large values of U.

For such a complicated system as the mercury atom, the calculation of either Bohr's Eq. (8) or Bethe's Eq. (10) becomes extremely laborious. In view of the fact that the ionization potentials of the electrons in the inner shells are only approximately known, a rigorous calculation of (10) is hardly practicable. A fairly close approximation to Eq. (10) can be obtained, for large values of U, from the following considerations. For values of V large compared with any V_i, (for which the ionization is appreciable), the logarithmic factors change only slightly and hence, to a first approximation, may be considered constants. Eq. (10) thus becomes

$$\epsilon_0=\frac{n\pi e^2(300)^2}{V}\sum\frac{C_lZ_l}{(V_i)_l}k, \quad (12)$$

where $k=$ constant for large values of V.

Furthermore, each V_i can be written as a constant times the first ionization potential, so that

$$\epsilon_0=\frac{n\pi e^2(300)^2}{V}\sum\frac{C_lZ_l}{\alpha_lV_i}k,$$

or

$$\epsilon_0=\frac{n\pi e^2(300)^2}{VV_i}\sum\frac{C_lZ_l}{\alpha_l}k.$$

and hence

$$\epsilon_0=(K_{Hg}/U)\sum(C_lZ_l/\alpha_l)k, \qquad (13)$$

where

$$K_{Hg}=n\pi e^2(300)^2/(10.4)^2. \qquad (14)$$

Comparing Eqs. (13) and (9) it is seen that they have essentially the same form if the factor $2b$ in (9) is written

$$\sum C_lZ_l/\alpha_l=2b \qquad (15)$$

and if

$$k\geqq\ln 4U/B. \qquad (16)$$

A suitable choice for the constant b in (9) should therefore yield a close approximation to (10), (for large values of U), for even as complex an atom as mercury. If Bethe's approximate value for B $(=1)$ is used, and if the values of ϵ are matched at the maximum U, then

$$\sum\frac{C_lZ_l}{\alpha_l}=2b=\frac{\epsilon U}{K_{Hg}\ln 4U}=5.64,$$

where $\epsilon=0.940$, $U=1057$ and

$$K_{Hg}=K_{He}(24.5/10.4)^2=21.1.$$

The large value of b obtained in this manner must be considered to be the sum of a large number of b's, each one probably less than unity.

The calculated values of ϵ_B, with $b=2.82$ and $B=1$ are shown in Fig. 8. Considering the approximations made, it is felt that the agreement is surprisingly good and hence that the theory, at least for large values of U, is quite accurate.

The agreement at high values of U and the disagreement at low values of U is of exactly the same type as that found in helium. Again, it should be noted that an increase in B would lower the values of ϵ_B at low U's but would cause the curve to drop further under the experimental curve for intermediate U's. The choice $B=1$ thus apparently gives almost as good a fit as can be obtained.

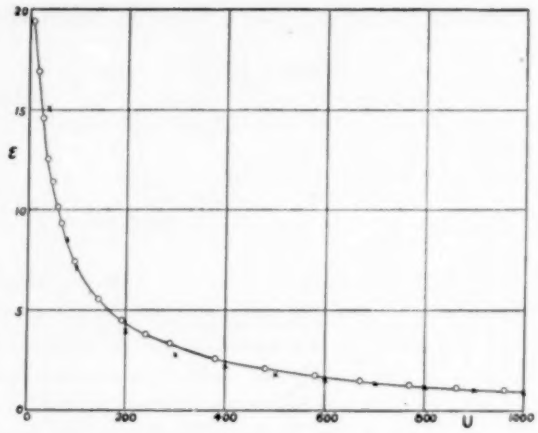

FIG. 8. Comparison of theory with experimental data on Hg. The circles are experimental values; crosses are calculated from Bethe's formula.

Reviewing the evidence presented, it is seen that the wave-mechanical solution of the problem yields results which agree with experiment over a considerably larger range of velocities than the classical solutions. Refinements in theory are still necessary, however, in order to bring theoretical values into agreement with experiment at low values of U.

In conclusion, the writer wishes to take this opportunity to express his gratitude to Dr. J. T. Tate, who suggested the problem and whose constant and keen interest during its solution was an inspiring aid. Thanks are also due to Dr. P. T. Smith for many helpful and interesting discussions during the course of the work. It is a pleasure too, to acknowledge with thanks, the assistance and suggestions of Messrs. C. H. Dane, E. Greinke and W. B. Haliday.

A Direct Experimental Test of the Principle of Spectroscopic Stability

OTTO HALPERN, *New York University*,
AND
EM. WASSER, *Leningrad*

(Received December 11, 1933)

The spectroscopic stability required by quantum mechanics is subjected to a direct test, and it is demonstrated that the atoms of saturated thallium vapor exhibit no double refraction due to spatial quantization in a magnetic field up to 1200 gauss. The accuracy of the measurement permits of the assertion that if present at all the phase-difference between the component of the electric vector at right angles and that parallel to the field, is less tha 10^{-4} of the wave-length employed. At the pressures employed this establishes a constancy of atomic refractivity to one part in 10^4.

I. STATEMENT OF PROBLEM

ACCORDING to the old Bohr theory one expects hydrogenic atoms to exhibit spatial quantization in magnetic fields however weak. This spatial quantization has been directly demonstrated by deflection experiments in an inhomogeneous magnetic field and Stern[1] surmised that it should also become observable by the occurrence of double refraction in a magnetic field. The essential feature of this double refraction effect should be found in the fact that it would occur even at a very small value of the field strength and would be substantially independent of its magnitude. Various attempts at demonstrating the effect have been undertaken by a number of authors, but with negative results in every case. R. Fraser[2] and W. Schuetz[3] observed the variation of the index of refraction for various gases in a longitudinal and in a transverse magnetic field. The work of W. Schuetz is notable for the high degree of sensitivity achieved. It should have permitted the observation of a phase difference of 10^{-4} of the wave-length, but no sign of anisotropic behavior could be ascertained.[4]

The result to be expected from the point of view of the new theory of quantum mechanics is fundamentally different from that to be expected on the basis of the old Bohr theory. The principle of spectroscopic stability, introduced originally with the help of the correspondence principle, is derivable from the fundamental equations of quantum mechanics. The negative result of these tests is therefore, in the light of the new theory, entirely to be expected, although in the particular case of Na and the other gases tested the experiments cannot be considered as testing spectroscopic stability since the orbital properties of S terms are spherically symmetrical.

The matter takes on a different aspect for atoms having no S term in the normal state. In this case according to the picture given by the old theory of quantum mechanics optical anisotropy is to be expected, while according to the new theory the principle of spectroscopic stability implies the absence of double refraction.

In the experiments described here Tl-atoms in $6p_1$ states were used. The atomic refractivity was found to be constant to within 1 part in 10^4 in fields as high as 1200 gauss. These experiments may be regarded as proving the validity of spectroscopic stability directly because the orbital wave functions have an angular dependence.

II. ARRANGEMENT OF THE APPARATUS

In its normal state $6p_1$ Tl absorbs the lines of the sharp and the diffuse series which lie in the ultraviolet. This fact is very favorable to the investigation of double refraction remote from the points of anomalous dispersion. In the visible range the known green thallium line 5350.46A appears only at higher temperatures, when sufficient atoms have been brought to the somewhat higher state $^2p_1$. By the employment

[1] O. Stern, Zeits. f. Physik **7**, 249 (1921).
[2] R. Fraser, Phil. Mag. **1**, 885 (1926).
[3] W. Schuetz, Zeits. f. Physik **38**, 853 (1926).
[4] For analogous tests in the field of gas kinetics, which are likewise negative in result, cf. for instance A. Sommerfeld, *Wave Mechanics*.

of a suitable light filter in the visible range it becomes readily possible to separate the phenomena attendant on anomalous dispersion in the magnetic field from the double refraction sought for.

For the purpose of the present tests a commercial preparation (Kahlbaum) was employed. The only impurities were slight traces of lead. The material was degassed by repeated heating in a high vacuum, but no further purification was carried out.

The arrangement of the apparatus is shown in Fig. 1. The first observations were taken with

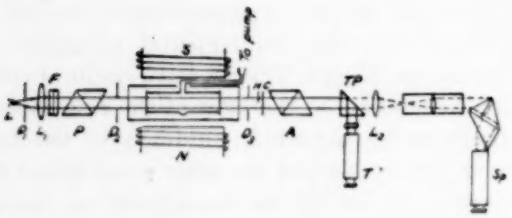

FIG. 1. L = source of light; D_1, D_2, D_3 iris diaphragms; L_1, L_2 lenses; F, filter; P, polarizer; N, S poles of magnet; H, half-shadow plate; C, compensator plate; A, analyzer; TP, totally-reflecting prism; T, telescope; Sp, spectrograph.

monochromatic light. The source of light employed was a quartz bulb mercury vapor point-light lamp of high intrinsic brilliancy the light from which was made monochromatic by a Zeiss filter. This filter lets through 80 percent of the green Hg line while it absorbs all but 0.003 percent and 0.1 percent, respectively, of the blue and yellow lines. The pencil rays emitted by the lamp are rendered parallel by a lens of great focal length, and limited by a number of iris diaphragms arranged in series.

In the experiments two absorption chambers of transparent quartz having plane-parallel windows fused on without strains were employed. Both quartz tubes were 1 cm in diameter; the one used at the start was 20 cm, the other 15 cm long. They were connected with the pumping device by means of ground joints. In this manner the diffusion of the thallium vapor from the absorption vessel was prevented.

In order to be able to produce any desired pressure of the saturated thallium vapor, the absorption tube was inserted in a two-part electric furnace consisting of a fire-brick tube about which a nickel-chromium strip was non-inductively wound; this eliminated the influence of longitudinal magnetic fields. Since the furnace was twice as long as the absorption vessels and was, moreover, well insulated against loss of heat, the temperature could be maintained fairly constant through the length of the vessels. The measurements were made at temperatures from 600°C to 950°C as measured by means of a thermocouple. This range of temperature corresponds to a variation in the vapor pressure of thallium from 0.05 to 10.5 mm Hg.

For the detection of double refraction there was employed a highly sensitive Brace half-shadow compensator constructed by the writers following Szivessy.[5] Since the principle of this apparatus has been amply described elsewhere, it is sufficient to refer briefly to the peculiarities of the half-shadow compensator here employed. The half-shadow and the compensator plates were each connected to a vernier and could be rotated independently in their respective planes. The accuracy of reading amounted to 1/3 minute. The compensator plate was made up of two mica leaves which were cemented between two plates of glass. Its retardation for Na light was 0.045λ. The half-shadow plate was composed as follows: A thin sheet of mica with a retardation of 0.020λ for Na light, was used to cover one-half of the field of vision of 10 mm diameter; the necessary weak double refraction was produced by means of a rectangular cover glass plate of 0.1 mm thickness which could be pressed parallel to two edges. In this manner any desired double refraction of the cover glass plate could be produced, and the sensitivity of the apparatus could be increased to some three times that obtainable with the use of the mica half-shadow plate. The adjustment of the apparatus was made as follows. The two nicols were first crossed, the direction of oscillation of the polarizer being inclined 45° to the horizontal magnetic field. The half-shadow plate was then inserted, and its direction of oscillation likewise turned to 45° with reference to the zero azimuth of the analyzer. This could be approximately done by turning the half-shadow plate in its plane until the two halves of the field of vision

[5] G. Szivessy, Zeits. f. Physik **6**, 311 (1931).

showed the strongest contrast in brightness. The more accurate adjustment could then be carried out after the insertion of the compensator plate. If this latter be rotated through 360° in its plane, the whole field of vision is darkened four times. For the angle of rotation of the compensator from the zero azimuth the following relation is valid:[5]

$$2\alpha = \pi/2 - (p_2 - p_1) = (p_3 - p_2) - \pi/2$$
$$= \pi/2 - (p_4 - p_3) = (p_1 - p_4) - \pi/2,$$

in which p_1, p_2, p_3, p_4 represent the readings on the arc of the compensator in the four half-shadow positions. The equality of the angle 2α, as calculated from the four readings, is a criterion for the correct setting of the half-shadow plate.

The beam of light emerging from the analyzer fell, as can be seen from Fig. 1, on a totally reflecting prism, and was here deflected into a telescope mounted at right angles to the direction of the beam, and accurately focussed on the limiting edge of the half-shadow plate. It was possible, by rotation of the totally reflecting prism, to throw the beam of light on the slit of a spectrograph. In this manner it was possible to keep a check on the composition of the light traversing the absorption chamber, and more particularly to detect the occurrence of any absorption lines. The spectrograph with a direct wave-length scale employed for this purpose was a Hilger instrument which separated the *D*-lines by about 1 mm.

The magnetic field was produced by a magnet built in the laboratory with poles of circular cross section 20 cm in diameter. The spacing of the poles had to be increased to 4.6 cm in order to accommodate the electric furnace, for which reason the maximum field strength obtainable was 1200 gauss. The poles of the magnet were fixed at this distance from each other by means of brass spacers since it was found that otherwise the poles approached each other by a few millimeters when the current was switched on. In spite of the wide spacing of the poles, the homogeneity of the field except for small distances from the edge was maintained by the large superficial area of the poles.

A vacuum of 10^{-5} mm Hg was maintained during the experiments by means of a rotary oil pump in series with a mercury vapor pump.

III. Experimental Results

In order to ascertain empirically the sensitivity of the half-shadow arrangement for the detection of double refraction, the Cotton-Mouton effect was observed with benzene. For this purpose benzene (specially refined for molecular weight determination) was placed between the poles of the magnet in a 15 cm tube with plane-parallel windows. The double refraction in the transverse magnetic field corresponded to a rotation of the compensator plate through 7 minutes. From the relation $\Delta = (\sin \varphi / \sin 2\beta)(\sin 2\alpha' - \sin 2\alpha)$ there resulted for the phase-difference of movement of the components of the electric vector oscillating at right angles to and parallel to the magnetic field, respectively, the value $5.9 \times 10^{-6}\lambda$($\lambda = 5461$A), or for the difference $n_1 - n_2$ in the refractive indices the value 2.2×10^{-10}. In the formula just given φ denotes the retardation of the compensator plate, β the azimuth of the half-shadow plate (in the present instance $\beta = \pi/4$), α and α' the azimuths of the compensator plate without and with the magnetic field. Since, as above mentioned, the readings of the arc were accurate to 1/3 minute, the error in the above value is presumably about 5 percent. Now in the calibration just performed the difference in intensity between the two halves of the field of vision was so great that a much smaller double refraction could have been detected with certainty. Thus a phase-difference of $1 \times 10^{-6}\lambda$ would be easily observable.

The saturated thallium vapor was first tested in monochromatic light of wave-length 5461A at temperatures varying between 600° and 800°C. Up to this latter temperature the thallium atoms are in the normal state; at all events the number of excited atoms present is negligibly small. The above-mentioned range of temperature corresponds to a pressure interval of the saturated thallium vapor of from 0.05 to 1.5 mm Hg. The absorption spectrum of thallium shows, at the temperatures mentioned, the lines of both subordinate series, starting from the lowest level $^2P_\frac{1}{2}$, and all lying in the ultraviolet. No absorp-

tion line appears in the visible range, up to about 800°C.

As proved by repeated measurements under the described conditions, *no double refraction of the thallium vapor could be ascertained within the given limits of sensitivity up to 800°C.* It should be noted that in the above experiments the magnetic field was varied through a wide range. Thus the effect of space quantization could not have been accidentally masked by effects due to a small longitudinal component of the magnetic field since this effect varies with the field while the double refraction looked for is independent of it.

As a check on the proper functioning of the apparatus we observed the magneto-optic effect in the neighborhood of 5350A. The effect was largest at about 850°C corresponding to a vapor pressure of about 4 mm Hg. It should be emphasized that this effect is not in contradiction to the principle of spectroscopic stability being just another form of anomalous dispersion.

Electron Scattering by Atomic Electrons

A. L. HUGHES* AND R. C. HERGENROTHER, *Washington University, St. Louis*

(Received June 13, 1934)

The velocity distributions of electrons scattered by helium atoms, at angles ranging from 10° to 60°, have been measured for electrons having energies of 800, 1000, and 1200 volts. The curves have a well-defined narrow maximum where the scattered electrons have the same velocity as the primary electrons, this being the well-known elastic scattering. In addition, for each angle of scattering, a single broad peak is superposed on the continuous distribution of velocities ranging from the maximum down to zero. This represents the inelastically scattered electrons. The position of each peak is such that the velocity corresponding to it, is given approximately by $v = u \cos\theta$, where u is the velocity of the electron before impact and θ the angle of scattering. This is the formula for the velocity of an electron when scattered through θ, by a free electron initially at rest. The inference is that we may associate these inelastic peaks with collisions between the incident electrons and the atomic electrons when the binding energy is small in comparison with the energy transfers during the collision. Jauncey's theory of the breadth of the modified line in the Compton effect is discussed in relation to the breadth of the inelastic peak, on replacing the photon by the incident electron.

INTRODUCTION

WHEN an electron is moving with a velocity u towards another electron, initially at rest, application of the principles of conservation of energy and momentum lead to the conclusion that if the first electron is deviated through an angle θ, its velocity will be given by $v_1 = u \cos\theta$, while that of the second electron will be given by $v_2 = u \sin\theta$, a result which implies that the two paths after collision are necessarily at right angles.[1] It is not possible to make a direct test of this result because of the difficulty of securing a sufficient density of free electrons. However, a close approximation to the ideal case is realized when a beam of beta-rays is passed through matter of low atomic number, a condition which insures that the binding energy of the atomic electrons may be neglected in comparison with the energy transfer involved during a collision. Experiments show that the beta-ray tracks in a Wilson cloud chamber are frequently forked and that the angle between the tracks is close to 90°.[2] This implies that the fork results from a collision between the beta-ray and an atomic electron, the nucleus playing no part. The beta-ray, because of its high speed, has to pass so close either to an atomic electron, or to the nucleus, in order to suffer an appreciable deflection, that the observed deflection can be attributed to a

* This investigation was made possible by a grant to the first named author from a fund given by the Rockefeller Foundation to Washington University for research in science.

[1] This follows easily from Eqs. (3) and (4) (given later) on omitting the binding energy.

[2] Rutherford, Chadwick and Ellis, *Radiations from Radioactive Substances*, p. 238 (Macmillan).

collision either with one or the other. If the beta-ray passes close to the nucleus, it is deviated without loss of velocity, but if it passes close to an atomic electron, it may go off in any direction θ with the reduced speed $u \cos \theta$, while the atomic electron recoils with the speed $u \sin \theta$. Thus the distribution of velocities of electrons scattered by such an idealized atom should, in principle, consist of just two groups of electrons, one having the full original speed u, and the other having the speed $u \cos \theta$. (Recoil electrons, with speed $u \sin \theta$, will of course be present.) Experimentally, it is found that, for electrons of moderate speed (say 100 to 2000 volts), the scattered electrons have a continuous distribution of velocities from a maximum down to zero. Renninger[3] investigated the distribution of energy of electrons scattered by nitrogen, neon, and argon, and found that the distribution of energy curves had very weak broad maxima at the energy $V_1 = V_0 \cos^2 \theta$, when the energy of impact V_0 was 2000 volts. The maxima disappeared completely for $V_0 = 500$ volts. The explanation is that, as the energy of the incident electron is diminished, it is more and more inaccurate to regard the nucleus and the atomic electrons as independent scattering centers. It becomes increasingly necessary to consider the complete atom as the scattering agent. Thus the scattering effect of an individual atomic electron, which is clearly shown for fast electrons by the 90° beta-ray fork referred to, is to be recognized with difficulty in Renninger's 2000 volt curves, and disappears completely from his 500 volt curves.

The purpose of the present investigation is to ascertain whether, with electrons of energy of the order of 1000 volts, the curves for the distribution of energies of electrons scattered at any selected angle, indicate effects which can be attributed to collisions between the incident electrons and the atomic electrons. The criterion is the presence of a maximum, at the energy value $V_1 = V_0 \cos^2 \theta$, in the energy distribution curve for electrons scattered at θ. Helium was chosen as the working gas because the energy of binding of its atomic electrons is very small and one would expect its electrons to approximate more to free electrons than the electrons in the gases investigated by Renninger. (Because of its lower ionization potential, hydrogen would probably show the effect more prominently than helium.)

[3] M. Renninger, Ann. d. Physik **9**, 295 (1931); **10**, 111 (1931).

Experimental Method

The apparatus is shown diagrammatically in Fig. 1. An electron gun, G, with slits 1 mm by 6 mm and 14 mm apart, is mounted so that it can be rotated about the center of a bulb which forms the collision chamber. The electron gun is attached to a support (not shown in the diagram) which is carried on a tungsten pivot in a side tube joined to the bulb so that the axis of

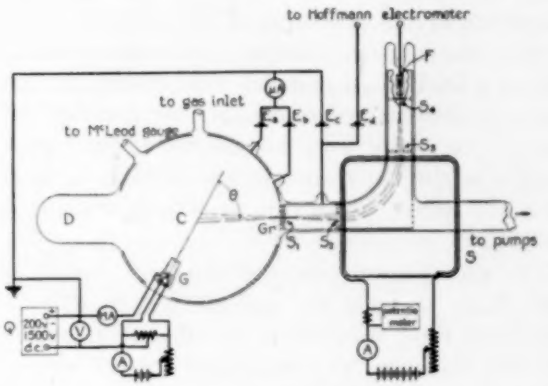

FIG. 1. Experimental apparatus.

rotation passes through C perpendicularly to the plane of the diagram. When the filament needs replacing, the electron gun is detached from its support and removed by cutting the side tube D. At the lower end of the support and sufficiently far removed from the collision center C, so as not to affect the electron paths, is a ring of soft iron. By means of an electromagnet which can be brought up from outside, the electron gun can be turned to any desired position. The bulb is lined with a layer of evaporated platinum, shown in the diagram by a thick line just inside the thin line representing the glass bulb. In front of the slit S_1 is a grid Gr made of fine platinum wires and connected to the outside by an independent lead. The angular width of the beam of electrons scattered at the collision center C,

into the analyzer, is defined by the slits S_1 and S_2 (0.20 mm by 6.0 mm, and 1.25 mm by 6.0 mm, respectively). The analyzer for separating out electrons of any desired velocity is of the new magnetic refocusing type recently described by Stephens.[4] For full details, the reader is referred to the paper cited. It is sufficient here to state that S represents the cross section of a square solenoid, and that S_1, S_2, S_3 and S_4 are the defining slits. The metal tube carrying the slits S_1 and S_2 fits the glass tube sufficiently well to insure that, because of the small dimensions of the slit S_1, a considerably lower pressure could be maintained in the analyzer than in the collision chamber. Helium, purified by passing it through charcoal in liquid air, is passed into the apparatus through a very fine capillary tube and pumped out continuously through the analyzer giving pressures of the order of 0.001 mm in the collision chamber. (On some occasions, when a fairly high pressure was needed, the gas was allowed to accumulate to the pressure desired.) As there were no greased ground glass joints in the apparatus, it was possible to bake out the whole apparatus at a temperature of 400°C.

As the electron gun, the platinum coating of the bulb, the grid *Gr*, and the slit S_1 with its carrying tube, were made of different materials, it was necessary to compensate for the various contact potentials to secure a really field-free collision region. This was secured by suitable voltages, provided by cell and potentiometer combinations represented by E_a, E_b and E_c. The correction was of course not so necessary for the high energies used in the investigation now reported as for the study of the much slower ejected electrons of energies below 5 or 10 volts, for which the apparatus was designed.

The high voltage d.c. supply unit, Q, which was used in place of B batteries had unusually good regulation. The ratio of the variation in the output voltage to that in the input voltage (about 110 volts) was 1 to 50, and the ratio of the variation in the output voltage to that in the load, at the load for which the unit was designed, was 1 to 1000. We are much indebted to Mr. O. H. A. Schmitt for designing the unit, an account of which will be published later.

[4] W. E. Stephens, Phys. Rev. **45**, 513 (1934).

The earth's magnetic field, in the vicinity of the apparatus was neutralized by a pair of Helmholtz coils. The current around the solenoid was measured by a potentiometer method, as in many cases a change of 0.1 percent in the magnetic field deflecting the electrons made a considerable change in the electron currents passing through the slit S_4 to the Faraday cylinder F. These electron currents were measured by a Hoffmann electrometer. (A battery, E_d, provided a retarding potential between F and S_4, when necessary for certain measurements.)

The experimental procedure was to set the electron gun so that the analyzer would accept the electrons scattered at a selected angle θ. Then by varying the deflecting magnetic field step by step, the distribution of velocities among the scattered electrons could be measured.

Results

The values of the electron currents to the collector in the analyzer are plotted as functions of the current, I_H, producing the deflecting magnetic field, for various angular settings of the electron gun. The values have been adjusted so that they all refer to the same gas pressure and to the same electron current from the gun. The usual correction for the change in length of the scattering path with θ has been made by multiplying the experimental values by the corresponding sin θ.

The curves obtained can be converted into true velocity distribution curves by dividing each ordinate by the numerical value of I_H. This comes about from the fact that the range of velocities, δv, accepted by the analyzer increases linearly with v (or I_H). It is well known in the technique of beta-ray analysis that this applies to the *continuous* spectrum of velocities, but does not apply to a *line* spectrum. For our present purpose, however, it is unnecessary to make this correction.

The various curves, assembled in Figs. 2, 3 and 4, are arranged so as to show the progressive shift in the positions of the inelastic peaks as the angle of scattering is increased from 11.9° to 31.9°. The magnitude of the scattered electron currents may be inferred from the scale alongside each curve. Figs. 5, 6 and 7, complete the results so far obtained. On account of the small scattered currents at these large angles the measurements were difficult. However these three

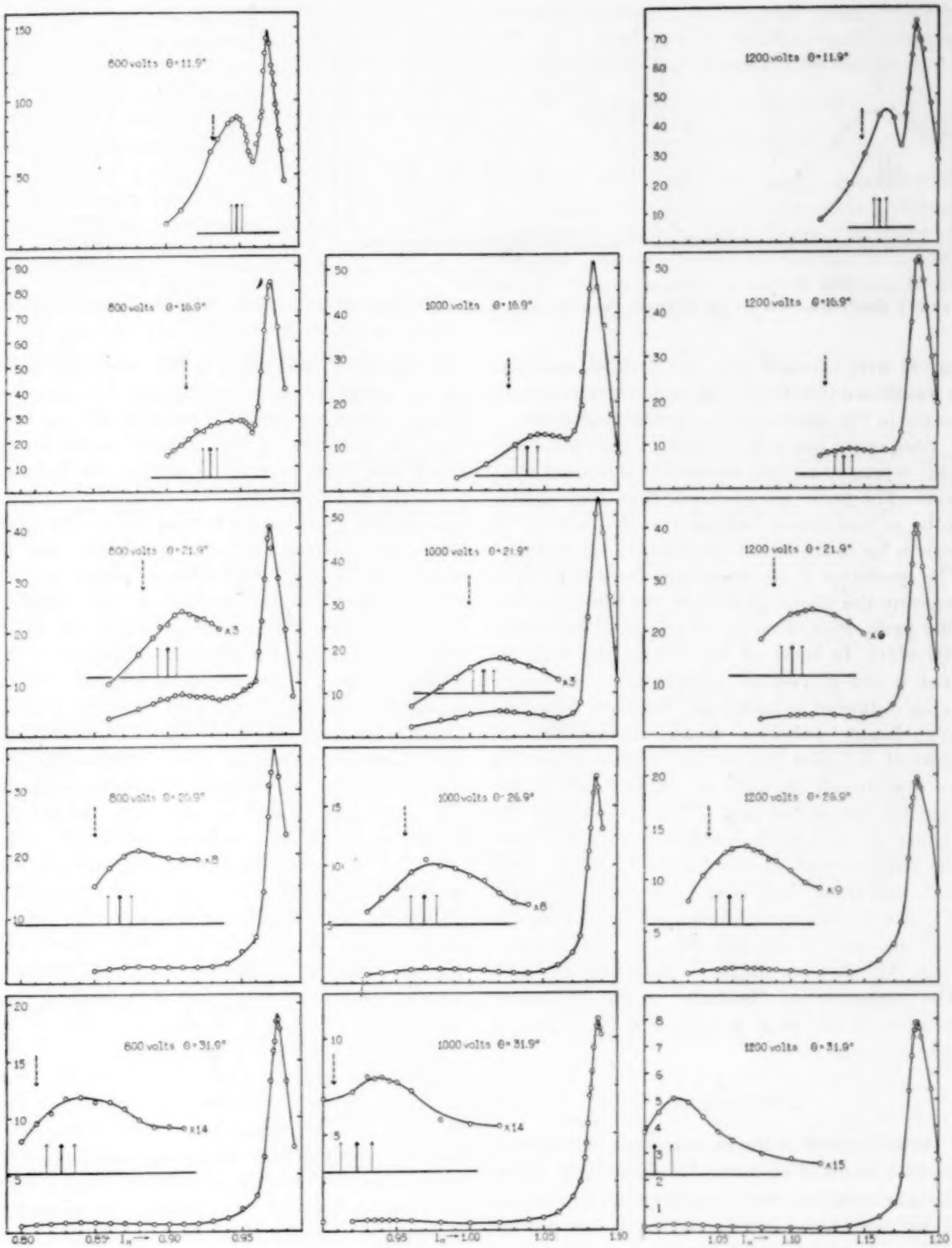

FIG. 2. FIG. 3. FIG. 4.

Velocity distribution curves for 800 to 1200 volt electrons scattered at angles between 11.9° and 31.9°. The $\dot{I}_H$ scale is identical for all curves in the same vertical column.

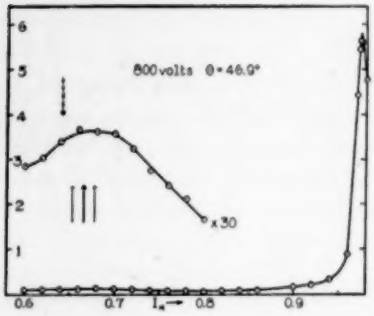

FIG. 5.

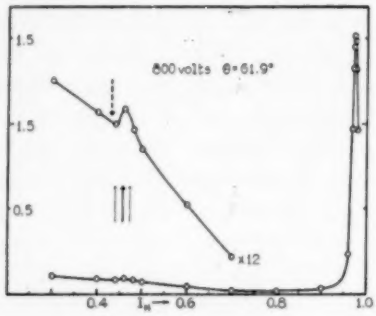

FIG. 6.

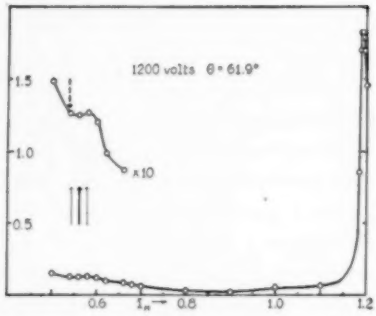

FIG. 7.

Velocity distribution curves for 800 volt electrons scattered at 46.9° and 61.9°, and for 1200 volt electrons at 61.9°.

curves were checked over and verified, and also it was shown that the background scattering with no gas in the apparatus was almost negligible.

Each curve has a sharp peak at the right-hand end, representing the elastically scattered electrons. The peaks are narrower than they appear to be at first glance because the zero for the I_H scale is far to the left of the origin of coordinates. The resolution of the apparatus is insufficient to separate the elastic peak from the lowest excitation peak, with electrons of energy above about 500 volts. In most of the graphs the inelastic peak is also plotted on a larger scale, the factor being indicated in each case. We have indicated by a heavy, unbroken arrow, the velocity (in units of I_H) that the electron should have if it were scattered through an angle θ, by a free electron initially at rest. (This is given by the change of velocity formula, $v_1 = u \cos \theta$.) Since the electron gun cannot be set to better than 0.5°, and since there may be an error of about 0.5° due to the electron beam not being collinear with the axis of the gun slits, we may assume that the effective angle is uncertain to $\pm 1°$. The corresponding "latitude" in the theoretical position of the peak is indicated by a pair of lighter arrows.

DISCUSSION

As was stated in the introduction, the scattering of a beam of electrons by an atom in which the scattering may be done either by the nucleus or by one of the atomic electrons, but not by both, leads to a clear-cut distribution of velocities consisting of just two groups of electrons, those in the group scattered by the nucleus having the full velocity u, and those in the group scattered by an atomic electron, all having the same reduced velocity $u \cos \theta$. Experimentally we find that the positions of the inelastic peaks are in every case close to those given by the formula $v_1 = u \cos \theta$. There is however, in addition, a wide distribution of velocities among the inelastically scattered electrons. We can retain the idea of scattering by individual atomic electrons and still account for the spread in the velocity distribution, by taking over Jauncey's theory in which the finite width of the modified line in the Compton effect is accounted for. (It may not be superfluous to point out that there is a close analogy between the scattering of electrons and the Compton effect in x-ray scattering. The monochromatic unmodified line corresponds to the elastically scattered electrons, while the broad modified line corresponds to the distribution of velocities among the inelastically scattered electrons.) The simple derivation of the change of wave-length in the Compton effect assumes the atomic electron, with which the photon collides, to be at rest, and yields a monochromatic modified line. By assuming that the atomic electron is in motion, and may be moving in any direction whatsoever at the instant the photon strikes it, Jauncey[5] was able to explain the observed width of the modified line. To obtain the corresponding solution for the electron scattering problem, Professor Jauncey merely substitutes the energy and momentum of the incident electron for those of the photon in his theory.[6] The velocity

[5] G. E. M. Jauncey, Phys. Rev. **25**, 314, 723 (1925).

[6] We take pleasure in thanking Professor Jauncey for his interest in this problem.

w of the electron in the hydrogen atom is, according to the Bohr theory for circular orbits, given by $(1/2)mw^2 = Ve$, where V is the ionization potential. We may assume that this relation is true also for helium. The problem to be solved is that of finding the range in the velocity v_1 of the incident electron after collision with an atomic electron having a velocity w and moving in any direction whatsoever. The solution is

$$v_1 = u\cos\theta \pm [1 - 2(u/v_1)\cos\theta + (u/v_1)^2]^{\frac{1}{2}}, \quad (1)$$

where u is the velocity of the incident electron and θ the angle of scattering. When u is considerably larger than w this reduces to

$$v_1 = u\cos\theta[1 \pm (w/u)\sin\theta/\cos^2\theta]. \quad (2)$$

For w/u we may substitute the square root of the ionization potential (25 volts) divided by the energy of the incident electron expressed in volts, and obtain for 1200, 1000 and 800 volt electrons, the values, 0.102, 0.112 and 0.125. Then on substituting for θ we can get the "spread" of the energy distribution of electrons scattered by a free electron when this is moving in any direction with the assumed speed. The extent of this theoretical "spread" is indicated in the graphs (for scattering at angles up to 30°) by a horizontal line below the inelastic peak. It seems evident that the theory gives at least the order of magnitude of the observed spread. In view of the fact that formula (2) is only approximate in the range considered and that the peaks are evidently superposed on a considerable "background," it seems better to postpone further comments until results are available for the range 2000 to 10,000 volts, where we may expect the assumptions to hold better.

The v_1 in the expression $v_1 = u\cos\theta$, is obtained on the assumption that the atomic electron may be regarded as perfectly free. Following a procedure which was used in discussing the Compton effect shortly after its discovery, we may introduce the ionization potential of the atom, V, through the relation $Ve = (1/2)mw^2$ into the energy equation

$$(1/2)mu^2 = (1/2)mv_1^2 + (1/2)mv_2^2 + (1/2)mw^2, \quad (3)$$

where the last term takes care of the energy used for ionization, u and v_1 are the velocities of the incident electron before and after collision, and v_2 is the velocity of the recoil electron initially at rest. The momentum equations are

$$\begin{aligned} mu &= mv_1\cos\theta + mv_2\cos\phi \\ 0 &= mv_1\sin\theta + mv_2\sin\phi. \end{aligned} \quad (4)$$

(It will be noticed that the energy equation now takes notice of the fact that an atom is involved, although this is ignored in the momentum equation. The principal excuse for this simplification is that it enables a usable solution to be obtained.) The solutions are

$$\begin{aligned} v_1 &= u\cos\theta(1 - w^2/2u^2\cos^2\theta), \\ v_2 &= u\cos\phi(1 - w^2/2u^2\cos^2\phi), \end{aligned} \quad (5)$$

when w^2 is small compared to u^2. These equations state that the velocities of both the scattered electron and the recoil electron are reduced when the binding energy is taken into account. The values of the velocities of the scattered electrons, calculated in this way, are indicated in the graphs by a vertical *dotted* arrow. The "spread" of velocities about this new position calculated by Jauncey's formula would obviously be the same as before but displaced so as to be symmetrical about the vertical dotted arrow. The experimental results show that the peaks come closer to the theoretical position calculated when the binding energy is neglected. Too much importance should not be attached to this result as it may be due in part to an oversimplification of the problem leading to a slight displacement of the position of the peak, quite apart from considerations of the binding energy.

The expression[7] for the probability of finding an electron moving down unit solid angle, in a direction θ with the original direction of motion of a beam of electrons of velocity u approaching a free electron, initially at rest, is

$$(e^4/m^2u^4)4\cos\theta(1/\sin^4\theta + 1/\cos^4\theta). \quad (6)$$

This expression, because it includes also the probability of finding the recoil electron in the same solid angle as the scattered electron is useful in discussing experimental results since we cannot distinguish between the two electrons by

[7] O. Klemperer, *Einfuhrung in die Elektronik*, p. 206 (Springer). Originally given by Darwin in a somewhat different form.

an experiment. The expression has a very pronounced minimum at $\theta=45°$. This is in accord with the experimental fact that the scattered electron currents were exceptionally small at 45°.

It is to be recognized that there is a certain artificiality in simplifying the problem by assuming that the incident electron may be deviated either by the nucleus or by one of the atomic electrons, but the experimental results justify this as a rough approximation which should become better at higher speeds. Although the step from 800 to 1200 volts is relatively small, our results indicate that the peaks show a decided tendency to become sharper at the higher velocities.

Whenever classical methods of attacking a problem in atomic physics fail to give results in agreement with experiment it is generally found that better agreement may be obtained by the methods of wave mechanics, provided that a solution in a usable form can be found. We do not know of any explicit expression obtained by wave mechanics methods which can be used to check our results, but certain observations of Mott and Massey[8] have a qualitative bearing. The wave mechanics method, in which the atom is treated as a whole, leads to the result that while there is inelastic scattering at all angles with a wide range of velocities, the scattering is a maximum when the velocities and directions of the scattered and ejected electrons are such that momentum is conserved. They also state that interference effects may be expected when the ejected and scattered electrons have approximately the same energies, that is, in the neighborhood of 45°. Although, in accordance with Eq. (6) the scattering is very small near 45°, we have made careful measurements of the velocity distribution of the 800 volt electrons to see if any evidence of interference could be found. (Mott and Massey, of course, stated that the interference should be looked for in the angular distribution curve; they made no prediction as to what one should expect in a velocity distribution curve.) The curve obtained was smooth; no oscillations of appreciable magnitude were to be found (Fig. 5).

As the results of this investigation were being prepared for publication, a paper by Mohr and Nicoll[9] appeared on a related topic. Their method differed from ours in that they selected electrons with a certain loss of energy after collision and studied their angular distribution. They find definite evidence for collisions with the atomic electrons in hydrogen when the energy is as low as 100 volts. In the case of helium, the evidence is much less marked, appearing as very slight humps, and then only on the curves for the higher energy losses. Comparison with our results cannot be effected, as they did not use electrons with more than 300 volts energy.

The results already obtained suggest an extension of the investigation over a far wider range of electron velocities. It is desirable to investigate, whether or not, as we go to higher velocities the inelastically scattered electrons tend to crowd into a progressively narrowing peak at $v_1=u\cos\theta$, while the background becomes relatively less and less. Investigation with different gases should be made to test the view that atoms of high atomic number, and therefore of higher average binding energy, should have less pronounced peaks in the energy distribution curves than atoms of helium or hydrogen.

Had time permitted we should have liked to extend the scope of this investigation and to determine the shapes of the curves more accurately. However, the transfer of all the equipment of the department to a new physics laboratory will certainly involve a serious delay in the resumption of the work. This, together with the fact that one of the authors is unable to continue with the collaboration, is a logical reason for publishing the results as they are.

[8] Mott and Massey, *The Theory of Atomic Collisions*, pp. 167–172 (Oxford University Press).

[9] C. B. O. Mohr and F. H. Nicoll, Proc. Roy. Soc. **A144**, 596 (1934).

Magnetic Double Refraction in Liquids

HENRY A. BOORSE, *Physics Department, Columbia University*
(Received May 31, 1934)

An apparatus for measuring magnetic double refraction (Cotton-Mouton effect) in liquids is described. The chief feature of the apparatus is a very sensitive variable order compensator which is discussed in detail. Measurements made with this instrument indicate that path differences as small as $3\times10^{-5}\lambda$ can be determined with a precision of about 12 percent provided use is made of very intense light having a wave-length lying within the region which corresponds to maximum visual response. The Cotton-Mouton constants of water and several organic liquids of the aliphatic series including four normal alcohols and five normal acetates are reported and compared with the previous determinations made by other investigators. Certain discrepancies are noted and discussed.

I. INTRODUCTION

IN 1907 Cotton and Mouton[1] discovered that certain isotropic organic liquids when placed in a strong transverse magnetic field acquire the doubly-refracting property of a uniaxial crystal with the optic axis in the direction of the field (H). Thus if a plane-polarized beam of light with a ray direction perpendicular to H is incident on such a liquid, the light will in general be transmitted through it as two component waves with the electric field in one wave vibrating in a plane parallel to H and the electric field in the other in a plane perpendicular to H. If n_p and n_s denote, respectively, the indices of refraction for these two waves, a simple calculation shows that they will emerge with a path difference Δ (expressed in number of wave-lengths):

$$\Delta = L(n_p - n_s)/\lambda, \qquad (1)$$

where L is the length of the specimen in the field H and λ is the wave-length of the light in vacuum. As path differences so produced are small, the emergent light will be characterized by a weak elliptic polarization and the experimental problem in researches on the "Cotton-Mouton effect" therefore consists essentially of an accurate measurement of this elliptic polarization.

The relation between the variables Δ, L and H was found by experiment[2] to be:

$$\Delta = C_m L H^2, \qquad (2)$$

"C_m" being a proportionality factor which is now usually referred to as the "Cotton-Mouton constant." This constant is different for different substances, being positive in some and negative in others; it also varies with their temperature and the wave-length of the incident light.[3]

The classical theory of magnetic (and electric) double refraction developed by Langevin and Born[4] accounts for these relationships on the basis of anisotropic electric and magnetic polarizabilities of molecules. While this theory is strictly applicable only in the case of gases, such experiments in magnetic double refraction have hitherto presented almost insuperable difficulties and the theory has therefore been applied to liquids only, where in most instances it has been found to predict approximately the experimental results.[5] The new quantum mechanics has yielded little more than the classical theory.[5]

As Raman[6] has pointed out, the importance of magnetic double refraction measurements from the standpoint of the general theory of magnetism is due to the use that can be made of Cotton-Mouton constants in evaluating the magnetic anisotropy of molecules. Suggestive attempts in this direction have been made by Ramanadham[7] and Chinchalkar[8] for the simpler organic molecules of the aliphatic series by means of the Langevin-Born theory. As the value of C_m is generally very small in aliphatic liquids,

[1] Cotton and Mouton, C.R. **145**, 870 (1907).
[2] Cotton and Mouton, J. de Physique **1**, 16 (1911).
[3] For a general resumé and complete references see Beams, Rev. Mod. Phys. **4**, 160–172 (1932).
[4] See Debye, Marx Handbuch der Radiologie **6**, 754–769, Leipzig (1925).
[5] Van Vleck, *Electric and Magnetic Susceptibilities*, Oxford Univ. Press (1932), p. 367 para. 84.
[6] Raman, Phys. Soc. Proc. **42**, 309 (1929).
[7] Ramanadham, Ind. J. Phys. **4**, 15 (1929–30).
[8] Chinchalkar, Ind. J. Phys. **6**, 165 (1931).

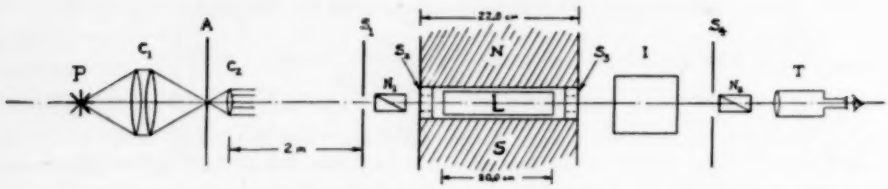

FIG. 1. Schematic diagram of the apparatus.

an apparatus of high sensitivity is needed for precise measurements. It is the purpose of this paper to describe such an apparatus and to present the results which have been obtained with it.

II. Apparatus and Procedure

A schematic diagram of the apparatus is given in Fig. 1: P is a 110 watt Pointolite lamp; C_1 is the condenser arranged to focus the bright bead in the lamp upon a circular aperture of 1 mm diameter in the screen A. This aperture acts as a "point" source of light for an achromatic collimating lens C_2. S_1 and S_4 are the mountings for the polarizing and analyzing prisms, N_1 and N_2, a combination discussed later in more detail. S_2 and S_3 are brass blocks, 6.10 mm wide, pierced along the axial line of the optical system with holes 5 mm in diameter; these blocks serve both as spacers for the pole-pieces N and S of the magnet and as diaphragms in the optical system. Under these conditions the light passing through the specimen tube L is parallel to at least 0.8°.

Failure to secure parallelism of the beam or to align it in a direction perpendicular to H results in the appearance of the Faraday effect, which acts to reduce the sensitivity of the apparatus. A convenient test of the fulfillment of these two conditions consists in placing carbon tetrachloride in the specimen tube, whereupon, if the lens system is properly adjusted, application or removal of the magnetic field will produce no noticeable optical effect since this substance shows no magnetic double refraction. Parasitic reflection of light in the system, which also reduces the sensitivity, was practically eliminated by using copper specimen tubes the walls of which were exposed to moist hydrogen sulfide, thus giving them a low reflecting power surface and also leaving them chemically inert. The tubes were 20.0 cm long with a rectangular cross-section 12 mm high and 6 mm wide with a square aperture 6 mm high and 5 mm wide sealed with carefully annealed microscope cover glass.

The cements suggested by previous investigators in this field for pasting the glass to the metal tube were found to be unsuitable as they dried hard and caused strains to be set up in the glass, resulting in a troublesome residual double refraction. To avoid this effect, very viscous and non-drying cements were used. In experiments on the alcohols a small amount of Merck's anhydrous lanolin was melted and titrated through a large amount of the alcohol to be examined. After repeated heating and stirring the insoluble part was recovered and the titration process repeated. The remaining insoluble part constituted a satisfactory cement. For the acetates the cement consisted of a mixture of dextrin, dextro-mannitol and glycerine treated with the respective acetates in a similar manner. It was found important to have the end glasses perpendicular to the axis of the tube and for this reason very thin layers of cement were used.

In Fig. 1, S_1 and S_4 represent twelve inch circular duraluminum disks graduated in quarter degrees; by means of verniers these circles could be read to 0.01° directly. The maximum error of graduation of the circles was found not to exceed the width of the ruling at any position and was thus estimated to be not greater than 30″ of arc. Both circles carried polarizing prisms, N_1 and N_2, of the Glan-Thompson type with square end faces 12 mm on a side. These prisms have two distinct advantages over the usual type of nicol: (1) they give more nearly plane-polarized light, (2) when turned they do not cause the usual rotational displacement of the light beam. With the optical system diaphragmed as described Landolt's fringe is not visible when the nicols are crossed, indicating that the light traversing

the specimen is plane-polarized and of a single azimuth.

The pole pieces N and S were specially designed for this investigation; their construction is indicated by an end section shown in Fig. 2. The high permeability of the "Weiss" iron insert allows higher field strengths to be obtained than would be the case if the pole pieces were constructed entirely of Swedish iron. With the magnet coils connected in parallel a total exciting current of 26 amp. was found to produce an average field of 22,600 gauss. The field strength was measured by suspending a current element in the gap and measuring the pull on the element by means of a balance. By mounting the balance on tracks above the magnet it was possible to make a point to point plot of the field. The error in measuring H was estimated to be less than 2 percent.

The instrument I in Fig. 1 represents the compensator used to measure the double refraction. It is of the "variable order" type and was first described by Palmer.[9] It consists essentially of three strain-free pieces of microscope cover glass arranged as shown in Fig. 3. The two horizontal strips are 25 mm long, 5 mm wide and about 0.2 mm thick. The lower, hereafter designated the "half-shade," may be subjected to pure tensile stress in a horizontal direction by the arrangement shown in the figure. The upper glass is kept strain-free and can be adjusted to lie in a plane which is parallel and adjacent to that of the half-shade. If the contiguous edges of the two strips have been ground and polished

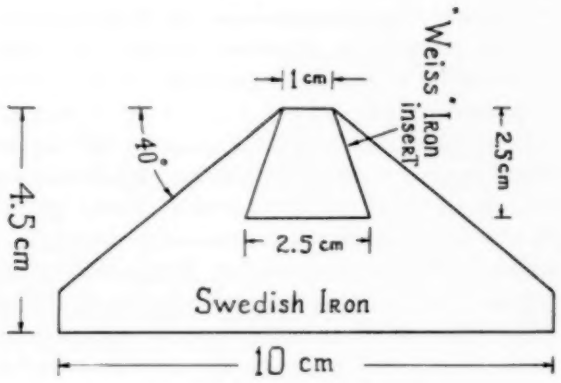

FIG. 2. End section of pole pieces.

[9] Palmer, Phys. Rev. **17**, 409 (1921).

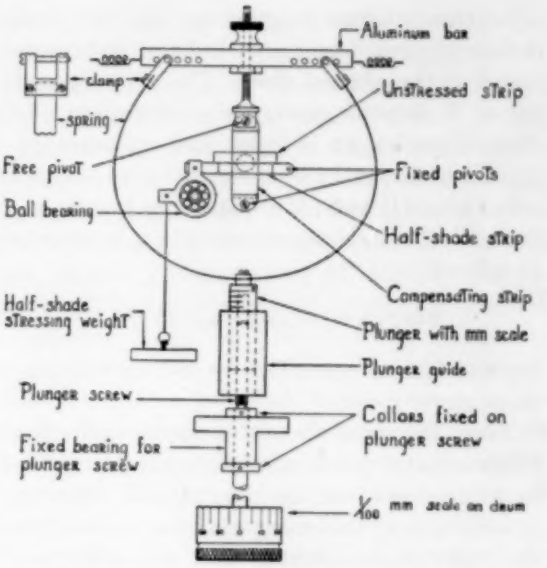

FIG. 3. Arrangement of microscope cover glasses.

to an optical flat and are not chipped, the dividing line between the two halves of the field of view (indicated by the dashed circle in Fig. 3) can be made, by careful adjustment, to vanish almost completely when the intensity of light in both is the same. In making observations the strips are viewed through the short-focus, low-power observing telescope T (Fig. 1) which is focussed upon their edges. The third glass of the same length and thickness as the horizontal ones, but 12 mm wide, is mounted behind them and covers the whole field of view. This strip, hereafter called the "compensating" strip, can be given pure tensile stress in the vertical direction by means of the indicated flat steel spring.

Since glass under tension behaves as a positive uniaxial crystal with the optic axis in the direction of the applied stress, the half-shade and compensating plates are therefore equivalent to crossed positive doubly-refracting plates of variable thickness. Photoelastic investigations have shown that the relation between the tensile stress applied to a glass plate and the resulting double refraction is linear,[10] hence:

$$n_e - n_0 = KT. \tag{3}$$

[10] Coker and Filon, *Photoelasticity*, Cambridge Univ. Press, 1931, p. 185, para. 3.03.

In this relation n_e and n_0 are the "extraordinary" and "ordinary" indices, respectively, and T is the applied stress. The proportionality factor K depends upon the composition of the glass, wave-length of light, and temperature (a point which will be considered later). With the aid of Eqs. (1) and (3) a quantity δ known as the "order" of a birefringent plate can be expressed as follows:

$$\delta \equiv 2\pi\Delta = 2\pi L(n_p - n_s)/\lambda = K'T. \qquad (4)$$

Eq. (4) has been verified by Palmer[9] for microscope cover glass.

From the usual theory of double refraction it follows that if two birefringent plates with "fast" axes at right angles are placed between a polarizing and analyzing nicol the intensity I of the light wave leaving the analyzer can be expressed as follows:

$$I = \tfrac{1}{2}A^2[\cos^2\theta + \sin 2\rho \sin 2(\theta-\rho) \sin^2 (\delta_1-\delta_2)/2], \qquad (5)$$

where A is the amplitude of the electric vector in the plane-polarized wave leaving the polarizer, θ is the angle between the transmission azimuth of the analyzer and the transmission azimuth of the polarizer (the latter serving as a convenient fiducial azimuth from which all angles are measured), ρ is the angle which locates the azimuth of the "fast" axis of the compensator plate, and δ_1 and δ_2 represent the "order" of the half-shade and compensator plates, respectively. Eq. (5) serves to define the intensity of light in the lower half of the field of view (as shown in Fig. 3) and will be denoted by I_1. Since there is only one birefringent plate in the upper half of the field of view, the corresponding intensity I_2 is expressed by:

$$I_2 = \tfrac{1}{2}A^2[\cos^2\theta + \sin 2\rho \sin 2(\theta-\rho) \sin^2 \delta_2/2]. \qquad (6)$$

I_1 and I_2 are evidently equal when:

$$\delta_1 = 2\delta_2. \qquad (7)$$

From Eqs. (1) and (4) the condition for a matched field may also be written:

$$T_1 = 2T_2. \qquad (8)$$

To measure the order δ_3 of a third doubly-refracting medium introduced into the optical system, e.g. (the double refraction of a liquid brought about by the action of the magnetic field), the simplest procedure is, perhaps, to orientate its optic axis so as to coincide with that of the half-shade plate. Since the optic axis of the liquid in magnetic birefringence is coincident in direction with H, and H and T_1 are both horizontal, this condition is already fulfilled. Thus, if a liquid shows *positive* double refraction of order δ_3, the effect in the compensator is exactly the same as an increase in T_1, for now δ_3 and δ_1 are both appropriate to positive plates of the same azimuth. If δ_1 is kept fixed, Eqs. (5) and (6) show that the match of the half-shade field will be restored when:

$$\delta_1 + \delta_3 - \delta_2' = \delta_2' - \delta_3, \qquad \therefore \quad \delta_1 = 2(\delta_2' - \delta_3). \qquad (9)$$

From Eq. (7) it therefore follows that $\delta_2' > \delta_2$, or from Eq. (8) that $T_2' > T_2$.

Similarly for *negative* double refraction;

$$\delta_1 = 2(\delta_2' + \delta_3), \qquad (10)$$

with $\delta_2' < \delta_2$ and $T_2' < T_2$.

From Eqs. (4), (7) and (9):

$$\delta_3 = K' \cdot \Delta T_2 \qquad (11)$$

where $\Delta T_2 = (T_2' - T_2)$. Eq. (11) provides a convenient criterion for both the sign and the magnitude of the double refraction of the liquid under investigation.

In terms of the physical adjustment of the compensator, T_1 being kept fixed, Eq. (11) shows that if after application of the magnetic field it is necessary to increase the tension on the compensating strip to restore the balance of the optical field then the liquid exhibits positive double refraction; negative double refraction requires the tension to be decreased if the match is to be restored.

It is important to note that Eq. (11) is true whether or not the nicols are crossed. Reference to Eqs. (5) and (6) for I_1 and I_2 shows that if they were originally equal then any change in θ will not destroy this equality. From this fact it follows that the appearance of the Faraday effect will not act to unbalance the optical field, and will not therefore be interpreted as a double refraction.

To define a measure of the sensitivity of the compensator let us suppose that the compen-

sating strip is given an increment of double refraction $\Delta\delta_2$ over and above the double refraction δ_2 corresponding to some match point. The absolute change in intensity in the upper half of the field, owing to this increment, is expressed by:

$$\Delta I_2 = (\partial I_2/\partial\delta_2)_{\text{match}} \cdot \Delta\delta_2, \qquad (12)$$

and the corresponding change in intensity in the lower half by:

$$\Delta I_1 = (\partial I_1/\partial\delta_2)_{\text{match}} \cdot \Delta\delta_2. \qquad (13)$$

Account must be taken of the response characteristics of the eye, hence an appropriate definition of the sensitivity S is:

$$S = |\Delta I_2/I_2 - \Delta I_1/I_1|, \qquad (14)$$

which in virtue of Eqs. (12) and (13) may be written:

$$S = \left| \left(\frac{\partial I_2/\partial\delta_2 - \partial I_1/\partial\delta_2}{I_2} \right)_{\text{match}} \cdot \Delta\delta_2 \right|$$

provided $\Delta\delta_2$ is considered very small. With the aid of Eqs. (5) and (6) it follows that:

$$S = \left| \frac{\sin 2\rho \sin 2(\theta-\rho) \sin\delta_2}{\cos^2\theta + \sin 2\rho \sin 2(\theta-\rho) \sin^2 \delta_2/2} \cdot \Delta\delta_2 \right|. \qquad (15)$$

Excluding the values $\theta = 0$, $\rho = 0$, the variables θ, ρ and δ are all independent and the condition that each must satisfy in order that S shall be a maximum may be found in the usual way by setting:

$$\partial S/\partial\theta = 0, \qquad \partial S/\partial\rho = 0, \qquad \partial S/\partial\delta = 0.$$

These conditions are satisfied for:

$$\theta = \pi/2, \qquad \rho = \pi/4, \qquad \delta_2 = 0. \qquad (16)$$

Hence, for maximum sensitivity the nicols should be crossed, the light vector should make an angle of 45° with the fast axis of the compensating plate, and the tension *on the half-shade* should be as small as is consistent with the desired range of the instrument. It should be noted that under these conditions the intensity of light in the half-shade field will appear quite low and the best results can therefore be obtained only when the observer's eye is dark-adapted.

As the above sensitivity analysis shows that the maximum rate of change of intensity of the half-shade field with double refraction of the glass strips is secured when the light vector makes an angle of 45° with the axes of the strips; it therefore follows that, since the axes of the liquid coincide with those of the strips, the rate of change of intensity in the compensator with double refraction induced in the liquid will also be a maximum for the same orientation of the light vector. To secure this 45° setting, the direction of H was determined by placing a liquid of relatively large double refraction (nitrobenzene) in the tube, and moving the transmission azimuth of the polarizer slowly through the horizontal direction, the compensator having been rotated through 45° to preserve its sensitivity. Under these conditions the disappearance of double refraction signalizes the coincidence in direction of the light vector and the magnetic force H. This coincidence could be determined to within $\pm 1'$ of arc.

The method of determining δ_2 was a comparative one and was based upon the magnetic double refraction of acetone as a standard. The procedure consisted in applying a given stress to the half-shade strip by hanging a weight on the stressing mechanism shown in Fig. 3. With the light beam traversing the specimen whose birefringence was to be measured, the corresponding reading of the deflection of the compensator spring was then observed when the optical field was matched. With a given weight on the half-shade six to nine readings were taken to determine this match point. This procedure was repeated with about four or five different weights, usually 20, 50, 70, 100 and 150 grams. The match points were then plotted as shown in Fig. 4, and double refractions determined by means of Eq. (11) in conjunction with this "calibration" curve. If, for instance, acetone were placed in the specimen tube and the field matched with 50 grams on the half-shade, application of the magnetic field would destroy this match. In order to rematch the optical field, it was found necessary to increase the tension on the compensating strip until the spring deflection reading was about 710. Referring to the calibration curve this reading will be seen to correspond to about 123 grams; application of the magnetic field therefore produces a double refraction in acetone which is the same as that

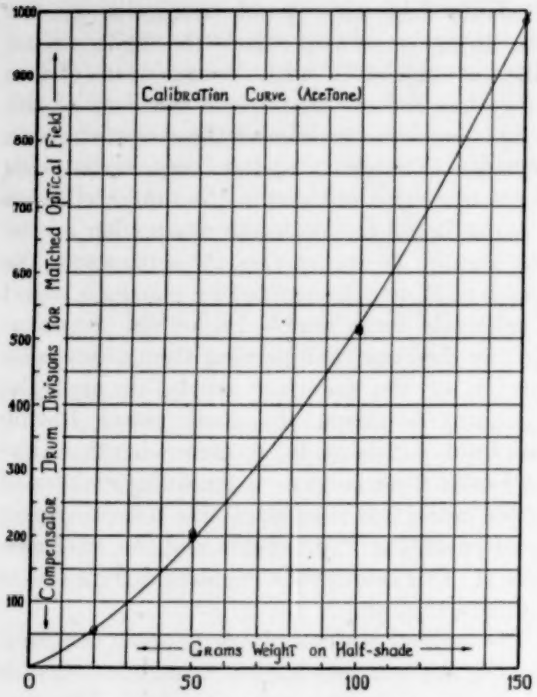

FIG. 4. Calibration curve of acetone.

produced by the application of an additional weight of 73 grams to the half-shade straining mechanism. If methyl acetate were placed in the tube, all other conditions remaining the same, the result found in this way would correspond to an increase of about 37.4 grams. If these increments are taken as a measure of the change in tension on the compensating strip, and are represented as ΔT_2 and $\Delta T_2'$, we may write:

$$\Delta T_2/\Delta T_2' = C_m/C_m' \qquad (17)$$

in virtue of the definition of order and Eqs. (2) and (11). It is usual to compare the double refraction of a given liquid with that of nitrobenzene under the same conditions, the latter being arbitrarily chosen to have a constant of 100. Cotton and Mouton[11] have found that on this scale acetone has a constant of 1.6. From Eq. (17) the relative constant of methyl acetate would therefore be:

$$C_m/1.6(0) = 37.4/73.0, \qquad C_m = 0.82.$$

As it was necessary to increase the tension T_2 to rematch the optical field in both cases, Eq. (11) indicates that the sign of the constants is positive.

Early experiments carried out with a glass straining system similar to that described by Palmer[9] showed that the calibration curves were not reproducible. The match points were found to be exceedingly unstable; overnight shifts of 200 drum divisions often occurred even though the tension on the strips had been completely relieved. Attempts to eliminate this difficulty by making the stressing systems as frictionless as possible led to the arrangement shown in Fig. 3. Although these efforts resulted in some improvement, the fundamental trouble was not located until a careful investigation disclosed that the instability of the calibration was due to the effects of small temperature fluctuations upon the compensator, a change of 3°C accounting for a shift in the match points of about 200 drum divisions. From the reported temperature coefficients[12] of K in Eq. (3) it appears that changes of this magnitude are too large to be attributed to variations in the birefringence of strained glass with temperature; whether or not the effect is only incidental to the stressing systems employed is not known. When the compensator was placed in a constant temperature housing in which the fluctuations were less than 0.1°C, the calibration curves were found to be reproducible within the experimental error of the determination of the match points, which seldom exceeded 10 drum divisions.

The accuracy of determinations of Cotton-Mouton constants by the comparative method described above is obviously dependent upon the purity of the calibrating substance (acetone). Specimens of acetone from three different sources were therefore checked against each other. Sample (1) was Merck's "Reagent," (2) Baker Chemical Company's "Analyzed," (3) a sample of exceptional purity obtained through the kindness of Professor L. P. Hammett of the Chemistry Department of Columbia University. This sample was purified by refluxing the liquid over solid calcium oxide and solid potassium permanganate for about five hours to dehydrate it and oxidize the organic impurities that might be present; it was then carefully distilled.

[11] Cotton and Mouton, Ann. de Chem. et Phys. **28**, 236 (1913).

[12] Coker and Filon, *Photoelasticity*, Cambridge Univ. Press, 1931, p. 243, para. 3.26.

The values of ΔT_2 obtained from these three samples were found to be, respectively: (1) 72.8±1.0 grams, (2) 74.1±0.4 grams, (3) 72.8±0.9 grams. Each of the above values is the average of four or more separate determinations and each single determination represents a mean of from five to nine readings with the magnetic field applied. The maximum deviation of any single determination from the mean of its set was 1.5 grams, and the average deviation of the single determinations is represented above as the precision measure of the set. The same statements, with the exception of the deviation of single determinations, apply to the values of ΔT_2 given in column (3) of Table II. As no special treatment was given samples (1) and (2), the final result for acetone was taken as:

$$\Delta T_2 = 72.8 \pm 1.0 \text{ grams.}$$

As a further check on this standard the constants of chloroform, ethylene dichloride and nitromethane were determined relative to acetone and then compared with those published by Cotton and Mouton[11] who used an absolute method. Because of its high sensitivity the range of the compensator was too small to measure the double refraction of these substances when contained in a 20.0 cm tube, hence for this comparison a shorter tube (length 7.04 cm) was substituted. The chloroform and ethylene dichloride were obtained from Eimer and Amend; the former liquid was of "tested purity" and carried an analysis; the latter was twice distilled before being used. The nitromethane was purchased from the Eastman Kodak Company (designated by E. K. C. in column 9, Table II) and was specified to have a boiling point between 98 and 101°C. The results are listed in Table I.

The above values of C_m given by Cotton and Mouton were calculated from measurements made with approximately monochromatic light of mean wave-length $\lambda = 578$ mμ (yellow lines of the mercury arc). Preliminary experiments with the above-described compensator showed that high sensitivity could not be obtained with the monochromatic sources available or by the use of filters owing to their high absorption. By using the unmodified radiation from the Pointolite lamp under the condition corresponding to maximum sensitivity of the compensator (low intensity of the half-shade field) it was found that not only were color effects absent but the match point of the field was very sharp. Measurements were therefore carried out in this way. Because of the excellent agreement shown in Table I between the author's and Cotton and Mouton's very reliable values for C_m, and the small dispersion of the substances investigated (Table II), it is considered appropriate to associate the various constants listed in Table II with $\lambda = 578$ mμ.

TABLE I. *Results.*

Liquid	Values	ΔT_2	Mean	C_m Boorse	C_m Cotton-Mouton
Acetone	25.0	25.0	25.0	+1.60	+1.6
Ethylene dichloride	31.5	33.5	32.5	−2.08	−2.1
Chloroform	43.5	43.5	43.5	−2.78	−2.8
Nitromethane	56.0	56.0	56.0	+3.58	+3.6

Psychological errors in the measurements were avoided as far as possible by the employment of two observers; one matched the optical field while the other recorded the corresponding deflection of the spring regulating the tension on the compensating strip. It was not until after a complete set of readings for a given specimen was made that the calibration curve was plotted and the value of ΔT_2 calculated. (Because of the presence of small residual double refraction, slight variations were found in the calibration curves for different specimens, and hence calibration readings were taken in every case before measurements were made with the magnetic field applied.)

An idea of the purity of the liquids examined, can be obtained from column (9) of Table II which indicates their source, the range in which the manufacturer specified their boiling point to lie, and whether or not they were distilled immediately before use. The three liquids which are noted as having received special treatment were prepared as follows. Sample (3) of methyl alcohol was treated with $AgNO_3$ to change the aldehydes present to acids and with KOH to neutralize the acids thus formed; a fractional distillation was then made. Sample (1) of "absolute" ethyl alcohol was refluxed over solid calcium oxide for five hours to remove traces of moisture and then distilled in the presence of dry air. Ethyl ether, supplied by the Merck Chemical Company, and specified

TABLE II. *Cotton-Mouton constant for various liquids.*
Scale: Acetone = 1.60; $t = 22°C$.

Liquid	Formula	ΔT_2	C_m Boorse	C_m Chinchalkar	C_m C.S.	C_m/d	C_m(abs.) $\times 10^{14}$	Chemical information
Water	H·OH	6.6±0.8	−.15	−.15	−.14₆[1]	− .14	− .37	Distilled
Methyl alcohol (1)	CH_3·OH	15.0±0.5	−.33	−.57		− .42		Mallinckrodt's "absolute"
Methyl alcohol (2)		14.1±0.6	−.31			− .39		Baker's "absolute" (distilled)
Methyl alcohol (3)		5.6±0.4	−.12			− .16	− .30	Chem. Dept. C.U. −99.5% special treatment
Ethyl alcohol (1)	C_2H_5·OH	9.5±0.8	−.21	−.38	−.39[1]	− .26	− .52	U. S. Industrial Chem. Co. special treatment
Ethyl alcohol (2)		9.4±0.6	−.21			− .26		Chem. Dept. C.U. "absolute"
n-Propyl alcohol	C_3H_7·OH	13.3±0.5	−.29	−.58		− .37	− .71	Chem. Dept. C.U. distilled over sodium hydroxide
n-Butyl alcohol	C_4H_9·OH	16.0±0.8	−.35	−.67		− .43	− .86	E.K.C. b.p. 116–118°C—distilled
n-Heptane	C_7H_{16}	21.4±0.8	−.47	−.77	−.50[2]	− .69	−1.16	E.K.C. b.p. 98–98.5°C distilled
Ethyl formate	H·COO·C_2H_5	41.9±0.4	+.92	+.95		+1.00	+2.26	E.K.C. b.p. 54–55.5°C
Methyl acetate	CH_3·COO·CH_3	37.4±1.1	+.82	+.81		+ .88	+2.02	E.K.C. b.p. 56.5–57°C "anhydrous"—distilled
Ethyl acetate (1)	CH_3·COO·C_2H_5	30.9±0.9	+.68	+.72		+ .75	+1.66	E.K.C. b.p. 76–77°C "anhydrous"
Ethyl acetate (2)		30.7±0.9	+.67					Merck's "Reagent"
n-Propyl acetate	CH_3·COO·C_3H_7	22.4±0.6	+.49	+.49		+ .56	+1.21	E.K.C. b.p. 99–102°C
n-Butyl acetate	CH_3·COO·C_4H_9	15.1±0.7	+.33			+ .38	+ .81	E.K.C. b.p. 124–126°C
n-Amyl acetate	CH_3·COO·C_5H_{11}	10.4±0.7	+.23			+ .26	+ .57	E.K.C. b.p. 145–147°C, distilled
Ethyl ether	C_2H_5·O·C_2H_5	17.9±0.4	−.39	−.70		− .55	− .96	Merck's "anhydrous" special treatment
n-Butyl ether	C_4H_9·O·C_4H_9	19.4±0.4	−.43			− .56	−1.06	E.K.C. b.p. 142–144°C

[1] Haque, C.R. **190**, 789 (1930).
[2] Extrapolated from Scherer, C.R. **192**, 1223 (1931).
b.p. = boiling point.

as "anhydrous-distilled over sodium" was further treated with metallic sodium to dry it and then distilled under the same conditions as ethyl alcohol above.

III. RESULTS

The Cotton-Mouton constants for the liquids investigated are listed in Table II. Column (4) of this table gives the values of the constants found by the author, column (5) the corresponding values found by Chinchalkar and column (6) values found by several of Cotton's students, reference to the original papers in the latter case being given in footnotes. Column (7) gives the specific birefringence (values in column 4 divided by the density of the liquid), and column (8) the absolute Cotton-Mouton constants calculated from the values given in column (4) and the absolute constant of nitrobenzene,[13] *viz.*, 2.46×10^{-12} at 20°C, $\lambda = 578$ mμ.

The values of ΔT_2 listed in column (3) represent the average of from four to nine separate determinations. The maximum difference between *single* determinations in any set was 3.0 grams, and the minimum, 1.0 gram. Methyl alcohol sample (3) showed the smallest path difference of all the liquids examined; from the known values of L, H^2 and its absolute Cotton-Mouton constant, we may write in virtue of Eq. (2):

$$\Delta \equiv d/\lambda = 0.30\times10^{-14}\times20\times5.1\times10^{8},$$

where d represents path difference in cm. From the precision of the measurements of L, H^2, C_m for methyl alcohol (obtained from the precision

[13] Salceanu, C.R. **190**, 737 (1930); **191**, 486 (1930).

of ΔT_2 for this liquid and acetone) and C_m(abs.) for nitrobenzene, estimated at less than 1 percent from Salceanu's paper:

$$d = 3.06 \times 10^{-5} \lambda \pm 12 \text{ percent}$$

$$= 1.8 \pm 0.2 \times 10^{-9} \text{ cm.}$$

From the standpoint of the precision of the *optical measurements alone*, it would appear that since ΔT_2 for this methyl alcohol sample was determined to within about 7 percent (see Table II),

$$d = \lambda/32{,}000 \pm \lambda/450{,}000,$$

provided no systematic errors were present.

Inspection of Table II shows that there is good agreement between Chinchalkar's and the author's values of C_m in the case of substances having positive constants; the negative constants, however, show a systematic difference of about 0.3 in all liquids except water and ethyl alcohol. All measurements on the former of these two substances show excellent agreement, especially in view of the fact that the precision of the determinations is uniformly low. From the papers of Chinchalkar and Haque their precision appears to be about 20 percent, hence the fact that Haque's measurements were made at 16.6°C with the green line of mercury need not be taken into consideration in the comparison, since temperature and dispersion effects are not comparable with this experimental error.

As regards the case of ethyl alcohol Chinchalkar and Haque are also in agreement, while the value reported here is roughly 50 percent different. Neither of these investigators reports the estimated purity of his alcohol nor lists any special precaution taken in its purification. (Haque's measurements were made under the same conditions as his water determination.) As both methyl and ethyl alcohol are difficult to secure in a highly-purified anhydrous state, it seems desirable that further measurements be made on samples of known purity.

Further evidence of systematic variation between the negative constants obtained by Chinchalkar and the author appears in the case of methyl alcohol. His reported value for this liquid is -0.57; he secures the same value within the experimental error for the constant of *n*-propyl alcohol given as -0.58. The same kind of agreement can be noted in column (4) Table II if comparison is made between the constant found for a commercial sample of absolute methyl alcohol (distilled before use) with that of *n*-propyl alcohol. General evidence[7, 8] shows that a lengthening of the aliphatic carbon-hydrogen chain, provided unsaturated valence bonds are not thereby introduced, acts to increase negative or to decrease positive birefringence. By examining the values of the specific birefringence, it is evident that the acetates are in accord with this generalization; the alcohols will also be if the value of C_m for methyl alcohol is chosen as -0.12. This choice would also have been made from two other considerations: first, it places methyl alcohol between water and ethyl alcohol as regards specific birefringence, second, it is the most probable value on the grounds of the chemical purity of the three methyl alcohol specimens.

The value of the Cotton-Mouton constant for *n*-heptane can be extrapolated from Scherer's measurements on five members of the saturated hydrocarbon series C_nH_{2n+2} between C_8H_{18} and $C_{14}H_{30}$. The average difference between values of C_m for successive members of this series is 0.10 and C_m for C_8H_{18} is given as -0.6, so that on this basis C_7H_{16} should have a constant of -0.5 for $\lambda = 578$ mμ. This is in good agreement with the value for *n*-heptane reported here.

In conclusion the author wishes to thank Dr. R. M. Bozorth of the Bell Telephone Laboratories for the gift of the Weiss iron used in the pole pieces, Dr. J. A. Greenspan of the Chemistry Department of Columbia University for the gift of several highly purified alcohols, the members of the shop force for their aid in constructing the apparatus, particularly Mr. S. Cooey for his excellent machine work on the compensator, Mr. L. H. Rouillion and Mrs. H. A. Boorse for their assistance, Professor A. deF. Palmer of the Physics Department of Brown University for demonstrating his compensator and for helpful correspondence, the Physics Department of Columbia University for the award of the Barnard Fellowship, and Professor A. P. Wills for suggesting the problem and for his continued interest and encouragement while the investigation was being carried out.

Radioactivity of Neodymium and Samarium

W. F. LIBBY, *Department of Chemistry, University of California, Berkeley, California*

(Received June 11, 1934)

Descriptions of methods for determining (*a*) absolute activity of an element, (*b*) the penetrating power of its radiation, (*c*) the deflectability in a magnetic field and (*d*) the sign of the charge of the radiation are given. The methods involve the use of Geiger-Müller counters with screen walls. Neodymium emits beta-rays of maximum $H\rho$ value 355 and 2.4 mm of air penetrating power. The half-life is slightly less than 1.5×10^{12} years. The range of the samarium alpha-particle has been found to be 1.23 ± 0.05 cm in air at N.T.P. and its half-life 6.3×10^{11} years. Gadolinium, praseodymium, tin, iodine and beryllium have been found inactive. They cannot have half-lives less than 10^{14} years if they emit particles of ranges greater than 1 cm. The limit for Be is 10^{15} years.

THE problem of the detection of radioactivity among the lighter elements has become of greater importance during the last few years because of our increasing knowledge of nuclear properties. In this investigation several elements have been examined and the activities of two of them substantiated. As Hevesy, Pahl and Hosemann[1] have stated, the general average stability of the elements does not rule out the existence of relatively active scarce isotopes. The methods of detection are so sensitive that the presence of so small an amount of radium as 10^{-12} parts per unit weight of sample is easily established. However, it is not necessarily true that such activities be attributed to less abundant isotopes. Activities of the abundant isotopes sufficiently low to prevent detection by this procedure can be established by counter methods in general and in particular by the one used in this research.

DESCRIPTION OF APPARATUS

Detection of feeble activity obviously cannot be better accomplished than by the use of an instrument capable of counting single particles emitted from a sample of large area. As the closest approach to this at present available, Geiger-Müller counters modified by the use of wide-mesh screen walls to allow free entrance of particles of the lowest possible energies have been used throughout this work.

Since there are so many ionizing particles being produced under normal conditions by cosmic rays and small amounts of strongly active substances, the presence of any radiation of the kind sought can obviously be established only by a differential method which will allow an accurate correction to be made for this background radiation.

The apparatus used for the general detection and measurement of activities is shown in Fig. 1a.

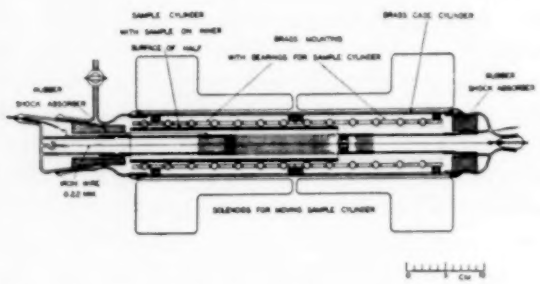

FIG. 1a. Apparatus used for general detection and measurement of activities.

A screen wall counter is placed in a chamber in such a way that a sample deposited on the inner surface of half a steel cylinder concentric with the counter can be brought directly over the counter and removed by moving the sample cylinder through half its length. The steel cylinder was mounted in a sleeve of brass bearings and the whole chamber placed inside of two solenoids capable of giving fields sufficiently intense to move the cylinder. The solenoids were used alternately to move the cylinder from the exposed to the unexposed position at intervals of five minutes. The timing mechanism consisted of a half-minute telechron clock from which a twenty-notch ratchet wheel device operated to close the

[1] G. v. Hevesy, M. Pahl and R. Hosemann, Zeits. f. Physik **83**, 43 (1933).

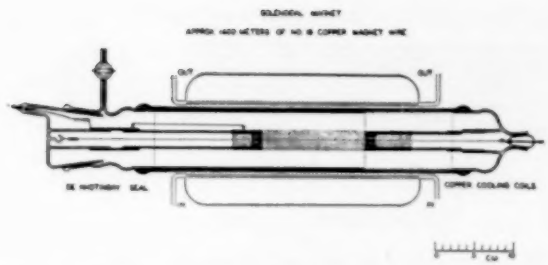

FIG. 1b. Apparatus used for determination of magnetic deflectabilities.

magnet circuits. The whole counter was placed in an iron shield as shown in Fig. 2. The shield affords a protection of at least a foot of iron in every direction and reduces the background count from approximately 25 per half-minute when unshielded to about 15.

The chamber was generally filled with oxygen, air, hydrogen, argon or helium at 2 or 3 cm of Hg pressure. The voltage necessary for counting ranged between 600 and 1500 under these conditions. The sample cylinder and chamber wall were usually kept at a potential about 45 volts positive with respect to the counter to stabilize the counts and render the effect of leakage currents less important.

By placing the sample cylinder at a sufficiently high negative bias with respect to the counter wall it is possible to increase the effective diameter of the counter to the size of the sample cylinder and effectively place the sample inside the counter.

The amplifying circuit is represented diagrammatically in Fig. 3. Essentially, the count phenomenon in the counter produces a fall in potential of the wire which lasts a time determined by the value of the shunt resistance to the ground represented in the figure as a three-element tube with filament and grid connected together to the counter wire and the plate to the ground. It seems essential that the value of this resistance be adjusted to certain values between 10^8 and 10^{10} ohms, somewhat dependent upon the counter being used. This has been mentioned in an earlier publication[2] in which the use of solution resistance units was advocated. The tube type of leak is more satisfactory because of its ready adjustability. The current heating the filament is varied by a sensitive rheostat. A milliammeter in the filament circuit insures reproducibility. Kovarik[3] first pointed out this general type of circuit for point counters. The tube resistance device is described by Rutherford, Chadwick and Ellis.[4]

The output in the plate circuit of the screen-grid tube has been used alternatively to operate a telegraph relay, a two-tube thyratron relay or

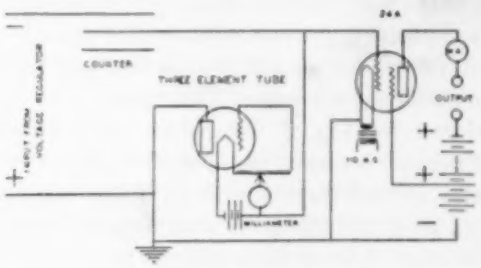

FIG. 3. Recording circuit.

coupled with a two-tube resistance coupled amplifier which gave output impulses of 10–20 m.a. to actuate the telephone relay. The latter was the most satisfactory.

An ordinary magnetic counter operated from the telephone relay to record the counts. A magnetically controlled automatic camera built to use standard 35 mm motion picture film was focussed to take pictures of the dial readings at intervals of 30 seconds. A telechron clock controlled the camera, as well as the sample-moving mechanism described above.

The whole assembly for activity determination functioned automatically, taking readings

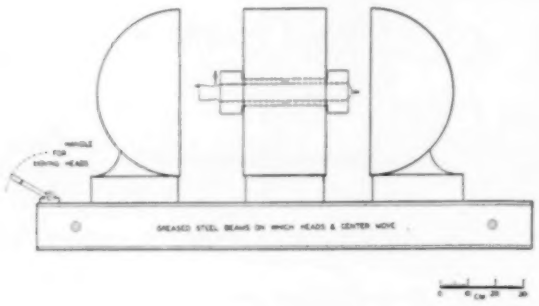

FIG. 2. Complete counter and shield assembly.

[2] Libby, Phys. Rev. **42**, 440 (1932).
[3] Kovarik, Phys. Rev. **13**, 272 (1919).
[4] Rutherford, Chadwick and Ellis, *Radiations from Radioactive Substances*, pp. 52–53, The Macmillan Co., 1930.

every half-minute with sample being moved either over or away from counter every five minutes for as long an interval as was necessary to establish definitely the value of the activity. An illustrative calculation of the time necessary for an effect of given size is given later.

Fig. 1b shows the apparatus used for the determination of magnetic deflectabilities. The chamber has a heavily wound water-cooled solenoid around the central portion where the counter is. The sample cylinder is enlarged to the size of the chamber wall. The magnet produces fields up to 900 gauss over the counter region. Since the distance from the sample to the counter is 1.7 cm, the radius of the circle of motion of the particle just missing the counter under the most advantageous conditions of energy and direction of emission must be 0.85 cm and the $H\rho$ value of this limiting particle is 0.85 of the field in gauss for this condition. Consequently the determination of the limiting $H\rho$ values for a radiation consists of plotting the curve of activity against field strength and noting the lowest field just capable of annihilating the effect. This type of curve is illustrated by Fig. 7 for Nd_2O_3 beta-radiation. The magnet is cooled by a layer of copper tubing wound around the chamber in bifilar manner so as to keep the chamber temperature uniform. Movement of the sample cylinder is accomplished by tipping the chamber and the use of the shield is foregone. Needless to say, this particular apparatus will serve for relatively low energy radiations only but can be modified by use of a larger chamber for higher energy particles. D. Bocciarelli and G. Occhialini[5] first suggested and used this geometrical arrangement in their work on potassium. The cooling coil next to the chamber is necessary to prevent a gradual rise in the counting voltage due to heating of the chamber.

The instrument used to determine the sign of the charge of a magnetically deflectable particle consists of the deflection instrument itself modified by the insertion of sloping vanes between sample and counter, as shown in Fig. 4. Four sets of readings are taken, two of them with sample over the counter and the field direction reversed automatically at regular intervals by an adaptation of the ratchet wheel mechanism mentioned

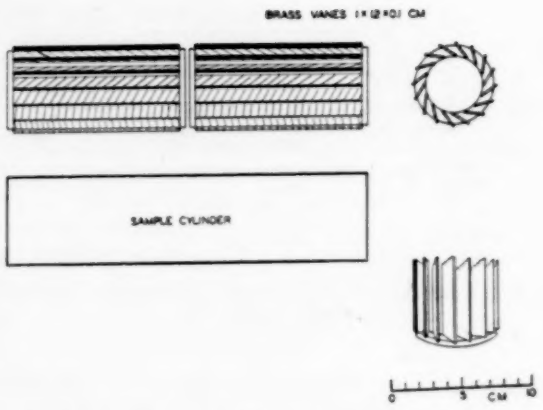

FIG. 4. Vanes for insertion in deflection apparatus to allow charge determination.

above; and the other two consisting of the readings with sample removed. The instrument was calibrated both by calculation of field directions and the effect with potassium radiation. The particles bending up from the sample when starting originally parallel to the vanes will obviously reach the counter more frequently than those curving oppositely.

The ranges of radiations in various gases are measured in the apparatus shown in Fig. 5. Two counters of approximately the same construction are placed in a large chamber with the sample deposited on the chamber wall over one of them. Two curves of count rate against pressure of gas are then run. The range of the radiation is determined from the lowest pressure at which the two curves start paralleling each other. The difference between the two count rates can be traced to the point at which it assumed a constant value. Curves of this kind are shown in Fig. 8 for

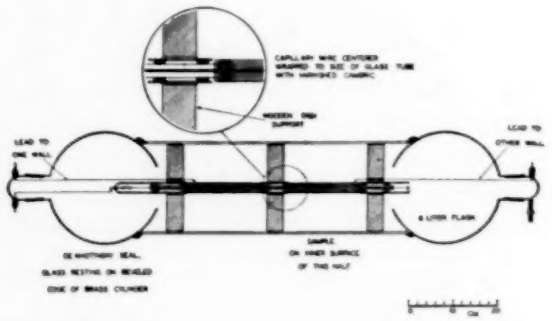

FIG. 5. Apparatus for determining ranges of α-particles in various gases.

[5] D. Bocciarelli, Nature **128**, 375 (1931).

samarium alpha-radiation. For the instrument shown the sample counter distance is 8.7 cm so a particle of 1 cm range should cease to be effective at a pressure of 8.7 cm of air, i.e., 76/87.

Characteristics of Counters

The general properties of screenwall counters are these: (1) In general, the properties of the counters agree with those of the solid wall type studied and reported upon so extensively by many workers.[6] (2) Each counter when in proper counting condition has a voltage range of from 10 to 100 volts within which the applied voltage can be varied without changing the count rate. However, the size of the "kicks" varies with the voltage in this interval and the amplification must be sufficient to prevent variation of kick size causing failure of mechanical counting. (3) Counters have been made with copper, aluminum and steel walls combined with wires of tungsten and of the above materials in the various possible ways. In none of these cases has it proved essential that the materials be cleaned or treated in any way other than to remove moisture. (4) The voltage-pressure curves are very dependent on the character of the gas. The noble gases apparently give flat portions at low pressures in the curves of voltage against pressure. (5) Very pure helium is not a good gas to use. It is difficult to get the voltage adjusted correctly, and the permissible voltage range appears to be smaller than for the less pure gas. (6) Counter heads should have high resistances to prevent spurious counts due to leakage currents from wall to wire. They should center the wire accurately to insure the maximum size of the counting voltage range. (7) The counters are often photoelectrically sensitive, especially if aluminum is present. Copper and iron both show the effect under the proper conditions.

Photoelectric Effect and Sensitivity of the Counters

Necessarily, the question of the sensitivity of the counters to particles of the lowest energy must be considered because of its bearing on the significance of negative results obtained from certain elements. Certainly one cannot say with assurance that failure to observe radiations of the more common ionizing powers indicates inactivity of any sort, especially in view of the low energy radiations from samarium and neodymium discussed below.

Fortunately, the photoelectric effect serves to establish the requisite sensitivity. Experimentally, the effect is most obvious with counters having aluminum screen walls. In fact, as many as 100 photoelectrons per minute have been counted from a wall area of 2 or 3 cm^2 with a 150-watt tungsten lamp at 5 or 6 feet. The chamber walls of 2 mm Pyrex glass as well as the bulb glass intervened. The phenomenon must be associated with the screen wall rather than the wire of the counter, for changing from aluminum to copper screen of the same mesh and wire size changes none of the counter characteristics except the response to light. Copper and iron emit photoelectrons in appreciable number when illuminated by direct sunlight. Most screen aluminum shows the effect but certain samples were found which did not until they had been cleaned with acid.

Since the Pyrex glass used is known to pass no light below 3000A and the photoelectric thresholds for iron and copper are given values in the I. C. T. between 2665–3050A for mechanically cleaned surfaces, it becomes clear that the instrument must be capable of counting electrons of very low energy. As a further, more quantitative test, the photoelectric threshold of the aluminum screen was determined by means of a monochromator with a tungsten lamp source. The procedure was to build a counter about the length of the monochromator slit, shield it from all light except that coming from the slit and observe the setting of the monochromator when the count rate became equal to the zero rate. A value of 5000A was found. The highest value given in the I. C. T. is 4770 and the average of all values given is 3900.

At first thought one might conclude that these results are of little significance as to the ability of the counter to detect low energy electrons because the voltage applied to the counter constitutes an accelerating potential of about (but not exceeding) 2000 volts per cm. This objection is answered rather conclusively, however, by the

[6] F. Burger-Scheiflin, Ann. d. Physik (5) **12**, 283 (1932); W. Schulze, Zeits. f. Physik **78**, 92 (1932); C. Bosch, Ann. d. Physik **19**, 65 (1934).

work of Lawrence and Linford[7] on the effect of high electrostatic fields on the photoelectric threshold of alkali metal surfaces. They checked the Schottky formula for the effect rather well and showed the effect for these surfaces to be thoroughly predictable. As an example, they found a field of 69,000 volts per cm to shift the limit for a potassium film deposited on tungsten from 5600 to 5900A. Assuming that the aluminum surface is not greatly different from potassium as far as this effect is concerned and with the formula they verified, it appears that a field of the order of that used in the counters should shift the threshold by about 30A providing the true threshold in the absence of a field is 4800A. These figures indicate that electrons are counted almost down to the threshold where they emerge from the metal with practically zero energy. At least they are counted when they have energies of 1 volt or so, since 0.05 volt corresponds to a shift of about 100A in the region of 4800A and these considerations have shown that the threshold as determined by the counter method is most probably within 100A of the true value. Consequently, the instrument must be capable of detecting any beta-ray that might be emitted from a radioactive body.

Furthermore, since alpha-rays necessarily have higher ionizing powers than betas, the above conclusion applies to them also. Finally, since gammas are recorded through their photoelectric secondaries they, too, must be included and the general conclusion that the method is capable of detecting any radiations of these types which can be emitted by a radioactive body is established.

Counting Efficiency

Having established the ability of the counter to respond to all possible radiations to some extent it is only necessary to demonstrate the high percentage of the eligible particles actually counted to establish the method as one of precision.

For example, the counter in the absolute activity apparatus shown in Fig. 1a, having a copper screen wall presenting 71 percent open space can be calculated by consideration of the solid angle subtended at each part of the sample by the counter and adding over the sample surface, to offer free passage to 14 percent of the particles from the sample. Since potassium is known[8] to emit 27,500 particles per half-minute per mole, the number passing through the counter must be 3850 per half-minute per mole of sample. The calibration experiments for the activity apparatus of Fig. 1a showed 3740 ± 200 counts per half-minute per mole of KCl in sample. The check seems quite satisfactory.

Statistical Distribution of Counts and Calculation of Error Limits

The question of the statistical distribution in time of the background radiation is of importance to this research only in that it indicates how the limits of error of the average results should be fixed. Bateman[9] has shown that the particles emitted from a radioactive body should be distributed in time according to a law requiring that the standard deviation from the average rate observed should be just the square root of that rate. This simple result might be expected to hold for the zero count in this work. Many data have been obtained in the course of this work which substantiate this. The details of this aspect of the work are to be submitted for publication separately. The probable errors given below have been calculated on the assumption that the average rate is sufficiently high to warrant the use of the error law relation that the probable error is 0.67 times the standard deviation.

The validity of the law allows its use to calculate the length of the runs necessary to establish definitely an effect of given size. With the activity instrument in the shield the rate without sample, zero rate, usually is about 15 per half-minute. By using this value, the length of the shortest satisfactory run to establish an effect of 1.0 count per half-minute with probable error of $\frac{1}{3}$ the effect can be calculated from the relation

$$0.6745 \times 2^{\frac{1}{2}}(15/(n/2))^{\frac{1}{2}} = 0.3$$

to have the value 300, n being the total time in half-minutes and $n/2$ the number of intervals with and without sample exposed.

[7] Lawrence and Linford, Phys. Rev. **36**, 482 (1930).

[8] W. Mühlhoff, Ann. d. Physik **399**, 205 (1931).

[9] H. Bateman, Phil. Mag. **20**, 704 (1910).

Methods of Proving Specificity of Activities Observed

Probably the most difficult phase of the problem of establishing the activity of a weakly active element is the proof that the activity observed is not due to minute amounts of known strongly active substances. In general, impurities of this sort present in such small amounts as 10^{-12} grams per gram vitiate any effects that could be expected. Three general methods of attack are used. The first consists of chemical purification of the substance investigated, observing any change in the activity resulting; the second depends upon observation of marked differences between the properties of the radiation and that of any previously known type; and the third is the checking of the growth of the activity after purification to a constant final residual activity against the growth curves for known radioactive substances.

Removal of such small amounts of impurities is most easily accomplished by the general method of co-precipitation. A considerable amount of a homologue of the impurity being removed (for example, Ba^{++} for Ra^{++}) is placed in solution with the substance being purified and a reagent added to precipitate the homologue of the impurity without taking out the substance purified. The co-precipitation methods, in general, prove adequate if the operation is repeated once or twice. The removal seems to be unexpectedly thorough, possibly because of a general covering up of the radioactive precipitate before it has opportunity to come to equilibrium with the solution and redissolve. All of the known radioactive substances which have sufficiently long lives to contaminate seriously a sample are homologues of sodium, barium, lanthanum, zirconium, tellurium, lead or the noble gases.

Obviously, it will prove difficult, in general, to purify any one element from all of the above. For example, the rare earths cannot easily be freed of traces of actinium and mesothorium. Consequently, there usually remains some doubt as to the source of any residual activity after all of the possible purifications have been carried out. This can sometimes be removed by allowing the sample to stand and by determining its activity at intervals as well as noting any changes in its characteristics such as penetrating power, deflectability, etc. Since the most probable impurities are those which have no homologues precipitated chemically, the growth curves and general changes in penetrating power, etc., to be expected from them are known and generally make the data obtained highly pertinent. Of course, it is possible that the character of the radiation after purification may obviate the growth curve step.

Results

Beta-radioactivity of neodymium[9a]

Samples of neodymium salts prepared by the late Professor James of New Hampshire and by Professor B. S. Hopkins of Illinois, as well as others of unknown history, were used. The first measurements on all of them showed a definite activity which seemed to have about the same value for all. However, thorough purification reduced the activity to a final residual value which was the same for all of the samples. All samples were changed to Nd_2O_3.

Since the rare earths cannot be readily purified of traces of actinium, the significance of this final residual activity was not clear. One sample was therefore purified as thoroughly as possible for all other possible impurities, and allowed to stand for seven months. After that time the activity was found to be unchanged within fifty percent. In addition, absorption experiments showed that 5 mm of air completely absorbs the radiation. These tests were made by placing thin screens over the sample in the activity counter, Fig. 1a, and also by varying the gas pressure in the deflection instrument, Fig. 1b, when there was no magnetic field present. For example, a pressure of 3 cm of air in the last case gave an absorbing layer of 0.6 mm. The data from one of these runs are presented in Fig. 6.

Magnetic deflection experiments were then performed. It was found possible to bend the hardest of the radiation into circles of 7.5 mm radius or less by a field of 500 gauss. Fig. 7 shows these data. The abscissae are the $H\rho$ values of particles which would just miss the counter under the most favorable conditions of emission and with the given field. The maximum $H\rho$ value

[9a] A brief report on this work has appeared previously. Libby, Phys. Rev. **45**, 845 (1934).

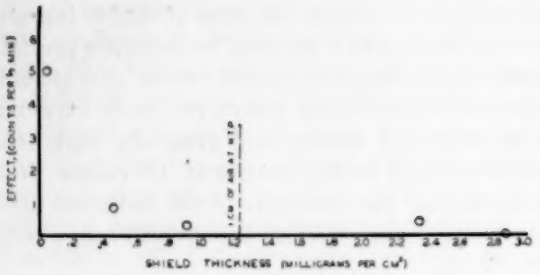

FIG. 6. Absorption curve for Nd beta-radiation.

apparently is close to 355, which agrees well with the observed range according to the data of Schonland[10] on cathode rays. This means a range of 2.4 mm in air at atmospheric pressure and 15°C.

These data seem to make the presence of any of the members of the known radioactive series in significant amounts extremely improbable. The possible presence of a rare earth impurity (such as element 61) which might emit such a radiation was checked by repetition of the deflection experiments with samples of samarium, lanthanum and praseodymium, none of which showed a deflectable radiation of intensity greater than one-third of that of neodymium. The intensity of the alpha-radiation from the samarium was about ten times that from the neodymium samples in the absence of a field.

There are two aspects of the growth curve data. The first is the relatively small change in the total activity and the second is the low penetrating power of the whole of the final radiation. Calculations for actinium itself show that there should have been over a two-fold increase in total activity but, more important, more than two-thirds of the final effect should have been due to alpha-rays, all of greater penetrating power, of course. It should be mentioned also that the whole notion of actinium itself acting as a detectable radioactive substance is improbable because of the known fact that its transition has never been detected except through its products. Calculations were also carried through for RaD, assuming that somehow it might give beta-rays of the right character. After seven months its activity should nearly have tripled in intensity and

[10] Schonland, Proc. Roy. Soc. (London) **A104**, 235 (1923); **A108**, 187 (1925).

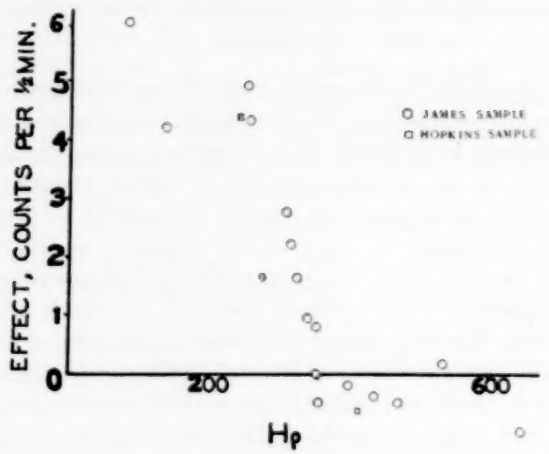

FIG. 7. Effect of magnetic field on Nd beta-radiation.

should have come to consist of 36 percent of beta-rays with $H\rho$ larger than 600 but less than 1200, 39 percent of betas with $H\rho$ larger than 1200, and 25 percent of alpha-radiation.

At this stage of the work the discovery of induced radioactivity with the emission of positrons from short-lived intermediates in transmutation processes was announced. It then seemed essential to determine whether the neodymium case was one of positron emission by definitely establishing the charge of the particles. This was done with the instrument previously described and shown in Figs. 1b and 4. Runs were made during which the sample was left in one position, either over the counter or away from it, readings were taken every half-minute, and the direction of the flow of the current was reversed every five minutes. The whole was done automatically as previously indicated. The best set of results is given in Table I.

TABLE I. *Count per half-minute.*

	Negatives pass	Positives pass	Effect
Sample present	23.37±0.108	23.07±0.107	0.30±0.15
Sample absent	23.38±0.108	23.98±0.110	−0.60±0.15

Each of the four values given is the mean of about 900 readings. The runs with sample present and sample absent were made on different days and the absolute values are therefore not significant. The effect, 0.90±0.22, of the addition of the sample appears conclusive. The effect indicating low energy positives from the wall in the absence

of the sample remains unexplained but definite. Further work will be done on this point.

Calculation of apparent half-life of neodymium

In order to calculate the specific activity it is necessary to calculate the thickness of the sample from which no emitted particles will fail to count because of self-absorption in the sample. It is assumed that this layer has a thickness just the range of the particle in the sample. Necessarily this introduces an error tending to make the effective sample assumed somewhat too large and making the rate of decay calculated too small. The data of Schonland[11] give 2.75×10^{-4} grams per cm² as the range of electrons of $H\rho$ value 355. This requires the saturated layer to have 8.18×10^{-7} moles per cm². The air interceding between sample and cylinder was 0.253×10^{-4} grams per cm², so the saturated Nd_2O_3 layer should have 7.43×10^{-7} moles per cm² or 1.435×10^{-4} moles for 193 cm².

Table II shows the results of three runs on the rate of emission of particles from the saturated layer.

TABLE II. *Counts per half-minute from 193 cm².*

46.1×10^{-7} moles/cm²	4.7 ± 0.7
90.8×10^{-7} moles/cm²	6.0 ± 0.9
Not measured, but approximately the same	5.0 ± 0.8
Average (weighted according to length of run)	5.2 ± 0.5

These data show that the effect per mole of sample is $(3.6\pm0.35)\times10^{4}$ counts per half-minute. A standardization run with KCl gave 3740 ± 220 for the effect from K. By assuming the neodymium betas to be just as efficient in counting as those of K because of the large openings in the screen wall and by using the data of Mühlhoff[12] on the activity of potassium, the decay constant has the value

$$\mathrm{Nd}=\frac{36{,}400\pm3500}{3740\pm220}\times1.5\times10^{-21}$$
$$=(1.46\pm0.20)\times10^{-20}\,\mathrm{sec.}^{-1}.$$

The apparent half-life of neodymium therefore cannot exceed 1.46×10^{12} years and is probably close to half that value.

Alpha-radioactivity of samarium

A samarium sample prepared by Professor James was used throughout this work. The activity of the element was easily detected and the extraordinary characteristics of the radiation in being wholly absorbed by a shield of stopping power 1.3 cm of air made it seem specific. Notice of the excellent work of Hevesy and Pahl[13] appeared at this time, clearly establishing the radiation as belonging to samarium itself. The range and decay constant were then measured.

The instrument shown in Fig. 5 was used to measure the range. Oxygen gas was employed at temperature of 25°C. Fig. 8 shows the data for

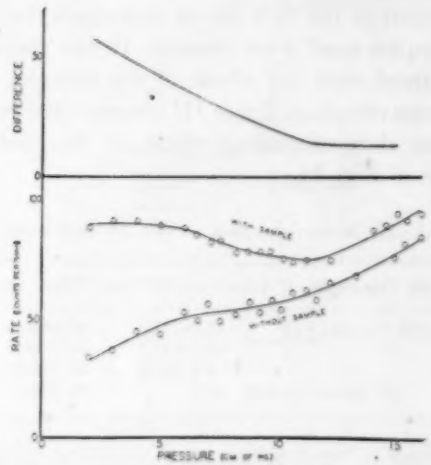

FIG. 8. Effect of pressure on count rates for counters in range finder with Sm sample.

one of the runs, the lower curve in both representing the activity of the counter without the samarium sample and the upper that with the sample. The significant pressure is, of course, that at which the difference between the two count rates becomes constant, showing that the samarium alphas are no longer counting. The curves apparently give the critical pressure at 11.2 cm of Hg. Another run gave the same value. Since the distance between the counter and the sample was 8.7 ± 0.1 cm, the equivalent distance at 76 cm at 15°C would be

$$8.7\times(11.2/76)\times(288/298)=1.236\text{ cm}$$

in oxygen which is the range value. The results of Gurney[14] on the relative stopping powers of oxygen and air for alpha-particles show that within one or two percent the average stopping

[11] Schonland, Proc. Roy. Soc. (London) **A104**, 235 (1923); **A108**, 187 (1925).
[12] Mühlhoff, Ann. d. Physik **399**, 205 (1931).
[13] Hevesy and Pahl, Nature, **130**, Dec. 3 (1932).
[14] Gurney, Proc. Roy. Soc. (London) **A107**, 340 (1925).

powers for alphas ranging uniformly from zero to 1.2 cm in range must be the same. Therefore the value for the range in air at N. T. P. found is 1.23 ± 0.05 cm, the error estimate being an upper limit.

The calculation of the range of the 1.23 cm particle in Sm_2O_3 is complicated by the deviations from the Bragg-Kleeman rule for atomic and molecular stopping powers for alpha-particles of short range. The best value is apparently close to 4.9×10^{-4} cm or 1.01×10^{-5} mole per cm^2. This figure is not of much importance to the following calculation of the half-life of samarium, because the samples used were thinner. It can therefore be assumed that the whole of the samples used have been effective. Table III presents the results of three determinations made in the activity counter of Fig. 1a.

TABLE III. *Samarium effect (counts per half-minute).*

Sample thickness	Effect for 193 cm^2	Effect per mole
0.0441×10^{-5} moles/cm^2	16.0 ± 0.9	$80,000\pm 6,000$
0.152	53.5 ± 0.2	$91,800\pm 3,400$
0.0153	5.1 ± 0.8	$89,500\pm13,000$
Weighted average		$88,900\pm 2,900$

$$\mathrm{Sm}=1.5\times10^{-21}\times\frac{88,900}{3740}$$
$$=(3.56\times0.1)\times10^{-20}\mathrm{sec.}^{-1}.$$

The value for the half-life is $(6.3\pm0.5)\times10^{11}$ years. Both the values for the range and activity differ somewhat from those of Hevesy, Pahl and Hosemann.[15] The range value is slightly larger than the 1.13 reported by these authors, in accordance with their belief that their value might be slightly low. The discrepancy between the values for the specific activity is perhaps larger than one might have hoped. It is perhaps pertinent that the samarium samples used in this research were never purified from radioactive impurities as carefully as possible because the radiation was found to have no component capable of penetrating more than 1.5 cm of air. If such a component were present it could not possibly have constituted more than 10 percent of the total radiation. It has been observed several times that thick samples gave concordant results only when the limitation of solid angle for deep particles was taken into account as in the formula of Evans.[15a] Application of this formula to the data of Hevesy, Pahl and Hosemann gives the half-life obtained in the present work.

Other elements

Praseodymium, gadolinium, tin and iodine have all been tested for activity. It is difficult to express the limiting values for the decay constants because they depend on the ranges of the particles which might be emitted. However, it can be said with considerable certainty that none of the above elements can emit particles of range greater than 1 cm of air and at the same time have a half-life less than 10^{14} years.

Beryllium

As previously reported,[16] no activity has been found in BeO samples purified sufficiently well. Measurements were made sometime ago with the activity counter represented in Fig. 1a when the sample cylinder was maintained at a sufficiently negative potential with respect to the counter wall to place the sample effectively inside the counter with the sample cylinder as its wall. These substantiated the limit of possible activity for particle emission mentioned in the above publication. The results can be summarized in the relation

$$t_{\frac{1}{2}}>1.1\times10^{15}R,$$

in which $t_{\frac{1}{2}}$ is the half-life in years and R is the range of any emitted particle in cm of air at N. T. P. This relation is most rigorous for alpha-particles but is not greatly in error for beta-particles.

The author wishes to express his deepest gratitude to Professor W. M. Latimer for the invaluable advice and criticism he has given the author throughout this work. He is also much indebted to Mr. D. E. Hull for assistance in the experimental work.

[15] Hevesy, Pahl and Hosemann, Zeits. f. Physik **83**, 43 (1933).

[15a] Evans, Phys. Rev. **45**, 29 (1934).

[16] Libby, Phys. Rev. **44**, 512 (1933).

Molecular Spectrum of Cadmium Vapor

S. Winston Cram, *University of Wisconsin*

(Received May 17, 1934)

The fluorescence and discharge spectra between 1900A and 5000A of Cd vapor were observed when the vapor was excited under various conditions. The observations include: emission of band spectra between 2212 and 2288 in both spectra, the process of excitation of some of the fluorescence spectrum, and a general summary of the Cd band spectra. Potential energy-nuclear separation curves for the Cd molecule are concluded from these observations and from the results to be presented in another paper.

THE band spectrum of Cd has been observed under a wide variety of conditions. It has not been possible to determine the molecular constants of Cd by the usual method of band analysis because none of the bands observed show rotational structure. The only way in which information concerning these constants has been obtained is through comparison of different types of spectra and through changes of intensity with variation in experimental conditions.

Previous observation on absorption, fluorescence and discharge spectra are summarized in Table I.

The limits of the bands change somewhat with change in vapor pressure—in this table the spectra listed are for a vapor pressure of approximately 80 mm of Hg unless otherwise stated.

The present work was undertaken to extend the observations on the band spectrum of Cd with the purpose of obtaining more information concerning the properties of the Cd molecule.

Experimental Procedure

The experimental arrangement is given by Fig. 1. The quartz tube AB was set in two adjoining furnaces allowing control of both temperature and pressure in the portion A. The vapor could be excited either by the light from a spark or by a low voltage Tesla coil through external electrodes. Condensed sparks between terminals of Cu, Zn or Al served as light sources. When the vapor was excited with light from a spark, the short wave-length limit and the intensity could be controlled by use of filters and mesh screens, respectively. The filters were thin pieces of Pyrex glass. The mesh screen used had a transmission coefficient of 25 percent. The

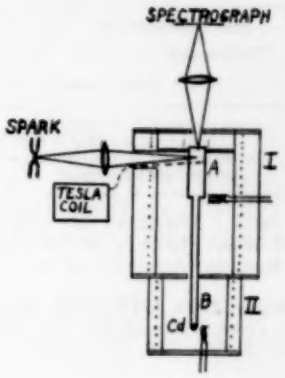

Fig. 1.

resulting emission from either type of excitation (fluorescence or discharge) was analyzed with a quartz spectrograph.

Exposures made with the tube cold showed that the intensity of scattered light was negligible.

Each tube (eight different ones were used) was prepared by evacuating and baking at 800°C for 32 hours and at 1000°C for eight hours. Cd was then distilled into the tube and it was sealed off. Five different samples of Cd were used. Tl was added to one sample and CdO to another to determine the effect of these impurities. The purest sample was electrolytic Cd which had been distilled five times in a vacuum. Unless otherwise stated, all exposures were taken at a temperature of 600°C (80 mm vapor pressure) in furnace II and about 650°C in furnace I.

Eastman Speedway and Process plates were used both with and without an oil coating. Exposures for fluorescence pictures varied from 15 minutes to eight hours. Electrodeless discharge exposures varied from one to 30 minutes.

TABLE I. *Previous observations of absorption, fluorescence and discharge spectra of Cd.*

Band Spectra of Cd

Absorption	Fluorescence: Wave-lengths in exciting light	Fluorescence: Bands observed	Discharge
a. 2125[1] a narrow band extending 1990–2150, maximum 2110–2140, faint from 1990–2110.	a. Below 2125	a. 2125[1] a narrow band extending 2110–2140.	a. 2125[7] a narrow band extending 2110–2140 with maximum at 2124.
b. 2212[2] a narrow band broadens toward long wave-lengths at high pressure.	b.	b.	b.*
c. 2288[3] a broad band extending 2212–3050 at high pressures. Flutings[5] between 2590–2825.	c. Below 3000	c. 2288[4] a broad band extending 2260–3050. Flutings 2700–3050.	c. 2288[7] continuous band extending 2191–3050 (pressure not given).
d. 3178[3] a narrow band at high pressures.	d. Below 3178	d. 3178[3] a narrow band.	d. 3178[7] a narrow band.
e. 3261[2] resonance line with band overlying it.	e. Below 3261 2600–3261	e. 3261[4] resonance line with band overlying it. 3261 appears with weak intensity.	e. 3261[7] resonance line with band over lying it.
	f. Below 3000	f. 4000[6] broad band extending 3800–5000.	f. 4058[7] a broad band extending 4058–5400.

Line Spectra of Cd

Fluorescence: Wave-lengths in exciting light	Fluorescence: Lines observed
a. 1850–2125	a. Sharp triplet[9, 10] ($5^3P_1 - 6^3S_1$) Diffuse triplet ($5^3P_1 - 5^3D_{123}$)
b. 2300–3050	b. Some lines of the exciting source re-emitted by the vapor.[9]

* 2212[2] a narrow band (pressure 0.1 mm) probably due to impurity.

[1] Jabłonski, Zeits. f. Physik **45**, 878 (1927).
[2] Mohler and Moore, J.O.S.A. **15**, 74 (1927).
[3] Jabłonski, Bull. de l'Acad. Pol. d. Sc. et d. L. **10A**, 163 (1928).
[4] Van der Lingen, Zeits. f. Physik **6**, 403 (1921).
[5] Mrozowski, Zeits. f. Physik **62**, 311 (1930).
[6] Kapuscinski, Nature **116**, 170 (1925).
[7] Hamada, Phil. Mag. **12**, 50 (1931).
[8] Robertson, Phil. Mag. **14**, 795 (1932).
[9] Kapuscinski, Zeits. f. Physik **41**, 214 (1927).
[10] Miss Kalinowska, Comptes Rendus **196**, 168 (1933), observed that this triplet was excited by a single absorption process at high vapor pressures.

RESULTS

Fluorescence

(a) When the vapor was excited by the total radiation from a Cu spark all the fluorescence bands and lines described in Table I were observed.

To determine the wave-lengths effective in exciting different lines and bands the wave-length and the intensity in the exciting light were varied.

With light of wave-length greater than 1990A from a Cu spark as source, the intensity of the 2125 band relative to the 2288 band was the same as with the total radiation from the Cu spark as source. The intensity of the sharp triplet was reduced to about 1/100, and the diffuse triplet could not be observed.

With light of wave-length greater than 1930 from an Al spark as source the 2125 band was too weak to be observed and the intensity of both the sharp and the diffuse triplet relative to the 2288 band was reduced to about 1/5 that with the total radiation from the Al spark as source.

Following a method used by Wood,[11] the amount of emitted radiation from the tube was reduced by placing the mesh screen first between the spark and the cell and then between the cell and the spectrograph. Equal intensity for the two cases indicated that the initial level for the transition was excited by a single absorption process. If the first case appears with 1/4 the intensity of that of the other case, a two-fold absorption process is indicated. The results distinctly showed the initial levels of the 2125 band and the sharp triplet to be populated primarily by a single stage absorption, and those of the diffuse triplet by a two-stage process. This agrees with Miss Kalinowska's[10] results for the sharp triplet.

(b) & (c) The Van der Lingen[4] fluorescence band (2288–3050) was found to extend from 2212–3050 (Fig. 2) with a broad reversed portion at 2288. The 2212–2288 part of the band was much weaker than the remainder of the band.

It was also found that lines from the exciting light of wave-lengths between 2212–2288 were re-

[11] Wood, Phil. Mag. **6**, 352 (1928).

FIG. 2. Cd fluorescence excited with Cu spark.

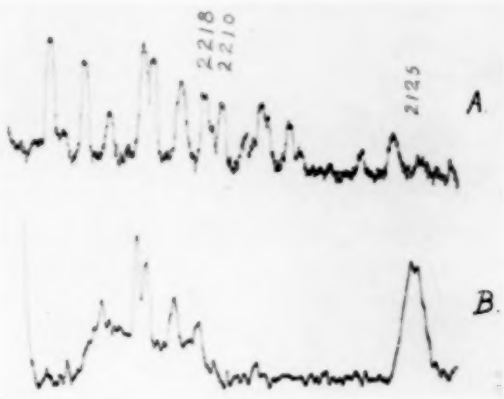

FIG. 3. Microphotometer curves: (A) Cu spark (B) Cd fluorescence.

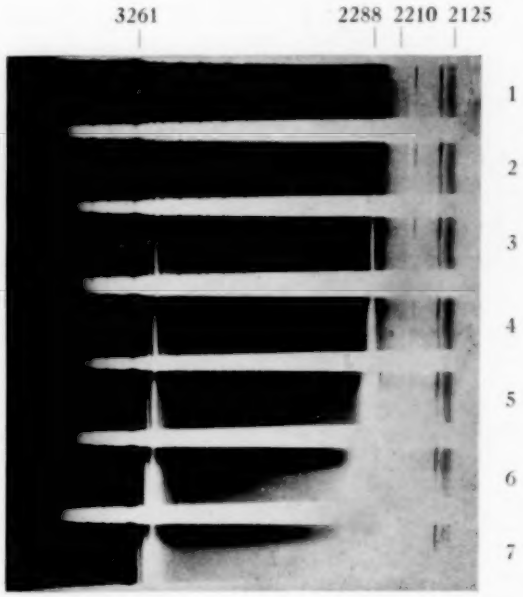

FIG. 4. Electrodeless discharge spectrum of Cd (1) 25 mm, (5) 125 mm, (7) 350 mm.

emitted by the Cd vapor in the same manner as previously found[9] for lines between 2300–3050. In Fig. 3 A and B are microphotometer records of the source and the fluorescence, respectively. The fluorescence showed a continuous band from 2212 to 2288 with five re-emitted Cu lines (2218, 2229, 2243, 2247, 2264) superimposed. If the lines were due to scattered light, the strong Cu lines between 2218 and 2125 should have appeared along with these five. The short wave-length limit for re-emission must fall between 2218 and 2210, since the 2210 Cu line does not appear. The short wave-length limit for the fluorescence band is about 2212.

Forty flutings were observed between 2560 and the long wave-length end of the 2288 band. These agreed within the error of measurement with the absorption flutings between 2590 and 2825 measured by Jablonski[3] and Mohler and Moore,[2] and the fluorescence flutings between 2627 and 3050 measured by Kapuscinski.[12]

Discharge spectra

(a) When the Cd vapor was excited by the Tesla coil, all the discharge bands described in Table I were observed except Robertson's[5] 2212 band.

Fig. 4 shows discharge spectra at different vapor pressures of Cd. At high pressures the 2125 band is reversed at the wave-length of maximum intensity for lower pressures (2124). This shows that the emission maximum coincides with the absorption maximum.

(b) & (c) At low pressures the 2288 band extends from 3070 to a sharp edge at 2210, and at high pressures the limits are 3070 and about 2300 as shown by Fig. 4. At high pressures the part from 2300–2210 is absorbed by the Cd vapor.

The 2288 band showed only six of the series of 40 flutings observed in fluorescence. These six coincide with the six fluorescence flutings between 2780 and 2870. Another set of flutings of smaller separation, originally found by Hamada, extending from 2890–3070 appeared with more intensity than the 2780–2870 flutings. However the intensity of the 2890–3070 flutings relative to that of the 2780–2870 flutings does not appreciably change with pressure.

The observation of only six of the 40 fluorescence flutings may be due to the superposition of the 2890–3070 series and the Cd arc lines on the 2288 band.

[12] Kapuscinski, Bull. de l'Acad. Pol. d. Sc. et d. L. **10A**, 1 (1927).

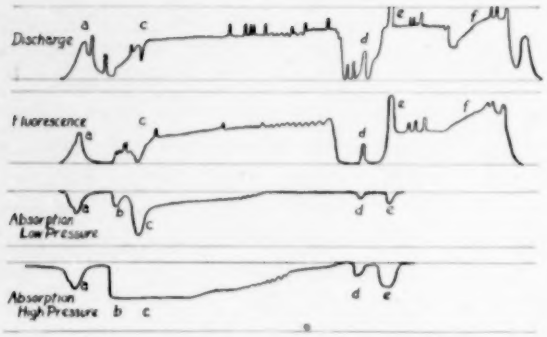

FIG. 5. Graphic description of Cd band spectra.

Effect of purity

Effects due to impurities were determined by comparing the spectra of the different samples of Cd. Very small amounts of impurity did not materially affect the observations made at high vapor pressures. In the discharge it was observed that lines due to impurities and Cd arc lines which appeared at low Cd pressures became very weak in comparison to the intensities of the Cd bands at high Cd pressures.

There was no evidence of the band at 2212 reported by Robertson.[8] Since he observed this band at low pressures, in fact much lower than those at which any other Cd band spectra has been observed, it was very likely due to an impurity.

Since the 2890–3070 discharge flutings do not become weaker at high pressures they are probably due to Cd.

Fig. 5 is a chart giving the absorption, fluorescence, and discharge spectra of Cd as they have been observed.

DISCUSSION

Since we interpret the observed bands in terms of absorption and emission by Cd molecules, it is interesting to see what knowledge of the potential energy-nuclear separation curves can be gained from the data.

A calculation giving the general characteristics of the potential energy-nuclear separation curves for molecules of this type will be published elsewhere by Professor J. H. Van Vleck.[13] These characteristics determine the general shapes of the curves concerned; the observed data were applied only to determine the relative position and magnitude of their maxima and minima. Fig. 6 gives the results of this application when due consideration is given the following general principles:

The Franck-Condon principle states that for all transitions the position and momentum of the nuclei are unchanged. Mulliken[14] has shown that the nuclear separation r_0 must be fairly small in stable molecules (i.e., large heat of dissociation D). It has been found empirically that for different states in one molecule the expression $\omega_0 r_0^2$ is approximately constant. If the intensity distribution in a band is the same in the absorption spectrum as it is in the emission spectrum, then r_0 of the initial state is equal to r_0 of the final state.

Kuhn's[15] recently determined value of D, as well as other previous evidence, shows that the minimum of curve b must be very shallow. The Van der Waal force associated with this curve varies as the inverse sixth power of the nuclear separation.

The $5^1S_0+5^1P_1$ level splits up into two components, b and c, at small values of r. The minima of these two components are at approximately the same r_0''. The broad 2288 band necessitates a very deep minimum in c (i.e., large D''), from this it follows that $r_0''<r_0'$ and therefore $\omega_0''>\omega_0'$. Thus the minimum of

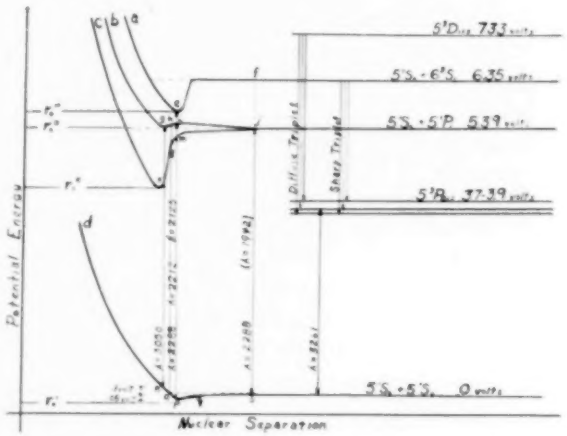

FIG. 6. Potential energy curves for the Cd molecule.

[13] Van Vleck, a paper to be published soon.

[14] Mulliken, Phys. Rev. **32**, 186 (1928).

[15] Kuhn and Arrhenius, Zeits. f. Physik **82**, 716 (1933).

curve c must be as shown in Fig. 6. Such a conclusion allows an explanation of other observations if the life period of molecules in this state is too short for a Boltzmann distribution of molecules among the vibrational levels to form. For this would account for the fairly intense emission between 2288 and 3050, as well as the re-emission of line spectra in this region, corresponding to transitions from all the vibrational levels along $k\,l\,m$ to $n\,o\,p$. The large separation and the breadth of the fluorescence flutings in the 2288 band can be understood from the steep slope of $k\,l$ and the fact that $n\,o$ is an unquantized portion of curve d.

The re-emission of line spectra by the vapor can be explained as a resonance absorption and emission process between the unquantized portion of the initial state and some vibrational level in the final state (curves b or c). A short life period in the excited state would give sharper resonance, i.e., if short enough so that the population of an excited level cannot be reduced materially through a collision process.

The maximum of curve b is apparently almost directly above p, with separation corresponding to a wave-length of 2212, since the short wave-length edge of the 2212–2288 band in emission coincides with the short wave-length edge of the 2212 band in absorption.

The behavior of the 2288 absorption band with increasing vapor-pressure[16] can perhaps be understood if $q\,s$ is quite long and flat for at low pressures the statistical number of quasi-molecules existing between q and s is greater than the number existing between o and p.

Curve a must have its minimum directly above that of curve d since the maximum of intensity of the 2125 band is at the same wave-length in both the absorption and the emission spectra; that is r_0''' is about equal to r_0' and ω_0''' nearly equal to ω_0'.

At high vapor pressures the sharp triplet can be excited by a single absorption process if the excitation energy is 6.2 volts or greater. This fact indicates that the potential energy curve associated with the 6^3S_1 atomic energy level has a minimum at nuclear separations of approximately r_0'. So it is natural to associate curve $a\,e$ with the 6^3S_1 level,[17] particularly since it is the first atomic level above e. If the life period of the molecules in this state is long, one would expect transitions only from the lowest vibrational levels of e.

These curves differ somewhat from those suggested by Kuhn.[15] The van der Waal forces involved in curves b and c have been found[13] to vary as the inverse cube power of the nuclear separation, but the sign of this force is the opposite for the two curves involved. Thus the van der Waal force associated with curve b is repulsive instead of attractive as the Kuhn[15] curves suggest. The reasons for the other differences between these and Kuhn's curves follow from the observations presented.

Finkelnburg[18] showed curve b for Hg_2 as a pure repulsion curve. For Cd_2 it is necessary for it to have a minimum in order to account for the re-emission of lines between 2288 and 2212. From curves b and d the energy of dissociation of Cd must be less than $(pi-sj)$, i.e., (0.2 volts) the value given by Winans.[16]

In conclusion the writer wishes to express his thanks and appreciation to Professor J. G. Winans under whose direction this work was carried out, and to Professor J. H. Van Vleck for his helpful advice.

[16] Winans, Phil. Mag. **7**, 555 (1929).

[17] There is, however, no positive proof that curve $a\,e$ is not associated with the 6^1S_0 atomic level.

[18] Finkelnburg, Phys. Zeits. **34**, 529 (1933).

On Abnormal Rotation of Molecules

O. OLDENBERG, *Physical Research Laboratory, Harvard University*

(Received June 9, 1934)

Hypothetical statements, explaining the abnormal rotation of molecules observed in band spectra, are tested by the investigation of the OH bands. It is known that the OH radicals are excited in the electric discharge through water vapor by simultaneous dissociation of H_2O and excitation of OH. As expected, strongly *abnormal* rotation is observed in the *emission* spectrum. On the other hand, the *absorption* spectrum of OH in the electric discharge showing *normal* rotation, confirms the assumption just mentioned regarding the excitation process. By addition of helium the rotation observed in emission is reduced to its normal value; no appreciable persistence of rotation in collisions is evident. In order to judge whether in a given source the temperature can be derived from the *rotational* structure of the band spectrum, tentative rules are deduced from a review of the known processes by which abnormal rotation may be produced or destroyed. The intensity distribution of the *vibrational* structure of a band spectrum indicates the temperature of the gas only in special cases.

I. PROBLEM AND PREVIOUS WORK

THE intensity distribution within a single band of a molecular spectrum, indicating the rotation of the molecules, is ordinarily determined by the temperature. Hence it serves for the measurement of temperatures in stellar atmospheres and electric discharges. In the electric discharge the molecules, emitting the spectrum which is being observed, have just suffered an excitation by electron impact; nevertheless their rotation indicates the temperature because it is not affected to any considerable extent by electron impact. This is understood on the basis of the laws of impact since in the collision between a light and a heavy body no appreciable exchange of kinetic energy takes place. Moreover, it is confirmed by experiments of Harries[1] investigating the kinetics of electrons diffusing through bimolecular gases.

In view of this important method for the determination of temperatures, some striking exceptions are of interest because the intensity distribution in single bands leads to apparent temperatures of several thousand degrees, although the experiments are performed at approximately room temperature. In previous papers[2] two elementary processes have been suggested hypothetically explaining these abnormal "rotational temperatures." An example for one process is the excitation of HgH molecules by impact of the second kind with excited Hg atoms; experimental proof for this process will be published soon by F. F. Rieke.[3] The other hypothetical process and its experimental confirmation are the objects of the present paper.

It was discovered by Lochte-Holtgreven[4] that the C_2 and CH bands excited in the electric discharge through acetylene (HCCH) gas show abnormal rotation. This has been interpreted by the following hypothesis: The excitation of the HCCH molecule by electron impact leads to a vibration so strong that the excited molecule dissociates into fragments, one of which is excited. This type of process is well known in a diatomic molecule such as I_2, which when dissociated by electron impact or absorption of light, goes over into a pair of atoms one of which might be excited. The energy of *translation* of the atoms so produced is abnormal—that is, independent of the temperature and in most cases much higher than the thermal value—and is determined by a relation between certain potential curves describing the laws of force of the normal and excited molecule. A *polyatomic* molecule in the analogous process ought to produce molecular fragments with abnormal *translation*, *vibration* and *rotation*. Again, all energies are determined not by thermal equilibrium but instead by a molecular excitation process best described by potential curves. The abnormal *translation* cannot be observed easily. The abnormal *vibration* is not characteristic for this process alone, since the vibration of the

[1] W. Harries, Zeits. f. Physik **42**, 26 (1927).
[2] O. Oldenberg, Phys. Rev. **37**, 194 (1931) and **37**, 1550 (1931).
[3] Cf. F. F. Rieke, Phys. Rev. **42**, 587 (1932).
[4] W. Lochte-Holtgreven, Zeits. f. Physik **67**, 590 (1931).

excited state far exceeds the thermal value anyway in most molecular spectra. The abnormal *rotation* of an excited fragment, for example CH, is to be observed unless it is reduced to the thermal value during the lifetime of the excited state by a large number of collisions. Evidently the simultaneous dissociation of the polyatomic molecule and excitation of one of the fragments are characteristic for this process.

The present paper deals, first, with an experimental proof for this hypothesis derived from the abnormal intensity distribution in the OH bands and, secondly, with the experimental reduction of this rotation to its normal value. In the last section some general rules are tentatively derived.

II. Abnormal Rotation of OH Radicals

It has been stated by Bonhoeffer and Pearson[5] that in the electric discharge through water vapor the well-known OH bands at 3064A are excited in one process by simultaneous dissociation of H_2O and excitation of OH. This is concluded from the fact that even for the smallest current, when hardly any OH radicals are present, the intensity of the band is considerable, approximately proportional to the current. The simultaneous dissociation of H_2O and excitation of OH requires an energy of about 9 volts. Obviously it is highly improbable that electron impact should provide just the minimum value of energy required, without any excess, so that the H atom and the OH radical when parting have the kinetic energies of all degrees of freedom within the narrow range of the thermal value of about 1/40 volt. In the normal H_2O molecule the atoms form an angle of 105°, as derived by Mecke and Baumann[6] from the band spectra. The H atom when flying away is producing very probably some rotation of the remaining OH radical. Therefore, our hypothesis leads us to predict abnormal rotation for the well-known OH bands.

Actually, in the spectrum the high rotational energy levels show up with an intensity impossible to reconcile with thermal distribution. For example, the line $P_1(29\frac{1}{2})$ comes out with considerable intensity, although from the temperature it is estimated that only one molecule in 10^{23} would have the corresponding rotational energy, evidently much too small a concentration. Thus the observation confirms the prediction that such a process of excitation leads to rotation entirely unrelated to the temperature.

This argument is supported by the absorption spectrum of OH radicals in the electric discharge. Since the fall of 1931 the absorption spectrum of OH has been studied at this laboratory by Dr. M. Grabau and the writer for the investigation of chemical processes. The spectra are to be calibrated with regard to the concentration of OH by an absorption spectrum of OH with known concentration.[7] Recently several failures to observe the absorption spectrum of OH at ordinary temperatures in experiments with electric discharges and chemical reactions have been reported.[8] A possible reason for these failures is that the experiments were undertaken with medium size spectrographs. Actually the most sensitive observation of *faint absorption* lines represents the same problem as the resolution of two *closely adjacent emission* lines. It requires a spectrograph of a resolving power comparable with the width of the absorption lines to be observed. Since the individual lines of the OH bands have a Doppler width of about 0.005A, the second order of a 21-foot grating, having a resolving power of 0.014A, is applicable although a still higher resolving power would be desirable. In this instrument, H_2O vapor with an electric discharge running clearly shows absorption of the strongest band 3064 of OH. The results of these experiments will be reported later.

For the present problem it is of interest that in absorption the single band is short; no trace of the high rotational lines appears. It is to be concluded that the radiating molecules with abnormal rotation do not originate from these OH radicals normally present in the discharge,

[5] K. F. Bonhoeffer and T. G. Pearson, Zeits. f. physik. Chemie **14**, 3 (1931); cf. W. H. Rodebush and M. H. Wahl, J. Chem. Phys. **1**, 606 (1933).

[6] R. Mecke and W. Baumann, Zeits. f. Physik **81**, 463 (1933).

[7] K. F. Bonhoeffer and H. Reichardt, Zeits. f. physik. Chemie **139**, 75 (1928), discovered the thermal dissociation of H_2O into OH and H at temperatures up to 1600°C.

[8] K. F. Bonhoeffer and T. G. Pearson, Zeits. f. physik. Chemie **14**, 1 (1931); P. Harteck, Trans. Faraday Soc. **30**, 139 (1934); W. Frankenburger and H. Klinkhardt, Zeits. f. physik. Chemie **15**, 440 (1932).

but instead from H_2O molecules by simultaneous dissociation and excitation. Evidently, after the radiation process the OH radicals are soon robbed of their abnormal rotation by thermal collisions and only after a somewhat greater interval are consumed in the chemical reaction.

III. The Reduction of the Rotation to its Normal Value

It seemed questionable whether or not the abnormal rotation could be reduced to its normal value by collisions during the lifetime of the excited state. In order to explain the abnormal rotation observed in some fluorescence experiments, alternative hypotheses have been offered, one assuming an extraordinary persistence of rotational energy even through thousands of collisions,[9] the other interpreting the observed spectra simply by the application of classical mechanics to the collision process.[10] These alternatives will be discussed in a paper by F. F. Rieke.

The persistence of rotation of the excited OH radicals is investigated in the following experiment. The rotation of OH is essentially a motion of a light particle, the H atom, circling about the heavier O atom. In order to give it a chance to dissipate its kinetic energy, we must provide for collisions with another light body, during the lifetime of the excited state. Addition of hydrogen might have an undesirable effect, since H_2 molecules may take away the electronic energy as well as the rotation, as is known from several cases of fluorescence radiation; a reduction of *total intensity* would result instead of the reduction of *rotation*.[11] Helium molecules, however, are known not to destroy the electronic excitation,[12] their mass ought to be sufficiently small to exchange kinetic energy with H atoms.

In Fig. 1 the OH band 3064, photographed with a Hilger E3 quartz spectrograph, is compared (a) in the discharge through water vapor of low pressure with (b) in the discharge through 20 cm helium with a trace of water vapor. The long and complicated band shrinks strikingly into a much shorter and simpler structure. About the origin, two simple branches are to be distinguished easily. The change is not due to a decrease of total intensity as can be seen by comparing the complete disappearance of the edge in the helium experiment with the high intensity of the edge in pure water vapor. Furthermore, the change is not to be described by the quenching of one or the other branch, but instead by the reduction of rotation in every

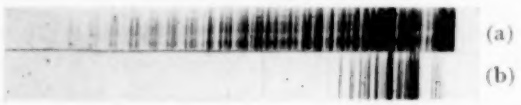

Fig. 1. Effect of admixture of 20 cm He on the intensity distribution of the OH band 3064 in the H_2O discharge. (a) H_2O. (b) H_2O+He.

branch. This was verified by the comparison of spectra taken with a 21-foot grating. (In Fig. 1 the faint branch fading away before it reaches the edge is R_1, the intense branch in the opposite direction, Q_1.) The intensity distribution estimated from the grating spectrum, leads to a temperature of about 670°K.

The comparison of the two spectra demonstrates, first, that in pure water vapor the rotation is highly abnormal and, secondly, that it can be reduced by collisions during the lifetime of the excited state. No particular persistence of rotation in collisions is evident.

An unexpected result is that the complicated band is simplified so strikingly by addition of a rare gas that it might be worth while to try the same method for other complicated bands. Obviously the labor of analyzing the band may eventually be made easier. An exposure taken with the second order of a 21-foot grating revealed the sharpness of the lines unspoiled by the addition even of 20 cm of helium.

[9] H. Beutler and E. Rabinowitsch, Zeits. f. physik. Chemie (B) **8**, 403 (1930).

[10] O. Oldenberg, Phys. Rev. **37**, 194 (1931). It has been pointed out by Franck and Eucken (Zeits. f. physik. Chemie **20**, 460 (1933)) that the transfer of *vibrational* energy in intermolecular collisions as well as in collisions between electrons and molecules, is not to be interpreted by the mechanical picture of dumb-bells colliding with one another. A strong persistence of vibration is assumed in some special cases on the basis of observations of the rates of monomolecular reactions and of dispersion of sound.

[11] The single bands of OH show about the same intensity distribution in water vapor of a few tenths of a mm and 15 mm pressure.

[12] L. v. Hamos, Zeits. f. Physik **74**, 379 (1931).

IV. General Rules for the Determination of the Temperature from Band Spectra

In order to judge whether in a given source the temperature can be derived from the *rotational* or *vibrational* structure of a band spectrum, it is of interest to review the processes determining the intensity distribution observed and in particular the known cases of abnormal distribution.[13]

The following processes are known to lead to abnormal distribution of rotational energy:

(1) Simultaneous dissociation of a *polyatomic* molecule (H_2O) and excitation of one of the fragments (OH) have been discussed in section I.

(2) Excitation of a *diatomic* molecule can under some circumstances result in excess vibration (explained by the Franck-Condon rule), the energy of which is subsequently partly transferred into *rotation* by a few impacts during the lifetime of the excited state. The occurrence of this process has been proved by F. F. Rieke in sensitized fluorescence radiation where the detail can better be followed (HgH bands). The same process must be expected to occur in electric discharges.[14] Experimentally, in the electric discharge through a diatomic gas, only a few cases of abnormal rotation are known, presumably on account of the fact that the accurate determination of the real temperature of the gas is made difficult by the presence of atoms and excited molecules, which show a tendency to deliver their energies to the walls of any thermometer. An example, which possibly might be explained by the principles discussed, has been discovered by Richardson.[15] The intensity distribution of certain hydrogen bands (in which the intensity is practically confined to the "diagonal bands" 0→0, 1→1, 2→2 and 3→3) changes by the admixture of helium. The high *vibrational* bands are *quenched* but within the 0→0 band the high *rotational* lines are relatively *strengthened*. It might be assumed that in the excitation by electron impact excited hydrogen molecules are produced with *normal rotation* but *high vibration*.[16] In collisions with helium atoms, probably the electronic excitation is not taken away but the excess vibrational energy is distributed over the degrees of freedom available, a part going into translation, another part into rotation of the hydrogen molecule. If only a few collisions take place during the lifetime of the excited state, the rotation might have a chance to pick up a part of the vibrational excess energy before the gradual dissipation of energy is interrupted by the radiation process observed. Thus we understand the appearance of abnormal rotation of the 0→0 band with increasing helium pressure. We expect the abnormal rotation to disappear again at a still higher pressure as described for the OH bands in section III.

(3) The third process to be mentioned, leading to abnormal rotation, is excitation by impact. Smyth and Arnott[17] discovered an abnormally large intensity of the higher rotational states in the N_2 bands when excited by a canal ray. This observation agrees with the theoretical conclusion that the heavy particle of the canal ray, rather than the light electron, is able to transfer energy of rotation to the molecule. The effect observed is not very pronounced. The same effect produced by *fast electrons* giving off a small fraction of their energy into rotation of N_2 molecules, has been observed by Duffendack.[18] It seems certain, however, that the slow electrons

---

[13] Cf. R. T. Birge, *Molecular Spectra in Gases*, 215–222 (1926); W. Weizel, *Bandenspektren*, 180–184 (1931); W. Jevons, *Band Spectra of Diatomic Molecules*, 133–139 (1932). Undoubtedly more cases are incidentally mentioned in the literature. The following observations of abnormal intensity distribution are left out since the experimental facts are not sufficiently well known: In the band spectrum of helium the band 4650 shows a certain anomaly (W. H. J. Childs, Proc. Roy. Soc. **A118**, 309 (1928)) while the band 6400 fails to show it although both bands belong to similar types of transition (C. W. W. Read, Proc. Roy. Soc. **A134**, 654 (1931)). A unique observation has been reported by N. Thompson (Proc. Phys. Soc. **46**, 440 (1934)), a rotational temperature derived from the N_2+ bands, lower than the temperature of the furnace surrounding the discharge tube.

[14] In the HgH bands, excited in a mixture of Hg and H_2, W. Kapuscinski and J. G. Eymers (Zeits. f. Physik **54**, 246 (1929)) observed an appreciable deviation from the thermal distribution of rotational energy. It is hardly possible, however, to analyze the process involved.

[15] O. W. Richardson, Proc. Roy. Soc. **A111**, 720 (1926) and *Molecular Hydrogen and its Spectrum*, p. 198 (1934); cf. A. S. Roy. Proc. Nat. Acad. Sci. **19**, 443 (1933).

[16] A large change of vibrational quantum number in the excitation process is to be expected from the Franck-Condon rule, since the upper state of the Fulcher bands has a much larger internuclear distance (1.136) than the normal state of the molecule (0.76).

[17] H. D. Smyth and E. G. F. Arnott, Phys. Rev. **36**, 1023 (1930).

[18] Private communication; cf. G. Herzberg, Zeits. f. Physik **49**, 761 (1928).

prevailing in most electric discharges are unable to excite rotation.

(4) An exceptional observation has been made by Gale and Monk[19] and confirmed by Aars.[20] They found the alternation of intensities varying within the individual fluorine bands so that the strong lines and the faint ones would yield different values of the temperature—as far as the observed intensities can be approximated by a thermal distribution. This irregularity is probably caused by a perturbation. A similar effect seems to exist in the CN band 3884.[21]

On the other hand, band spectra in which the rotation of molecules actually indicates the true temperature have been investigated in Ornstein's[22] laboratory. In general, we may expect the rotational structure of a band spectrum to indicate, at least approximately, the true temperature of a gas in the following cases: (1) absorption spectra, characteristic of molecules which have not just been disturbed by an excitation process; (2) emission spectra excited by heat,[23] provided that the intensities are not modified by self-absorption; (3) emission spectra of electric discharges at pressures so low that no collisions take place during the lifetime of the excited state;[24] (4) emission spectra at high pressure, in particular high pressure of added rare gases, characteristic of molecules which have a good chance to come to thermal equilibrium of rotation during the lifetime of the excited states (OH +He); (5) emission spectra of molecules like N_2 which do not pick up appreciable vibration or rotation—though for different reasons—in the excitation process. It is not claimed that this list is complete.

The rules just mentioned obviously fail to give a definite criterion deciding *a priori* whether or not in an actual spectrum exactly normal rotation is to be expected. It is certain, however, that in many experiments with electric or thermal excitation the rotation actually yields the correct temperature. Only the absorption method is *a priori* certain to indicate the real temperature of the gas by the molecular rotation.

Finally, the determination of the temperature from *vibrational* intensities is to be compared briefly with the method discussed, based on the rotation. In the electric discharge, the rotational intensity serves for this purpose mainly on account of the fact that the *rotational* energy is not appreciably changed in the excitation by slow electrons. The *vibrational* energy, however, is in many cases completely changed, as described by the Franck-Condon rule. Hence the vibrational intensity distribution in the excited state is only indirectly determined by the temperature[25] unless the vibration is brought back to the value of thermal equilibrium by a large number of collisions during the lifetime of the excited state. In many cases it is obviously not even possible to describe the vibrational distribution of the excited electronic level by a virtual temperature. For example, for the halogen molecules excitation by light or electron impact leads predominantly to *high* vibration of the excited level, whereas the thermal distribution of vibration, even for high temperatures, necessarily leads to the maximum population of the *lowest* vibrational level (Maxwell-Boltzmann distribution for one degree of freedom). This explains the failure of Rosseland and Steensholt[26] to derive consistent values of the temperature from

[19] H. G. Gale and G. L. Monk, Astrophys. J. **69**, 77 (1929).

[20] J. Aars, Zeits. f. Physik **79**, 122 (1932).

[21] M. Fassbender, Zeits. f. Physik **30**, 90 (1924).

[22] Examples are cited in a review by L. S. Ornstein, Phys. Zeits. **32**, 517 (1931).

[23] R. T. Birge, reference 13; L. S. Ornstein, H. Brinkman and A. Beunes, Zeits. f. Physik **77**, 72 (1932); D. T. J. Ter Horst and G. Krygsman, Physica **1**, 114 (1933).

[24] Even for no collisions and strict validity of the Franck-Condon rule a minor deviation of the rotational temperature from the thermal value is to be expected if a considerable change of internuclear distance takes place at the excitation process. For example, iodine molecules in the very moment of excitation by electron impact do not appreciably change their rotational energy or internuclear distance because of the small mass of the impinging electron. The excited molecule has a larger equilibrium value of the moment of inertia. Hence the energy quanta of rotation are smaller. The conservation of angular momentum leads to a conservation of *rotational quantum number*, hence to a reduction of *rotational energy*. The excess energy goes into the vibration. (This exchange of energy is easily understood on the basis of potential curves, Zeits. f. Physik **56**, 563 (1929).) Therefore, if no collisions take place during the lifetime of the excited state, the rotation of the excited molecules is expected to correspond to a lower temperature than the rotation of the normal molecules. The ratio of these temperatures is to be estimated from the ratio of the moments of inertia. (Cf. W. R. van Wijk, Zeits. f. Physik **75**, 584 (1932).)

[25] Cf. G. Herzberg, Zeits. f. Physik **49**, 761 (1928). For recent references cf. N. R. Tawde, Proc. Phys. Soc. **46**, 324 (1934).

[26] S. Rosseland and G. Steensholt, Univ. Observ. Oslo Publ. No. 7, p. 14.

the vibrational intensity distribution of the nitrogen bands observed in the aurora.[27] The conclusion is that the chances are not good for determining the temperature of a gas from the vibrational intensities observed in an *electric discharge*. This objection obviously does not hold against the emission spectrum excited by heat[28] or the absorption spectrum.[29]

The main conclusion is that hypothetical statements made previously for the interpretation of abnormal rotational intensity distribution in bands are confirmed by the investigation of the OH bands, and general rules are tentatively derived for the determination of the temperature from the rotational and vibrational intensity distribution in band spectra.

[27] The pressure of these layers of the atmosphere is so low that no collisions during the lifetime of the excited state are to be expected. Handbuch der Experimentalphysik **25**, Part 1, p. 435 (1928).

[28] L. S. Ornstein, H. Brinkmann and A. Beunes, Zeits. f. Physik **77**, 76 (1932).

[29] Cf. H. Kuhn, Zeits. f. Physik **39**, 77 (1926); E. Hutchisson, Phys. Rev. **36**, 416 (1930); K. Wurm, Zeits. f. Astrophys. **5**, 260 (1932).

The Thermal Resistivity and the Wiedemann-Franz Ratio of Single Crystal Zinc

C. A. CINNAMON, *Physical Laboratory, State University of Iowa*

(Received May 22, 1934)

The thermal resistivities at 57°C are measured for thirteen large, strain-free, single crystals of zinc. The guard tube method is used with the heat applied at the center of the specimen. The results show definitely that the thermal resistivity obeys the Voigt-Thomson symmetry relation. The principal resistivities are $\omega_0 = 0.991$ and $\omega_{90} = 0.936$ cm deg. C/watt, with the ratio $\omega_0/\omega_{90} = 1.058$[3]. The close agreement of this value with the ratio of the principal electrical resistivities previously determined in this laboratory shows that the W-F ratio is the same for all orientations of the zinc crystal. The value of this ratio is 7.15×10^{-6} watt ohm/deg. C at 57°C and agrees within 11 percent with the value predicted by the Sommerfeld theory. The two principal thermal conductivities are $\lambda_0 = 1.009$[2] and $\lambda_{90} = 1.068$[4] watts/cm deg. C at 57°C. Some observations are included on "optically mosaic" crystals and on the effects of permanent strain on the single and mosaic crystals.

INTRODUCTION

ALTHOUGH the thermal conductivities of some few zinc crystals of various orientations[1] have been previously measured,[2] only Bridgman has made a definite attempt to check the Voigt-Thomson symmetry relation for thermal conductivity. His results are, unfortunately, so scattered as to render the test inconclusive. From these data Bridgman further concluded that the Wiedemann-Franz ratio is not the same for all orientations of the zinc crystal. Goens and Grüneisen[2(a), (b)], however, find at 20°C nearly the same values for the two principal orientations ($\theta = 0°$ and $\theta = 90°$). The present work consists of an experimental determination of the thermal resistivities of a group of zinc crystals having orientations distributed throughout the possible range, undertaken for the express purpose of studying the variation of thermal resistivity with orientation and of testing the Wiedemann-Franz law.

For the zinc crystal the Voigt-Thomson symmetry relation takes the form

$$\lambda_\theta = \lambda_{90} + (\lambda_0 - \lambda_{90}) \cos^2 \theta, \qquad (1)$$

in which λ_θ is the thermal conductivity for orientation θ while λ_0 and λ_{90} are for orientations 0° and 90°, respectively. An exactly similar equation may be written for each of the three quantities: thermal resistivity, ω_θ; electrical conductivity, σ_θ; and electrical resistivity, ρ_θ.[3] Also, for the two principal orientations (0° and 90°) the following reciprocal relations hold:

$$\lambda_0 = 1/\omega_0, \quad \lambda_{90} = 1/\omega_{90}, \quad \sigma_0 = 1/\rho_0 \quad \text{and} \quad \sigma_{90} = 1/\rho_{90}. \qquad (2)$$

[1] The orientation is the angle, θ, between the normal to the (basal) cleavage plane and the length of the rod.

[2] (a) Grüneisen and Goens, Zeits. f. Instrumentenkunde **46**, 104 (1926); (b) Goens and Grüneisen, Ann. d. Physik **14**, 164 (1932); (c) P. W. Bridgman, Proc. Am. Acad. Arts Sc. **61**, 101 (1926); (d) C. C. Bidwell and E. J. Lewis, Phys. Rev. **33**, 249 (1929).

[3] W. Voigt, Lehrbuch der Kristallphysik, Ch. VI.

For intermediate orientations the resistivity (thermal or electrical) is not the reciprocal of the corresponding conductivity. The proper relation between the two is given by the following expression which may be easily derived from Eqs. (1) and (2):

$$\lambda_\theta = (\omega_{90} + \omega_0 - \omega_\theta)/\omega_0\omega_{90} \quad (3)$$

and

$$\omega_\theta = (\lambda_{90} + \lambda_0 - \lambda_\theta)/\lambda_0\lambda_{90}. \quad (4)$$

One also obtains from Eq. (1)

$$\lambda_\theta/\lambda_{90} = 1 + a\cos^2\theta, \quad (5)$$

where $a = (\lambda_0 - \lambda_{90})/\lambda_{90} = \lambda_0/\lambda_{90} - 1$

and similarly

$$\sigma_\theta/\sigma_{90} = 1 + b\cos^2\theta, \quad (6)$$

where

$$b = (\sigma_0 - \sigma_{90})/\sigma_{90} = (\rho_{90} - \rho_0)/\rho_0 = \rho_{90}/\rho_0 - 1,$$

from which

$$\lambda_\theta/\sigma_\theta = \lambda_{90}(1 + a\cos^2\theta)/\sigma_{90}(1 + b\cos^2\theta). \quad (7)$$

Thus, if the Voigt-Thomson relation is obeyed for the two resistivities and the two conductivities and if $a = b$, the Wiedemann-Franz constant becomes the same for all orientations, assuming that all constants are determined at the same temperature.

In the experimental determination of the electrical resistivity of a crystal rod having a relatively small but uniform cross section the usual assumption is that the current density is everywhere longitudinal since it is necessarily so at the insulated lateral surfaces. The current density thus has the same value at all points in the rod and may be determined from the total current divided by the cross-sectional area. Likewise the longitudinal component of the potential gradient is constant and equal to the average value. The resistivity is thus determined as the ratio of the longitudinal potential gradient to the average current density.[4] Except for crystals of the two principal orientations the equipotential surfaces in the crystal are not perpendicular to the length of the crystal.

The analogous situation for the flow of heat in a single crystal rod is precisely the same,[5] if the lateral loss of heat be prevented, a task that is much more difficult in the thermal case. The writer's experimental procedure, described below, seems to justify the assumptions of no lateral heat loss from the crystal and of no transverse heat flow at any point in any cross section. Therefore the measured constant, which is the ratio of the longitudinal temperature gradient to the average heat current density, is the thermal resistivity and not the reciprocal of the conductivity. It must be noted, in case this assumption appears questionable, that for zinc the thermal conductivity and resistivity are so nearly reciprocally related for any orientation that any error introduced by an incorrect assumption as to what is being measured will be less than the existing experimental error.[6]

Materials

The material from which the crystal specimens were grown was taken from a single 50 lb. slab of "Evanwall" zinc (99.99+ percent Zn). Spectroscopic comparison with a test sample which contained the following impurities:[7] Fe 0.0004 percent; Cd 0.0008 percent; Pb 0.0047 percent; Cu 0.0002 percent, showed no difference in the Pb, Ag and Cd. The two copper lines for the slab material were perhaps very slightly stronger, while the three faint iron lines found for the test sample were lacking. The method of growing the single crystals has been described elsewhere.[8] The specimens were 30 cm long and nearly square in cross section (actually trapezoidal) with an area of approximately 1.24 cm².

Apparatus and Experimental Procedure

Thermal resistivities were measured by a guard tube method, the details of which will be evident from the diagram in Fig. 1. The heater coils H, H_1, H_2 and H_3 were supplied with power from batteries and operated individually. The

[4] Voigt, reference 3, Sec. 181.

[5] Reddeman, Ann. d. Physik **14**, 139 (1932) sec. II, I. If in Voigt, Ch. VI, sec. 195, one equates $\bar{\chi}$ to zero (Eq. 164) and solves the differential equation for the steady state condition, one appears to reach the opposite conclusion, namely that the thermal conductivity is given by the ratio of "heat current density" to the temperature gradient. Voigt, however, considered as negligible two terms which if replaced, will certainly modify his result and should lead to the conclusion stated above.

[6] The greatest difference between the thermal resistivity and the reciprocal of the thermal conductivity occurs at $\theta = 45°$ and is about 0.1 percent.

[7] Spectrograms were made by Mr. A. W. Hanson, Phys. Rev. **45**, 324 (1934). He detected a trace of silver in the test sample in addition to the stated impurities.

[8] C. A. Cinnamon, R. S. I. **5**, 187 (1934).

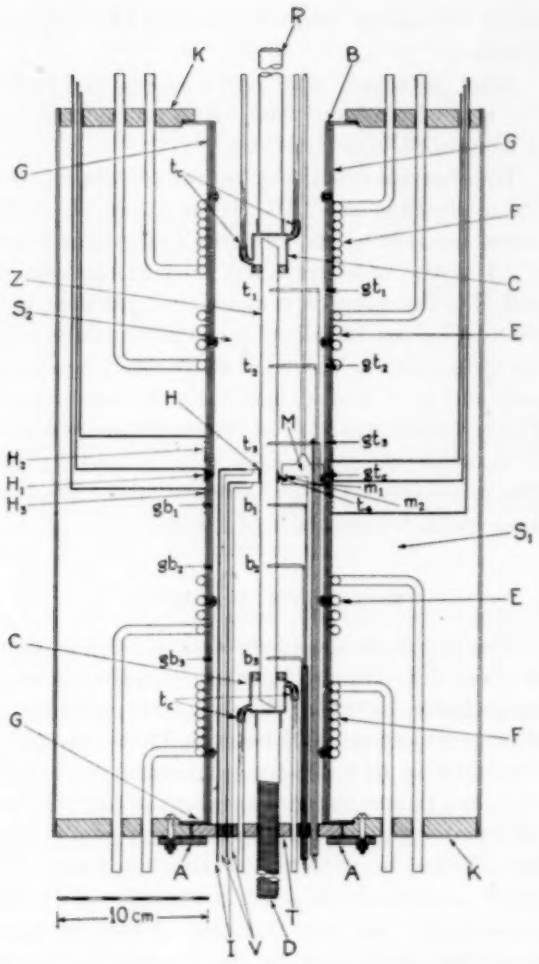

FIG. 1. Vertical section of the apparatus showing the assembled arrangement of the guard tube and crystal specimen. *Z*, crystal specimen; *G*, cylindrical brass guard tube; *H*, heater coil on crystal, about 6.5 ohms of No. 26 Chromel C wire; H_1, H_2, H_3, separate heater coils wound over guard tube, each 40 ohms of No. 26 B and S gauge Chromel C wire; *I* and *V*, current and voltage leads, respectively, to *H*; *C*, brass calorimeter cups fitted over ends of crystal and provided with hollow cylindrical flanges so as to fit securely over ends of rods *D* and *R*; *E* and *F*, individual cooling coils made of copper tubing, spiraled around guard tube and soldered thereto. t_1, t_2, t_3, b_1, b_2, b_3, copper-constantan thermocouple junctions on upper and lower halves, respectively, insulated from crystal by a thin strip of mica (0.02 mm thick, and 0.5 cm wide) and held in place by a small spring steel clamp 0.5 mm thick and 1.5 mm wide (not shown in diagram); t_4, thermocouple junction on outside of alundum cement covering coil *H*; m_1 and m_2, two extra thermocouples placed between *H* and H_1; *M*, thin strip of mica for holding m_1 and m_2; *tc*, thermocouple junctions sealed in tip of small glass tubes (not shown) which were fitted centrally within the inlet and outlet tubes leading to calorimeters; *B*, brass strips for holding thermocouples on guard tube and held thereto by screws; gt_1, gt_2, gt_3, gb_1, gb_2, gb_3, copper-constantan thermocouple junctions on guard tube; junctions are insulated by thin strip of mica (0.09 mm thick), accurately placed and clamped in position by clamps *B*; *T*, transite mounting base, used to support crystal, thermocouple leads, etc; *A*, clamps for holding mounting base; *D*, threaded hard rubber rod for adjusting position of crystal; *R*, hard rubber rod held at top by clamp (clamp not shown); S_2, fine 85 percent magnesia asbestos cement insulating crystal from guard tube; S_1, space between guard tube and outer cylinder filled with dried silica sand; *K*, transite end pieces.

water flow in each of the coils, *E* and *F*, and in the calorimeters, *C*, used for cooling the ends of the guard tube and crystal, respectively, was regulated by an individual needle valve. The water was supplied from a constant temperature and pressure tank.

Before placing the crystal specimen in the apparatus the positions for the thermocouples ($t_1t_2 = t_2t_3 = 5$ cm, $b_1b_2 = 4$ cm and $b_2b_3 = 6$ cm) were accurately marked on the specimen, by using a travelling microscope to assure accuracy of spacing. The heater coil, *H*, insulated electrically from the crystal by one layer of friction tape, was wrapped around the specimen by hand[9] and then covered with a thin layer of alundum cement, which when dried and baked by the heater current held the coil rigid and prevented short circuits between adjacent turns. The specimen was then held vertically while the ends were fitted into the calorimeter cups and sealed thereto with sealing wax. The transite base, *T*, together with rod *D*, the thermocouple wires, and the current and voltage leads to coil *H* were together removed from the guard tube as a single unit and supported vertically. The specimen was then mounted on the end of rod *D* by fitting over its end the hollow cylindrical flange at the base of the lower calorimeter cup. The assembly was then supported horizontally on special supports while the ends of the heater coil were fused to the current leads and the thermocouple junctions clamped in position on the crystal. It was finally supported vertically and the specimen accurately adjusted for height above the transite base by means of the threaded rod *D* so that the thermocouple junctions on the crystal would be placed exactly opposite the corresponding junctions on the guard tube when in operation. The specimen thus mounted was carefully placed within the guard tube, and held in position by

[9] Throughout the entire handling of the crystal every precaution was taken to avoid straining the specimen. This required both skill and knowledge of the properties of the crystals since certain orientations are much softer than others.

clamps A with the upper rod, R, centering the upper end of the crystal assembly. The space S_2 between the crystal and guard tube was filled with fine and fluffy,[10] previously dried magnesia asbestos cement, which was poured in from the top.

Starting with the known approximate adjustments for the power in the heater coils H, H_1, H_2, H_3, and the flow of water in the coils E, F, and calorimeters, C, it was possible in about 10 hrs. and by adjustments of the guard tube only, to establish a steady state in which the temperatures at corresponding points on the crystal and guard tube (for example points t_1 and gt_1) were the same within 0.3°C. At this balanced condition the temperature at t_4 exceeded that at gt_e by approximately 5°C. However, at positions m_2 and m_1 which were 4 mm from t_4 and gt_e, respectively, the temperatures were the same but lower than at gt_e. This condition was especially significant since it indicated definitely that no heat was conducted radially between the guard tube and the crystal in this central region.

An exact linear distribution of the temperature along each half of the crystal was not obtained. The amount and direction of the deviation from linearity were such as might be expected from the variation of thermal conductivity with temperature. Thus the temperature at the middle point t_2 (for the upper half of the crystal) fell below the mean of the temperatures at t_1 and t_3 by about 0.3°C. The corresponding deviation between the temperature at b_2 (not centered in the lower half) and the linear value obtained from the temperatures at b_1 and b_3 was about 0.25°C.

The cold thermocouple junctions were kept at the temperature of melting ice. All thermal e.m.f.'s were measured on a precision potentiometer[11] making possible reliable estimations to 0.2 microvolts (equivalent to 0.005°C). The input energy supplied to H was measured on the same potentiometer with the aid of a standard resistance and standard cell. The output energy, measured by the constant flow calorimeters, C (Fig. 1), was read, but in the computations use was made of only the electrical input for reasons which will appear under the section Discussion of Errors.

After the steady state had been reached two to five sets of readings were taken on each crystal at about one hour intervals.

The thermal resistivity, ω, was calculated from the expression, $\omega = 2AG/W$, in which W is the power input in watts delivered to the heater coil, H, A is the cross-sectional area of the crystal, and G is the average temperature gradient over the two halves, obtained in obvious fashion from the temperatures indicated by the thermocouples at t_1 and t_3, b_3 and b_1, and their distances apart. The temperatures at t_3 and b_1 were approximately 77°C while the temperatures at t_1 and b_3 were approximately 38°C so that the resistivities are for a mean temperature of about 57°C.

Discussion of Errors

The errors in the comparative measurements between different specimens were of the following magnitudes. Errors in the direct measurement of W were less than 0.001 percent. However, due to the inability to make the temperatures at corresponding points along the crystal and guard tube identical, there was undoubtedly a small radial flow of heat between the crystal and guard tube which introduces an error in the effective power input. By actual tests the effect of this difference in temperature between the crystal and guard tube over the entire 30 cm length of the crystal amounted to less than 0.06 watt per degree temperature difference. For about 10 watts input and for an arithmetical mean temperature difference not exceeding 0.3°C the error amounts to about 0.2 percent. The maximum temperature difference between the crystal and guard tube never exceeded 0.5°C and such a difference never extended over more than 5 cm of the crystal. Error in measuring the cross-sectional area was less than 0.10 percent. Errors in the distances t_1t_3 and b_1b_3, Fig. 1, each of which was equal to 10 cm, were less than 0.10 percent. The errors in the measurement of the corresponding temperature differences were less than 0.05 percent. Thus the total possible error amounts to less than 0.45 percent and represents the maximum variation to be expected between the observed value of the thermal resistivity and the most probable value.

[10] The ordinary 85 percent magnesia asbestos cement will become very fine and fluffy in texture after frequent use in the electric furnace during the process of growing crystals. It is this sort of fluffy material that was used.

[11] Leeds and Northrup type K-2.

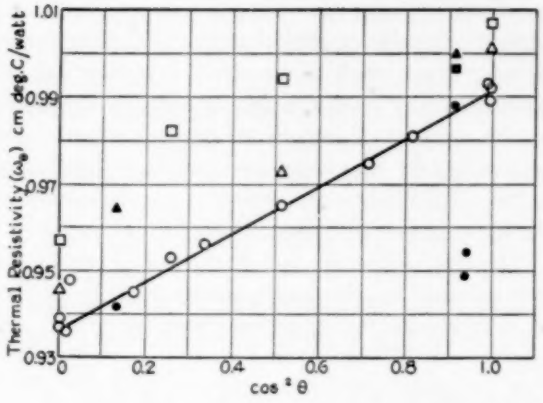

FIG. 2. The thermal resistivity of zinc crystals plotted against the square of the cosine of the orientation: unstrained crystals, open circle; strained single crystals, open squares; strained and annealed single crystals, open triangles; unstrained mosaics, solid circles; strained mosaics, solid square; strained and annealed mosaics, solid triangles. All data are for a mean temperature of 57°C.

In Fig. 2, all of the open circle points (with one exception) lie within this limit as judged by the deviation from the straight line.

A test of the reproducibility of values for a given crystal was made by comparing the results of two series of measurements between which the crystal had been removed from the apparatus, thermocouples at t_1, t_2, t_3, b_1, b_2, b_3, had been dismounted and replaced, and the apparatus reassembled. The results differed by about 0.3 percent. The maximum variation, given by the sum of all the above estimated errors, except that in measuring A, amounts to about 0.35 percent.

In addition to the sources of error mentioned above there are errors which will be the same for all crystals and which might therefore affect the absolute values without reducing the accuracy of the comparison of one crystal with another. Such errors may arise from the heat conducted by the power leads and thermocouple wires, and the longitudinal heat flow in the insulating material between the crystal and guard tube. All of the wires extended radially from the crystal to the mid-point between the crystal and guard tube where they were bent at right angles and continued longitudinally. The temperature difference over the radial portion of these wires did not exceed 0.3°C. It is estimated that the heat thus lost by conduction amounted to less than 0.04 percent of the total power input. The heat conducted longitudinally through the insulating material[12] found by calculation amounted to about 0.27 percent. The maximum estimated error in the absolute value thus amounts to less than 0.8 percent.

The output power, measured by calorimeters, C, was found to exceed the input by 2 percent. This difference is to be expected since no exact balance between the temperatures at corresponding points along the calorimeter cups and guard tube was possible, the temperatures on the guard tube being unavoidably higher, thereby permitting heat to flow into the calorimeters. For this reason the output power was not used in computing the resistivities.

RESULTS

In Fig. 2 the measured thermal resistivity of each crystal is plotted against the square of the cosine of the orientation. For the strain-free crystals, i.e., measured as grown with no intervening intentional strain (open circles) the Voigt-Thomson relation is fully substantiated. It is apparent from Fig. 2 that the effect of strain (open squares) is to raise the value of the thermal resistivity. Before taking these data each half of the crystal was placed horizontally on two supports 10 cm apart and pushed down at a point midway between the supports until this point was depressed a measured amount. The crystal was then straightened, similarly bent in the opposite direction the same amount and again straightened. The crystals represented by values of $\cos^2\theta$ equal to 0.001; 0.257; 0.514; and 0.996 were respectively given strains of the following amounts, expressed in centimeters of depression: 0.079; 0.114; 0.125; and 0.013. This effect of strain may well account for the extreme deviation from the line of the one point ($\cos^2\theta = 0.025$, $\omega = 0.9475$), assuming that the crystal was accidentally strained before the first measurement. It also very probably accounts for the uncertain and scattered results obtained by others[2(a, b, c)] in the past, particularly if the crystals used were small and thereby very easily strained in handling or during the process of growth. The strained specimens after a subsequent annealing of 11 hrs. at 380°C (open tri-

[12] The thermal conductivity of the insulating material was found by measurement to be 3.2×10^{-4} watt/cm deg. C.

angles), show a partial recovery towards their unstrained value.

The values of the two principal thermal conductivities, obtained from the curve (Fig. 2) by means of the reciprocal relations of Eq. (2), are, at 57°C: $\lambda_{90}=1.068^4$ watts/cm/deg. C; $\lambda_0=1.009^2$ watts/cm/deg. C with the ratio, $\lambda_{90}/\lambda_0=1.058^8$. This ratio agrees well within the limits of experimental precision with the ratio of the two principal electrical conductivities, $\sigma_{90}/\sigma_0=\rho_0/\rho_{90}=1.057$ for the K crystals of Tyndall and Hoyem.[13] Thus the constants a and b of Eqs. (5) and (6), respectively, are equal and by Eq. (7) the Wiedemann-Franz ratio becomes the same for all orientations. The value $\rho_{90}=5.86^8\times10^{-6}$ ohm/cm³ at 20°C, given by Tyndall and Hoyem corrected[14] for density and temperature gives $6.69^2\times10^{-6}$ ohm/cm³ at 57°C. This value for ρ_{90} together with the author's value for λ_{90} (at 57°C) give a W–F ratio of $\lambda_\theta/\sigma_\theta=7.15\times10^{-6}$ watt ohm/deg. C. This may be compared with the theoretical values of Drude, Lorentz and Sommerfeld which are 7.35, 4.9 and 8.06×10^{-6}, respectively, expressed in watt ohm/deg. C at 57°C.[15]

The thermal resistivities of four "optically mosaic" crystals[16] were measured. They are plotted as solid circles in Fig. 2. The two crystals represented by points lying close to the curve were grown from the same allotment of zinc as the previously discussed good crystals and under quite similar conditions. One of these crystals ($\omega=0.9417$, $\cos^2\theta=0.132$) was not mosaic throughout but was good on one end. The mosaic part was of type B of Schilling's classification. The other crystal ($\omega=0.988$, $\cos^2\theta=0.9116$) was entirely a mosaic of type C. The two crystals represented by the solid circles far from the curve (in the lower right hand portion of the figure) were from a different lot of Evanwall zinc (obtained from the manufacturer in the form of cast rods) and grown under somewhat different conditions. These two crystals were of Schilling's type A throughout their lengths. That these two mosaics have such abnormally low thermal resistivities may be due either to a slight difference in the amount of impurities present in this zinc or to the fact that they were mosaic. The latter is the more likely supposition as the difference in purity was not sufficient to explain the effect.

The effect of strain (solid square) on one of the two mosaics on the line together with the effect of a subsequent annealing (the two solid triangles) can be seen from Fig. 2. It is to be noted that for these specimens the anneal is not effective in partially removing the strain effect, as it was for the single crystals.

Previous determinations on the thermal conductivity of zinc single crystals are not in good agreement with each other nor with the present data. A comparison is given in Table I. The original data, when not taken at 57°C, have been reduced to this temperature by assuming that the conductivity decreases by one part in 1500 for every degree C rise in temperature.[17]

TABLE I. *Thermal conductivities of zinc crystals, in watts/cm deg. C, at 57°C.*

Bridgman[18]	highest	1.42
	lowest	1.28
Bidwell and Lewis	$\theta=90°$	1.23
Goens and Grüneisen	$\theta=3.6°$	1.17
	$\theta=8.7°$	1.21
	$\theta=79.7°$	1.21
Cinnamon	$\theta=0°$	1.009^2
	$\theta=90°$	1.068^4

It will be observed that the writer's values are distinctly lower than previously reported values. Even so the writer believes that his results are more reliable. It is obvious that the experimental method used herein is straightforward and free from weighty corrections. The crystals were grown under strain-free conditions, were specially guarded against the development of optical mosaics,[8] and were of much larger size than any previously used. The internal agreement of the results is excellent. The data presented herein are

[13] E. P. T. Tyndall and A. G. Hoyem, Phys. Rev. **38**, 820 (1931).

[14] The temperatures correction is made by using the temperature coefficient of resistivity $\alpha=4.009\times10^{-3}$ obtained by A. G. Hoyem, Phys. Rev. **38**, 1370 (1931). The correction for density is made by multiplying by 7.15/7.13. Tyndall and Hoyem used a density of 7.15 g/cc, but the value 7.13 seems preferable.

[15] Becker-Abraham, *Theorie d. Electricität*, vol. II, pp. 200, 206, 235.

[16] H. K. Schilling, Physics **5**, 1 (1934).

[17] From data given by F. H. Schofield, Proc. Roy. Soc. **A107**, 206 (1925).

[18] The orientations of Bridgman's crystals lay between 33° and 87°, individual values not being given.

for every crystal grown with none discarded because of lack of agreement. The independent measurement of the "output energy", which agreed within 2 percent with the input is a practical assurance against any systematic error in the measurement of the latter. The zinc was of such high purity that it is exceedingly unlikely that previous, higher results can be attributed to greater purity of material. That some of the crystals of previous workers may have been optically mosaic and therefore of high conductivity is quite possible.[19]

At least the production of optical mosaics having a higher conductivity than single crystals is a very strong argument against supposing that the highest attainable conductivity is indicative of the most nearly perfect single crystal.

In attempting a comparison with the previously obtained data on polycrystalline zinc specimens many factors must be considered. From considerations of symmetry only it may be concluded that a polycrystalline aggregate with randomly oriented grains should exhibit a conductivity somewhere between the two principal values ($\theta=0$, $\theta=90°$) of the single crystal, perhaps equal to the value at $\theta=54.5°$.[20] Such an assumption presupposes the existence of such an aggregate in which one may consider negligible the grain-boundary effects, effects of constraint of one grain on another, and permanent strains such as are undoubtedly present in zinc castings.[21] It is exceedingly doubtful that such an ideal polycrystalline specimen can ever be prepared. Where a polycrystalline casting has been subjected to mechanical working it departs still further from the ideal of randomly oriented, unstrained grains. Most of the above effects are usually assumed to raise the thermal conductivity and some experimental indications of this sort have been found for other metals as well as for zinc. The writer's results, however, do not support such a view. Thus the International Critical Tables give for polycrystalline zinc a weighted mean of 1.09, with a variation from 1.02 to 1.15 watts/cm deg. C, reduced to 57°C.[17] The value for the polycrystalline material computed from the resistivity curve of Fig. 2 (i.e., at $\theta=54.5°$) is 1.05, which lies within the lower part of the range of observed values of the polycrystal. Moreover, Schofield[17], using a method similar to the writer's but a distinctly less pure zinc, obtained 1.10 watts/cm deg. C. Bidwell and Lewis[2(d)] obtained 1.03 and 1.09 watts/cm deg. C for two polycrystalline rods, one cast in air and one in vacuum. Van Dusen and Shelton[22] obtained 1.14 at 57°C. Were the precise data on the specific heat of zinc available a valuable comparison could be made from Frazier's[23] recent determination on the thermal diffusivity of a polycrystalline casting of zinc of the same grade as the writer's. Adopting a value of specific heat 0.0902[24] and density 7.13 g/cm³, Frazier's value leads to a thermal conductivity of 1.065 watts/cm deg. C at 24°C, whereas the writer's value reduced to the same temperature is 1.073.

In conclusion, the author wishes to express his sincere thanks to Dr. E. P. T. Tyndall for suggesting and directing this problem and for his constructive criticism during the course of the research.

[19] There is abundant evidence in this laboratory to show the difficulty of growing truly single crystals from zinc of high purity. It thus appears exceedingly difficult to grow them by the Czochralski-Gomperz method, or in glass tubes as moulds, or in any shape of mould in which the crystal is constrained during growth. Further, it has recently been discovered by Professor Tyndall that with an addition of several tenths of one percent of cadmium to a zinc of the grade used herein, the growth of single crystals with no visible mosaic structure and exhibiting practically perfect, plane cleavage surfaces, is comparatively easy by the Czochralski-Gomperz method and presumptively by other methods. Thus the freer the zinc from cadmium the more it must be suspected of producing these mosaics unless care is taken to prevent them.

[20] Accepting the value determined by Linder, Phys. Rev. 29, 563 (1927) for the thermoelectric effects of the polycrystal.

[21] See comparison of the elastic behavior of a polycrystalline zinc rod and single crystal by A. W. Hanson, Phys. Rev. **45**, 324 (1934).

[22] Van Dusen and Shelton, Bur. Stand. J. Res. **12**, 429 (1934). Results are not absolute, but by comparison with lead.

[23] R. H. Frazier, Phys. Rev. **43**, 135 (1933).

[24] The average of the three best values taken from the curves on page 77, Circular of the Bureau of Standards, No. 395, *Zinc and Its Alloys.*

Vibrational Isotope Effects in Three Particle Systems. Part II

ARTHUR ADEL, *University of Michigan*

(Received June 8, 1934)

A quantum mechanical analysis of the general potential energy function of the linear, unsymmetrical, triatomic molecule X—Y—Z is developed in terms of the infrared spectrum of the molecule. The anharmonicity and mutual interactions of the several modes of vibration, as well as the coupling between rotation and vibration are taken into account. It is demonstrated that particular infrared data of two or more molecular isotopes suffice to define accurately the potential function.

I. INTRODUCTION

A PREVIOUS paper by this title, Part I,[1] was concerned with the shifts produced in the fundamental frequencies of a general triatomic molecule by the introduction of an isotope of one of its atoms. It was assumed that valence forces acted within the molecule and also that the forces between the atoms were invariant for an isotopic change of mass. Expressions for the frequency shifts were derived, and it was further shown that the analysis furnished a criterion by means of which the arrangement of the atoms within the molecule can be ascertained.

In the present paper it is proposed to solve the reverse problem. It will be shown how the infrared spectra of two or more molecular isotopes can be applied to the analysis of the actual potential function of the normal molecule. The single assumption to be made will be that of the invariance of the molecular force field under an isotopic change of mass. Unlike Part I, the results of this investigation will be applicable to the isotopes of hydrogen with the same high degree of accuracy with which they apply to the isotopes of heavier atoms.

To obtain a sufficient number of relations involving the potential energy coefficients, the analysis must include:

(a) the effect of the anharmonicity of the vibrations
(b) the interactions between the several modes of vibration
(c) the perturbation of vibration by rotation
(d) the perturbation of rotation by vibration.[2]

In conformity with the method of infinitesimal oscillations we shall begin the analysis by representing the molecule as a group of independent simple harmonic oscillators, two linear and one plane isotropic.

II. ANALYSIS

(A) The zeroth order potential energy of vibration

The normal modes of vibration of the linear molecule X—Y—Z are schematically indicated in Fig. 1.

In presenting the analysis we shall use the coordinates q, z, r, and ϕ in a manner similar

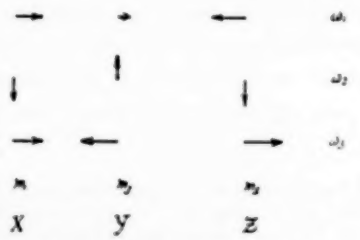

FIG. 1. Normal modes of vibration of the linear molecule.

to that in which they are employed in the corresponding treatment of the linear, symmetrical, triatomic molecule;[3] that is, q measures the relative separations of the end atoms, z the relative displacement of the interior atom with respect to the center of mass of the end atoms, measured parallel to the axis of the molecule, while r and ϕ are the polar coordinates of the interior atom in a plane perpendicular to the axis of the molecule, the origin of coordinates

[1] Adel, Phys. Rev. **45**, 56 (1934).

[2] The perturbation of rotation upon itself, responsible for the cubic convergence in the pure rotation spectrum involves primarily the quadratic potential and is, therefore, only of secondary interest.

[3] Adel and Dennison, Phys. Rev. **43**, 716 (1933).

lying at the center of mass of the end atoms. Since the potential energy function is subject to the geometric symmetry of the molecule, the quadratic potential takes the form:

$$V_0=\tfrac{1}{2}[k_{11}q^2+2k_{13}qz+k_{33}z^2+k_{22}r^2].$$

In virtue of the existence of $k_{13}\neq 0$, q and z are not normal coordinates. The solution of our problem is, however, greatly simplified by the introduction of normal coordinates and such a transformation will therefore be effected. r is already a normal coordinate and will be omitted from the following transformation. We require the kinetic energy of the vibrations ω_1 and ω_3. This is easily found to be $T=\tfrac{1}{2}[\mu_q\dot{q}^2+\mu_z\dot{z}^2]$ where $\mu_q=m_1m_2/(m_1+m_2)$ and $\mu_z=m_3(m_1+m_2)/(m_1+m_2+m_3)$. The secular determinantal equation of the normal coordinate transformation can now be constructed. It is

$$\begin{vmatrix}\mu_q\lambda-k_{11} & -k_{13}\\ -k_{13} & \mu_z\lambda-k_{33}\end{vmatrix}=0.$$

From this it follows that the normal coordinates are given by:

$$Q=\frac{\mu_q^{\frac{1}{2}}[\lambda_3-k_{11}/\mu_q]q-[k_{13}/(\mu_q)^{\frac{1}{2}}]z}{[\lambda_3-k_{11}/\mu_q][\lambda_1-k_{33}/\mu_z]-k_{13}^2/\mu_q\mu_z},$$

$$Z=\frac{\mu_z^{\frac{1}{2}}[\lambda_1-k_{33}/\mu_z]z-[k_{13}/(\mu_z)^{\frac{1}{2}}]q}{[\lambda_3-k_{11}/\mu_q][\lambda_1-k_{33}/\mu_z]-k_{13}^2/\mu_q\mu_z},$$

where $\lambda=4\pi^2\omega^2$. The potential and kinetic energies of the first and third modes of vibration may now be written:

$$V_0=\tfrac{1}{2}[\lambda_3^2-\lambda_1\lambda_3+(\lambda_1-\lambda_3)(k_{11}/\mu_q)][\lambda_1Q^2+\lambda_3Z^2],$$

$$T=\tfrac{1}{2}[\lambda_3^2-\lambda_1\lambda_3+(\lambda_1-\lambda_3)(k_{11}/\mu_q)][\dot{Q}^2+\dot{Z}^2].$$

The corresponding energies of the second mode of vibration are:

$$V_{\omega_2}=\tfrac{1}{2}k_{22}r^2,\quad T_{\omega_2}=\tfrac{1}{2}\mu_r[\dot{r}^2+r^2\dot{\varphi}^2],$$

where

$$\mu_r=\left[\frac{m_3(m_1+m_2)}{m_1+m_2+m_3}\right]^2\left[\frac{1}{m_1}\left(\frac{s_2}{r_0}\right)^2+\frac{1}{m_2}\left(\frac{s_1}{r_0}\right)^2+\frac{1}{m_3}\right].$$

The quantities s_1, s_2, and r_0, respectively, are the X—Y, Y—Z, and X—Z equilibrium separations; that is, $r_0=s_1+s_2$.

The coefficients of the quadratic potential may now be determined as follows. From the secular determinantal equation, the energy expressions, and the moment of inertia of the molecule we obtain the relations given below. Involved in them are the four independent potential coefficients k_{11}, k_{22}, k_{33}, k_{13} and the distances s_1 and s_2.

$$\lambda_1+\lambda_3=k_{11}/\mu_q+k_{33}/\mu_z,$$

$$\lambda_1\lambda_3=k_{11}k_{33}/\mu_q\mu_z-k_{13}/\mu_q\mu_z,$$

$$\lambda_2=k_{22}/\mu_r,$$

$$I_0=m_1s_1^2+m_2s_2^2-[1/(m_1+m_2+m_3)]\times[m_1^2s_1^2+m_2^2s_2^2-2m_1m_2s_1s_2].$$

From the I_0 values of two molecular isotopes the distances s_1 and s_2 can be computed. μ_r can then be evaluated and k_{22} determined from λ_2. It is clear that the solution for k_{11}, k_{33}, and k_{13} demands a knowledge of ω_1 and ω_3 of one of the molecular isotopes and information concerning at least one of the frequencies ω_1, ω_3 of a second isotope.

The zeroth order potential function and the molecular dimensions can thus be completely specified from infrared data on the fundamentals of two molecular isotopes. We turn now to an examination of the cubic and quartic terms in the correction to the potential energy of vibration.

(B) Higher terms in the potential energy of vibration

It proves convenient to introduce the dimensionless coordinates σ, ξ and ρ.

$$\sigma=[\lambda_1\{\lambda_3^2-\lambda_1\lambda_3+(\lambda_1-\lambda_3)(k_{11}/\mu_q)\}1/h\omega_1]^{\frac{1}{2}}Q,$$

$$\xi=[\lambda_3\{\lambda_3^2-\lambda_1\lambda_3+(\lambda_1-\lambda_3)(k_{11}/\mu_q)\}1/h\omega_3]^{\frac{1}{2}}Z,$$

$$\rho=[k_{22}/h\omega_2]^{\frac{1}{2}}r.$$

In terms of these coordinates the cubic and quartic terms of the potential may be given in two successive approximations as follows:

$$\lambda V_1=hc[a\sigma^3+b\sigma\rho^2+c\sigma\xi^2+\alpha\xi^3+\beta\xi\rho^2+\gamma\xi\sigma^2],$$

$$\lambda^2V_{11}=hc[d\sigma^4+e\rho^4+f\xi^4+g\sigma^2\rho^2+h\sigma^2\xi^2+i\rho^2\xi^2+j\sigma\xi^3+k\xi\sigma^3+l\sigma\xi\rho^2].$$

The perturbation calculations based upon these perturbing elements are especially tiresome, and since they do not differ in principle from those already discussed in connection with the analogous problem for the symmetrical molecule X—Y—X,[3] only the results of our analysis will be set forth here. These may be stated simply as follows:

The energy[4] of a vibrational level correct through a second order perturbation calculation on the anharmonicity and the interactions of the several modes of vibration possesses the quadratic form:

$$E_{\text{vib}}=\nu_1 V_1+\nu_2 V_2+\nu_3 V_3+X_{11}V_1^2+X_{22}V_2^2+X_{33}V_3^2+X_{ll}l^2+X_{12}V_1V_2+X_{13}V_1V_3+X_{23}V_2V_3+\text{cst.},$$

where V_1, V_2, V_3, and l are the quantum numbers of vibration and where

$$\nu_1=\omega_1+3d/2+g+h/2-3a[9a/8+b+c]/\omega_1-3\alpha[9\alpha/\gamma+\beta+\gamma]/\omega_3-(3/8)[a^2/\omega_1+\alpha^2/\omega_3]$$
$$-(1/2)\left[\frac{b^2}{\omega_1+2\omega_2}+\frac{\beta^2}{\omega_3+2\omega_2}\right]+(1/2)\left[\frac{b^2}{\omega_1-2\omega_2}+\frac{\beta^2}{\omega_3-2\omega_2}\right]$$
$$-(3/8)\left[\frac{c^2}{\omega_1+2\omega_3}+\frac{\gamma^2}{\omega_3+2\omega_1}\right]+(1/4)\left[\frac{c^2}{\omega_1-2\omega_3}+\frac{\gamma^2}{\omega_3-2\omega_1}\right],$$

$$\nu_2=\omega_2+3e+g/2+i/2-b[b+3a/2]/\omega_1-\beta[\beta+3\alpha/2]/\omega_3-(1/4)[b^2/(\omega_1+2\omega_2)+\beta^2/(\omega_3+2\omega_2)],$$

$$\nu_3=\omega_3+3f/2+h/2+i-c[6a+4b+c]/4\omega_1-\gamma[6\alpha+4\beta+\gamma]/4\omega_3-(3/8)[c^2/\omega_1+2\omega_3)+\gamma^2/(\omega_3+2\omega_1]$$
$$+(1/8)[c^2/(\omega_1-2\omega_3)+\gamma^2/(\omega_3-2\omega_1)],$$

$$X_{11}=3d/2-(57/8)[a^2/\omega_1+\alpha_2/\omega_3],$$

$$X_{22}=\frac{3e}{2}-(1/2)\left[\frac{b^2}{\omega_1}+\frac{\beta^2}{\omega_3}\right]-(1/8)\left[\frac{b^2}{\omega_1+2\omega_2}+\frac{b^2}{\omega_1-2\omega_2}+\frac{\beta^2}{\omega_3+2\omega_2}+\frac{\beta^2}{\omega_3-2\omega_2}\right],$$

$$X_{33}=\frac{3f}{2}-(1/2)\left[\frac{c^2}{\omega_1}+\frac{\gamma^2}{\omega_3}\right]-(1/8)\left[\frac{c^2}{\omega_1+2\omega_3}+\frac{c^2}{\omega_1-2\omega_3}+\frac{\gamma^2}{\omega_3+2\omega_1}+\frac{\gamma^2}{\omega_3-2\omega_1}\right],$$

$$X_{ll}=\frac{-e}{2}+(1/8)\left[\frac{b^2}{\omega_1+2\omega_2}+\frac{b^2}{\omega_1-2\omega_2}+\frac{\beta^2}{\omega_3+2\omega_2}+\frac{\beta^2}{\omega_3-2\omega_2}\right],$$

$$X_{12}=g-3\left[\frac{ab}{\omega_1}+\frac{\alpha\beta}{\omega_3}\right]-(1/4)\left[\frac{b^2}{\omega_1+2\omega_2}-\frac{b^2}{\omega_1-2\omega_2}+\frac{\beta^2}{\omega_3+2\omega_2}-\frac{\beta^2}{\omega_3-2\omega_2}\right],$$

$$X_{13}=h-3\left[\frac{ac}{\omega_1}+\frac{\alpha\gamma}{\omega_3}\right]-(3/8)\left[\frac{c^2}{\omega_1+2\omega_3}+\frac{\gamma^2}{\omega_3+2\omega_1}\right]+(1/2)\left[\frac{c^2}{\omega_1-2\omega_3}+\frac{\gamma^2}{\omega_3-2\omega_1}\right],$$

$$X_{23}=i.$$

The quantities ν_1—X_{23} may be evaluated from experiment and the above relations thus constitute a partial set of simultaneous equations in the unknowns a—i. The investigation of the interaction between the rotation and vibration of the molecule, to which we now proceed, will furnish a sufficient number of additional relations to make possible the solution of our problem; namely, the definition of the potential energy of vibration. (It is to be noted that even to the present order of approximation the terms $j\sigma\xi^3+k\xi\sigma^3+l\sigma\xi\rho^2$ furnish no contribution to the energy. They mark the difference between the molecules X—Y—Z and X—Y—X in second order approximation and may be expected to be very small.)

[4] $E_{\text{vib}}=E_0+\lambda E_I+\lambda^2 E_{II}$, where

(a) $E_0=h[\omega_1(V_1+\frac{1}{2})+\omega_2(V_2+1)+\omega_3(V_3+\frac{1}{2})]$,

(b) $\lambda E_I=0$,

(c) $[\lambda^2 V_{II}]_{nl}^{n'l}+\Sigma'_{n''l''}\{[H_1]_{nl}^{n''l''}\}^2/\{E_0^{n}-E_0^{n''}\}$.

The wave functions employed in the calculation are given by:

$$\Psi_{nl}=\Psi_{(\sigma)}{}^{V_1}\Psi_{(\xi)}{}^{V_3}R_{(\rho)}{}^{V_2 l}e^{\pm il\varphi},$$

where $\Psi_{(\sigma)}{}^{V_1}$ and $\Psi_{(\xi)}{}^{V_3}$ are Hermitian orthogonal functions with the arguments σ and ξ, respectively, and where

$$R_{(\rho)}{}^{V_2 l}=(k^*)^{\frac{1}{2}}\{(l+k)^*\}^{-\frac{1}{2}}\pi^{-\frac{1}{2}}\rho^l e^{-\rho^2/2}L_{l+k}{}^l(\rho^2),$$

$L_{l+k}{}^l(\rho^2)$ being the associated Laguerre polynomial of argument ρ^2 and k being equal to $(V_2-l)/2$.

(C) The interaction between rotation and vibration

As in the case of the perturbations on vibration, the present calculation does not differ principally from the analogous one discussed in the problem of the X—Y—X molecule.[5] Consequently, in conformity with our procedure, only the coupling potential and the results of the analysis will be given. The coupling potential is

$$\lambda^2 V_i = -\frac{h^2}{8\pi^2 I_0}[J(J+1)-l^2][P\sigma^2+Q\rho^2+R\xi^2],$$

where

$$P=\frac{C_1}{\mu_q}\left[\frac{\lambda_1-C}{M}\right]^2+\frac{C_2}{\mu_z}\left[\frac{B}{M}\right]^2 + \frac{C_4}{(\mu_q\mu_z)^{\frac{1}{2}}}\frac{\lambda_1-C}{M}\frac{B}{M}+3aF_1+\gamma F_2,$$

$$Q=h\omega_2 C_2/D+bF_1+\beta F_2,$$

$$R=\frac{C_1}{\mu_q}\left[\frac{B}{N}\right]^2+\frac{C_3}{\mu_z}\left[\frac{\lambda_3-A}{N}\right]^2 + \frac{C_4}{(\mu_q\mu_z)^{\frac{1}{2}}}\frac{\lambda_3-A}{N}\frac{B}{N}+CF_1+3\gamma F_2.^6$$

The correction to the energy of a rotation-vibration level is therefore given by:

$$\lambda^2 E_i = -\frac{h^2}{8\pi^2 I_0}[J(J+1)-l^2][P(V_1+\tfrac{1}{2}) +Q(V_2+1)+R(V_3+\tfrac{1}{2})].$$

It follows upon the introduction of the selection rules for the rotational quantum numbers that the convergence of fine structure in a band resulting in a transition from the ground state is given by

$$\lambda^2\nu_i = -\frac{h}{8\pi^2 I_0}[PV_1+QV_2+RV_3]N^2,$$

where N is the ordinal number of the line.[7]

III. Conclusion

It is apparent that there exist several methods of exploiting these relations to solve for the desired quantities a—i. The most precise, however, may be outlined simply as follows:

(a) By applying the results of section C to the observed fine structure convergences of the fundamentals of two molecular isotopes, the first order coefficients a—γ may be accurately determined.

(b) By introducing these values into the results of section B the second order coefficients d—i can be found.

It is hoped soon to make applications of this analysis, especially to the isotopes of H—C—N.[8]

Notes added in the proof: 1. The coordinates set forth as normal are not precisely the normal coordinates but are proportional to them; that is, in normal coordinates,

$$T=\tfrac{1}{2}\sum_i \dot{q}_i^2$$

$$V=\tfrac{1}{2}\sum_i \lambda_i q_i^2.$$

2. The lines of the pure rotation spectrum of the X—Y—Z molecule are given by the expression:

$$\nu_R=\frac{hJ}{4\pi^2 I_0 c}\left[1-\frac{J^2}{I_0}\left\{2\mu_q r_0 Y+\frac{2\mu_z}{S}(m_1s_1-m_2s_2)Z\right\}\alpha\right],$$

where,

$$Y=\frac{2k_{33}\mu_q r_0-2k_{13}(\mu_z/S)(m_1s_1-m_2s_2)}{I_0^2(k_{11}k_{33}-k_{13}^2)}$$

$$Z=\frac{2k_{11}(\mu_z/S)(m_1s_1-m_2s_2)-2k_{13}\mu_q r_0}{I_0^2(k_{11}k_{33}-k_{13}^2)}$$

$$\alpha=(h^2/8\pi^2)\{1-(P/2+Q+R/2)\}.$$

---

[5] Adel and Dennison, Phys. Rev. **44**, 99 (1933).

[6] $A=K_{11}/\mu_q$, $B=k_{13}/(\mu_q\mu_z)^{\frac{1}{2}}$, $C=k_{33}/\mu_z$,
$M^2=\lambda_1(\lambda_1-\lambda_3)(\lambda_1-C)/h\omega_1$,
$N^2=\lambda_3(\lambda_3-\lambda_1)(\lambda_3-A)/h\omega_3$,
$C_1=-(\mu_q/I_0)[(4\mu_q/I_0)r_0^2-1]$,
$C_2=\frac{1}{2}\mu_r/I_0$,
$C_3=-(2m_3/\Sigma I_0)^2[(m_1-m_2)s_1^2+m_1m_2(s_2-s_1)^2 -m_3(m_1-m_2)(s_2^2-s_1^2)-\Sigma SI_0/4m_3]$,
$C_4=-[8m_1m_2m_3/\Sigma SI_0^2]r_0[m_1s_1-m_2s_2]$,
$F_1=M/L[\mu_q^{\frac{1}{2}}(\lambda_3-A)\delta-B(m_3S/\Sigma)^{\frac{1}{2}}\Delta]$,
$F_2=N/L[-(\mu_z)^{\frac{1}{2}}B\delta+(\lambda_1-C)(m_3S/\Sigma)^{\frac{1}{2}}\Delta]$,
$L=(\lambda_1-C)(\lambda_3-A)-B^2$; $S=m_1+m_2$, $\Sigma=m_1+m_2+m_3$,
$\delta=[BC_6/(\mu_q\mu_z)^{\frac{1}{2}}]\lambda_1\lambda_3-C_5[1+B^2/\lambda_1\lambda_3]/\mu_qA$,
$\Delta=[k_{13}C_5-k_{11}C_6]/[k_{11}k_{33}-k_{13}^2]$,
$C_5=2\mu_q r_0/I_0$,
$C_6=(2m_3/\Sigma I_0)[m_1s_1-m_2s_2]$.

[7] As in the case of the symmetrical molecule X—Y—X, the interaction between rotation and vibration provides a correction to the moment of inertia of the molecule which amounts to about one percent of the total value. The corrected moment of inertia is to be computed from the following formula:

$$K=(h/4\pi^2 I_0)[1-\tfrac{1}{2}\{P(V_1+1)+Q(V_2+2)+R(V_3+1)\}],$$

where K is the interval between neighboring fine structure lines.

[8] Adel and Barker, Phys. Rev. **45**, 277 (1934).

LETTERS TO THE EDITOR

Prompt publication of brief reports of important discoveries in physics may be secured by addressing them to this department. Closing dates for this department are, for the first issue of the month, the twentieth of the preceding month; for the second issue, the fifth of the month. The Board of Editors does not hold itself responsible for the opinions expressed by the correspondents.

Surface Magnetization in Ferromagnetic Crystals

Deposits of a magnetic powder on a polished surface of a ferromagnetic crystal form under certain conditions a complicated pattern of lines related in some way to the crystalline space-lattice. Bitter, who published the first pictures of such patterns,[1] preferred a suspension in ethyl acetate of Fe_2O_3 particles about 1μ in diameter. Akulov and Degtiar[2] obtained more sharply defined patterns ("*S*-lines") with an alcohol suspension of the same material. Their Figs. 5 and 7 are particularly good. Becker and Freundlich[3] used a propyl alcohol suspension described as "almost colloidal" and show several photographs of the same region with different patterns depending upon the intensity of the applied magnetic field. All these observers applied magnetic fields parallel to the surface and report that the conspicuous lines of the patterns have different directions for different azimuths of the applied field. The spacing of parallel lines is different in different cases. In Bitter's Fig. 2 several horizontal lines near the lower right corner are spaced at about 100μ. Akulov and Degtiar report spacings of the order of 40μ. Becker and Freundlich's photographs show a few clearly resolved vertical lines, near the left of their Fig. 3, spaced at about 50μ. More conspicuous lines are farther apart, from 100μ upward.

We have improved the technique for observing such superficial heterogeneities of magnetization by using true sols of Fe_2O_3 in water (with a little KOH) which do not precipitate on iron.[4] The concentration of Fe_2O_3, however, is so much increased in regions where H is very non-uniform, that temporary swarms of particles in such regions can be photographed with ease. The mobility of the particles is a help rather than a hindrance, for in photographs with exposures of the order of a minute the sharpness of boundaries is not much affected by the size of individual particles. Furthermore, any change in the field-distribution is immediately followed by a migration of the swarms to new regions of highly non-uniform H. By these means we have been able to observe a new effect which throws some light on the distribution of magnetization to which the patterns are due.

In a particular experiment, a mono-crystal silicon iron[5] disk 0.6 cm in diameter and 0.04 cm thick was carefully polished on one side and mounted polished side up on the ground end surface of a vertical soft-iron bar 1.3 cm in diameter forming the core of a small electromagnet. A small rubber washer, a brass clamp with a hole in it, and a cover glass to cover the hole, formed the sides and top of the colloid cell. The cover glass had to be inclined to the horizontal to avoid troublesome reflections under vertical illumination. With this arrangement the applied magnetic field is normal to the surface and may easily be reversed in direction. Its magnitude can only be estimated as of the order of 1000. Fig. 1 shows the appearance of the same region for the two directions of the applied field. The time of exposure in each case was one minute and several minutes were allowed for the pattern to become stable before photographing it. It will be observed that the black lines on one pattern occupy the centers of the white spaces on the other. The spacing of adjacent parallel lines is about 4μ.

It was further observed (and photographed) that a very faint pattern, obtained after demagnetizing the core by reversals, comprised both of the patterns for large vertical applied fields. Moreover, a colloid containing smaller concentration of Fe_2O_3 gives patterns of the same dimensions but with narrower lines. There are in this specimen, two directions parallel to which lines run. These directions, nearly at right angles, agree in azimuth with the traces on the surface of the two planes of form {100} most nearly perpendicular to the surface. These traces were located by the analysis of a Laue diagram with about 30 fairly intense spots showing little internal strain in the disk. The lines are definitely not in the directions of the projections on the surface of <100> axes, which would require exchange of the acute angles, 86°, with the obtuse angles, 94°. Over considerable areas both sets of lines are equally developed and of the same average spacing. Where they are unequally developed the better developed set have the closer spacing. The longer lines are unequally black, blacker regions occurring at intervals of about 2μ. (This is particularly evident where lines are faintest, such lines appearing beaded.) As already reported by Akulov and Degtiar, ells and tees occur, but no crosses. We also note that H-patterns with cross-bars of minimum length are very unusual.

These findings seem to agree best with the hypothesis that the surface layer is composed of roughly cubical blocks

[1] F. Bitter, Phys. Rev. **41**, 507 (1932).
[2] N. [S.] Akulov, M. Degtiar, Ann. d. Physik **15**, 750 (1932).
[3] R. Becker, H. F. W. Freundlich, Zeits. f. Physik **80**, 292 (1932).
[4] We are indebted to Dr. L. A. Welo, of this laboratory, for the preparation of these sols in various concentrations.
[5] From a larger piece furnished by Dr. W. E. Ruder and more fully described by L. W. McKeehan and R. F. Clash, Jr., Phys. Rev. **45**, 839 (1934).

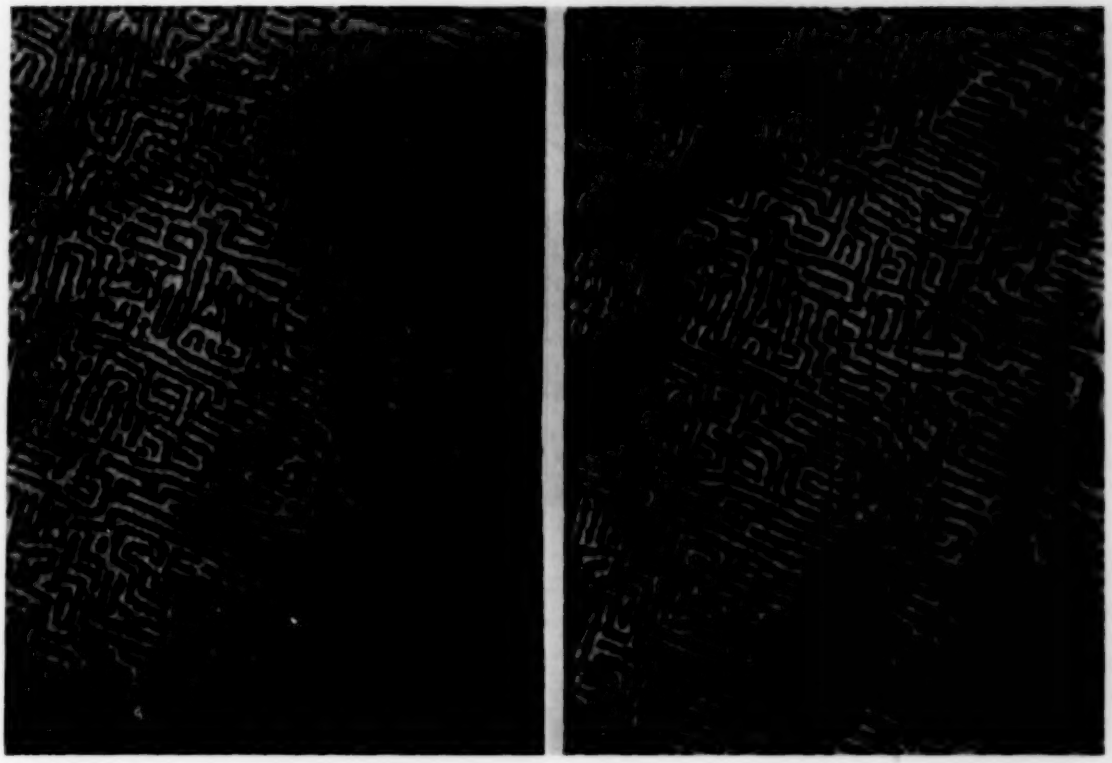

FIG. 1. Powder patterns with H normal to the surface. The group of 6 squares is about $70\mu \times 35\mu$.

about 2μ on each edge magnetized parallel to the surface either along a <100> direction or along a <110> direction. These blocks are so magnetized that the average magnetization over any small region is as small as possible. This requires opposing magnetizations normal to about half the block boundaries. In the absence of any applied field the stray field at these boundaries can produce some concentration of the colloid, producing a faint pattern with 2μ spacing. In the presence of a normal field half these boundaries have their stray field increased by the inclinations of the magnetizations in the adjacent blocks. The other half of the boundaries have stray field decreased by the same inclinations, as indicated in vertical cross section in Fig. 2. One of the denser patterns with 4μ spacing is then observed. A normal field in the opposite sense selects the other half of the original no-field pattern for enhancement. The blocks must be about as thick as they are wide to make these enhancements so striking.

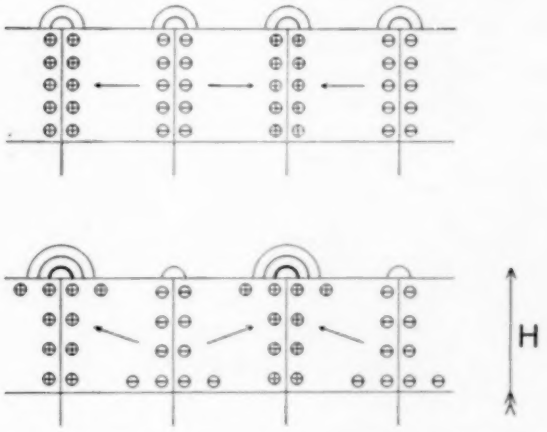

FIG. 2. Schematic diagram of magnetization in a plane perpendicular to the surface and of powder swarms at block boundaries, without H, and with H as indicated.

The particular scale of the patterns here shown seems to be accidental, for we have observed double spacings (in a normal field) as small as 1μ, and, as noted in the introductory paragraph, nearly rectangular patterns with much larger spacings have previously been observed by others.

More irregular streaks of much greater spacing are also observed on our specimens. Streaks of this sort may just be recognized in Fig. 1 and are seen to be parallel to one set of closely spaced lines. They are conspicuous at lower magnifications. These streaks also migrate when the normal field is reversed, so that light and dark regions interchange, as may be appreciated to some extent by studying the two photographs in Fig. 1. We attribute these also to variations in normal induction through the surface. The reversal of deeper lying layers with magnetic axes normal to the surface in both cases would account for the effect.

We are proceeding to study patterns in oblique applied fields by combining with the vertical bar electromagnet a larger electromagnet (Du Bois type) producing horizontal fields. The exchange of lines for spaces with change in the direction of the normal component persists as long as the fine lines are observable. In agreement with previous observers we find that the fine line pattern itself changes as the field parallel to the surface increases and may be made very nearly invisible.

L. W. McKeehan
W. C. Elmore

Sloane Physics Laboratory,
Yale University,
July 7, 1934.

Progression of Nuclear Resonance Levels with Atomic Number

In a recent letter to the *Physical Review*[1] one of us pointed out that the resonance levels for alpha-particle disintegration seem to vary linearly with the atomic number. A tentative explanation was given in terms of standing waves within the potential barrier. In the present note we offer a more adequate explanation in terms of particle interaction.

For the six elements Be, B, N, F, Mg, Al, resonance levels are found with energies differing by increments proportional to the change in nuclear charge. The mean increment for an increase in charge of two units (a difference of an alpha-particle) is $1.1\pm0.3\times10^{-6}$ ergs. A second series of levels is found with approximately the same increment although the experimental data are less complete. The straight lines joining the values of the resonance energies in each series plotted against nuclear charge are roughly parallel to the line joining the minimum penetration energies (or barrier heights) which are much harder to define and measure than the resonance energies themselves. The linear increase of barrier height with nuclear charge implies that the radius of the inside of the potential wall is at least approximately a constant.

Resonance levels correspond to energies of unoccupied alpha-particle states inside the nucleus. For approaching alpha-particles of these energies the penetration probability rises to unity. There is as yet no theoretical method of determining the actual positions of the virtual alpha-particle levels for a given nucleus. This is, however, not necessary if the *change* in energy of a particular level from nucleus to nucleus is considered. We make the suggestion that the difference between the energies of corresponding alpha-ray resonance levels in elements of atomic numbers Z and $Z+2$ is in general due to the interaction of two alpha-particles: (1) the alpha-particle added to the nucleus in passing from the first element to the second, (2) the alpha-particle, the virtual presence of which gives rise to the resonance. Since the radius of the inside of the barrier is sensibly constant for these elements, this interaction accounts very simply for the approximately linear increase in the resonance energy as we pass from, say, boron to nitrogen.

It is also possible, on the basis of simple assumptions, to explain the order of magnitude of the energy differences. Let us assume that one alpha-particle is localized near the center of the nucleus while the other is bound in one of the stationary states of the nucleus. If the latter is regarded as a barrier of infinite height and radius r_0, the radial part of the ψ-function for any one of the stationary states has the form

$$R=Ar^{-\frac{1}{2}}J_{l+\frac{1}{2}}(kr)$$

where k is determined by the condition that $J_{l+\frac{1}{2}}(kr_0)=0$. Let us assume the interaction to be of the Coulomb type. We then obtain for ΔE, the energy difference in question,

$$\Delta E=4e^2k\int_0^{\xi}J^2_{l+\frac{1}{2}}(x)dx/\int_0^{\xi}J^2_{l+\frac{1}{2}}(x)\cdot xdx,$$

where ξ is a root of $J_{l+\frac{1}{2}}(x)$. If we assume the alpha-particle to be bound in the lowest S-state ($l=0$, ξ is the first root) the result is: $\Delta E=2.3\times10^{-6}$ ergs, if it is in the lowest P-state ($l=1$, ξ is the first root) $\Delta E=1.7\times10^{-6}$ ergs. For higher states the results are somewhat smaller. The value for r_0 here chosen is 10^{-12} cm. This is probably not too high because the finite actual height of the barrier causes the charge of the alpha-particle to penetrate into the walls of the barrier.

The significant fact seems to be that the Coulomb energy alone produces the correct order of magnitude for ΔE, but that the results are numerically too high. This is in line with the known circumstance[2] that the deviations from Coulomb interaction between alpha-particles diminish the repulsion. As is seen, the correction here amounts to about 50 percent of the Coulomb energy itself.

The change in the position of the resonance level from one element to the next, e.g., from beryllium to boron, is to be understood in a similar manner. The increment in energy is here due to the interaction between a proton and an alpha-particle, and this should be approximately half the ΔE calculated above. A general linear progression in the position of nuclear resonance levels with atomic number is thus explained.

It is to be expected that the resonance level of B^{10} lies higher than that of B^{11}, for the latter contains one neutron more than the former, and a "free" neutron should produce a negative energy of interaction with an alpha-particle. The experimental results so far indicate that this is actually the case but are not sufficiently accurate to permit more than a speculative value for the difference.

The suggestions here presented may be of guidance in the absence of a correct nuclear theory. The similarity of this explanation with that of the progression of atomic resonance states is of course evident.

H. Margenau
E. Pollard*

Yale University,
June 13, 1934.

* Sterling Fellow.

[1] E. Pollard, Phys. Rev. **45**, 218 (1934).
[2] H. M. Taylor, P.R.S.A. **134**, 113 (1931).

Protons Emitted from Boron and Phosphorus Bombarded by High Energy Alpha-Particles

During the past year the writer has been privileged to use a strong source of thorium C′ at the University of Tübingen, Germany. By means of a proportional counter developed by Geiger it has been possible to examine the protons emitted by elements bombarded by the high energy alpha-particles from thorium C′. Proton emission at right angles to the direction of bombardment has been studied for both boron and phosphorus using these rays. The results are shown in Figs. 1 and 2.

Curves 1, 2, 3 and 4 show the results obtained for the protons from a thin layer of boron when bombarded with alpha-particles of 8.6 cm range—the full energy available—and with 7.6 cm range, 6.1 cm range, and 5.2 cm range, respectively. Curves 1 and 2 show three well resolved groups and a fourth group ending at about 37 cm in curve 1 but not so well resolved because of the geometry of the experiment. The characteristic energy, Q, for each of these groups was computed from curve 1 on the assumption that energy and momentum are conserved in the transformation and that the range-velocity data recently published by Duncanson[1] are correct. These Q's, in order of decreasing range, are (in electron-volts) $3.1 \cdot 10^6$; $0.35 \cdot 10^6$; $-0.78 \cdot 10^6$; $-1.86 \cdot 10^6$. Most of the previous work[2, 3, 4, 5] on boron has been done with alpha-particles from polonium and the greater energy available here gave a much larger velocity and corresponding range to the protons permitting a greater separation of these groups and a corresponding increased accuracy in the determination of their location. The two groups with positive energy have values for Q which check nicely with results obtained by Chadwick and mentioned in Duncanson's report. The group with the largest negative energy agrees with a similar one reported by Heidenreich. The other group whose Q is determined as $-0.78 \cdot 10^6$ e.v. has not been previously resolved. The yield of protons for this work was approximately the same as that found by others but, for the range of alpha-particles used, the results show definitely that the relative number of protons in each group emitted does not change as the energy of the bombarding alpha-particles is changed. This can readily be seen in Fig. 1 by noting the height of the several arrows which mark the ends of the groups for each range of alpha-particles used.

[1] Duncanson, Proc. Camb. Phil. Soc. **30**, 102 (1934).
[2] Chadwick, Constable and Pollard, Proc. Roy. Soc. London **A130**, 463 (1930).
[3] Bothe, Zeits. f. Physik **63**, 381 (1930).
[4] Heidenreich, Zeits. f. Physik **86**, 675 (1933).
[5] Pollard, Phys. Rev. **45**, 746 (1934); **45**, 555 (1934).

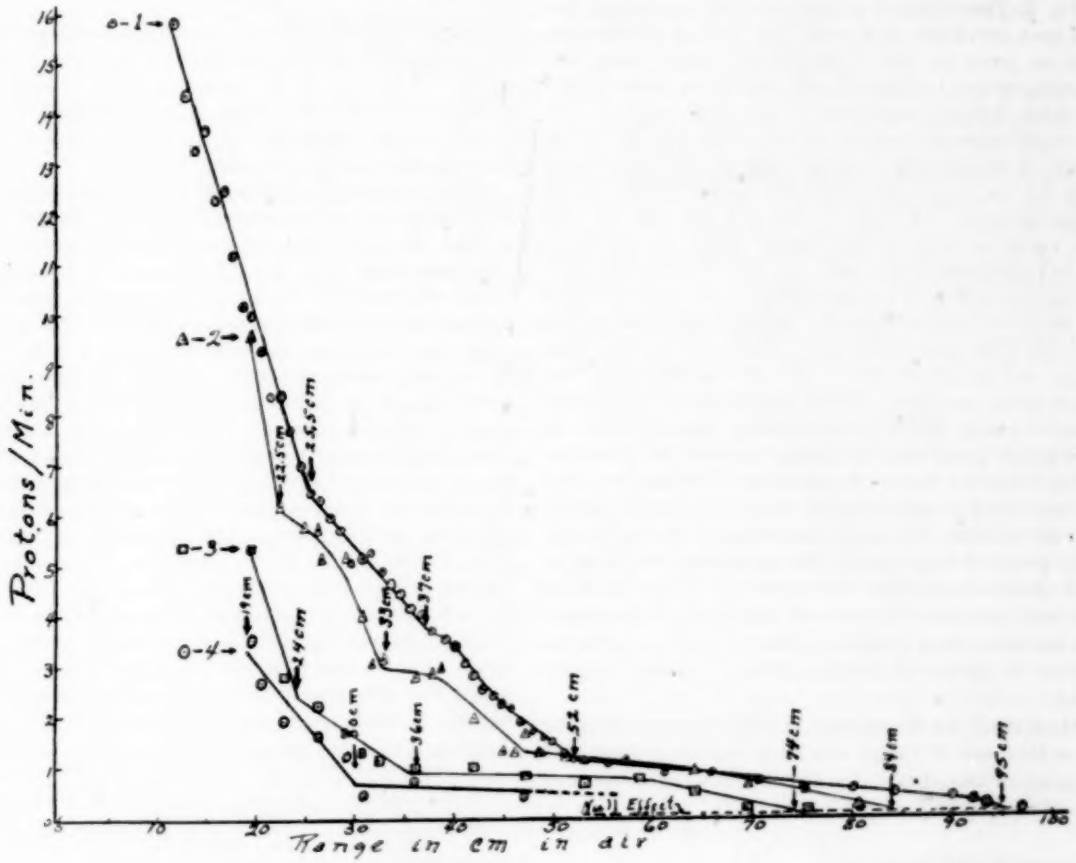

FIG. 1. Boron.

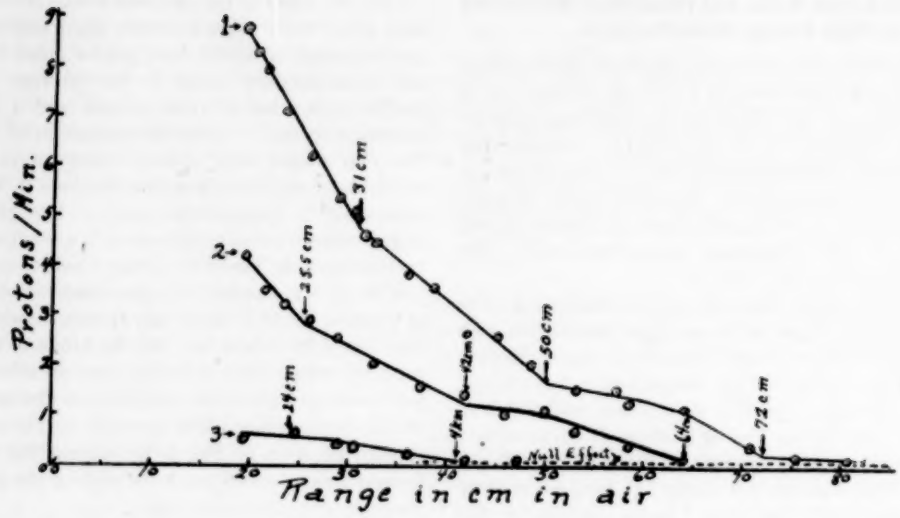

FIG. 2. Phosphorus.

Results surprisingly similar to those for boron are obtained with phosphorus and are summarized graphically in Fig. 2. Three distinct groups are found where only one had been previously observed.[2] The yield of protons was fully as great as that obtained from boron when the phosphorus was bombarded with the 8.6 cm range alpha-particles. But, as comparison of the three curves in the figure will show, the yield decreased rapidly with decreasing energy of bombarding alpha-particle, curve 1 being taken with 8.6 cm range alpha-particles, curve 2 with 7.6 cm alpha-particles, and curve 3 with 5.2 cm ones. In this last curve no trace of the middle group of protons in curve 1 appeared though these protons should be observable in this experiment at a range ending at 24 cm as indicated by the arrow. Values for the Q's for the three proton groups emitted from phosphorus, given in order of decreasing range, are 0; $-1.47\cdot10^6$; $-2.96\cdot10^6$ electron-volts. The single group previously found[2] was reported with a small positive energy but is probably to be identified with the zero energy group here. It should, however, be noted that curve 1 does not fall to the null value of the counter at 72 cm, remaining at approximately twice this value at both 75 and 81 cm. This may mean the presence of a fourth very faint group of larger range. But phosphorus is known to emit neutrons and, while the count observed in this range was from particles which did not penetrate 1 mm of lead, the existence of a group of protons ending somewhere beyond 81 cm can only be established by further experiment.

Much credit for the success of the experiments should be given Professor H. Geiger who suggested the problem and supplied all needed facilities. Dr. O. Haxel also cooperated actively in carrying out the work.

R. F. PATON

University of Illinois,
July 5, 1934.

On the Interpretation of Present Values of Nuclear Moments

Various writers[1, 2, 3, 4, 5, 6, 7] have published speculations on the magnetic moment and the nature of the neutron and proton. In view of the discordant results it appears proper to discuss the reliability of the g values for different nuclei as well as the plausibility of the explanations proposed from the point of view of nuclear structure.

(a) It is believed by Inglis and Landé[3] that the disagreement between Landé's[1] assumed value $g_p=4$ for the proton g factor, the molecular beam value[8] 5.0 ± 10 percent, and the atomic beam value[9] 6.4 ± 10 percent is to be attributed to the crudities of the theory used in all three cases. As far as we know this objection cannot apply to the R. K. Z. value. The only essential points presupposed in the theory of the experiment are: (1) the possibility of describing the interaction of the electron and the nucleus by assuming a nuclear magnetic moment, (2) the sufficient validity of Dirac's equation for a single electron as applied to hydrogen. It is possible that one or both of these suppositions are incorrect, but it seems impossible to discuss the problem definitely without either. The agreement between the S. E. F. and the R. K. Z. value may be regarded as a support of both. It should be remembered that the S. E. F. value is obtained by a direct measurement of the force on the magnetic moment of the proton and does not depend on interactions between electrons and protons a short distance apart. The corrections for the rotational magnetic moment of the molecule were made experimentally by using

[1] A. Landé, Phys. Rev. **44**, 1028 (1933).
[2] B. Venkataschar and T. Subbaraya, Zeits. f. Physik **85**, 264 (1933).
[3] D. R. Inglis and A. Landé, Phys. Rev. **45**, 842 (1934).
[4] H. Kallmann and A. Schueler, Zeits. f. Physik **88**, 210 (1934).
[5] H. Schueler, Zeits. f. Physik **88**, 323 (1934).
[6] H. Schueler and H. Westmeyer, Naturwiss. **21**, 674 (1933).
[7] T. Tamm and S. Altschuler, Comptes Rendus de L' Academie des Sciences de l' U.R.S.S. **1**, 458 (1934).
[8] Stern, Estermann and Frisch, Zeits. f. Physik **85**, 4, 17 (1933).
[9] Rabi, Kellogg and Zacharias, Phys. Rev. **45**, 761 (1934).

parahydrogen. The only vital assumption involved is that of the constancy of this magnetic moment to the corresponding mechanical angular momentum. We see no reason for seriously questioning this.

On the other hand, the nuclear g values used by Landé are questionable. With the exception of $g=2.19$ for Li^7 they are all obtained on the supposition that the many electron problem presented by an atom is approximated with sufficient accuracy by replacing the effect of all but the valence electrons by a suitable central field. In some cases corrections for perturbations have been made. In no case has a complete calculation been carried out. The magnitude of the error introduced by this assumption is at present unknown and there appears to be no valid reason for supposing it to be small.

It is possible to eliminate our lack of knowledge of absolute nuclear g values by paying attention to the ratios of the g factors of isotopes. The atomic wave functions cancel out in such a calculation. It is of interest to discuss such ratios for Z odd and M odd by using Landé's picture of i and μ as due to proton having a definite orbital angular momentum l. For Rb the only reasonable assignment of l is $l=1$ for Rb^{87} and $l=3$ for Rb^{85}. Other assignments lead to impossible ratios of $g(87)/g(85)$ or else to wrong signs of $g(87)$ or $g(85)$. Using the experimental value $g(87)/g(85)=3.46$ one obtains $g_s=3.97$ which is in excellent agreement with Landé's $g_s=4$ but disagrees violently with S. E. F.'s $g_s=5$ or R. K. Z.'s $g_s=6$, these values of g_s would require $g(87)/g(85)=5.4, 9.3$, respectively. Both of these values are excluded by the high accuracy of Kopfermann's experiments. For Sb the experimental value $g(121)/g(123)=1.80$ may be accounted for either by $g_s=3$ with $l=2$ for Sb^{121} ($i=5/2$) and $l=4$ for Sb^{123} ($i=7/2$) or else by $g_s=-3$, $l=3$ for Sb^{121} and Sb^{123}. The latter choice is in disagreement with Rb and so is $g_s=3$ because $g_s=4$ gives $g(121)/g(123)=2.4$ which can hardly be mistaken for 1.80. For Ga there appears to be no reasonable way of accounting for $g(71)/g(69)=1.27$, on Landé's picture.[1]

The theoretical values given in Table III of Tamm and Altschuler appear to satisfy the isotope ratio for Sb very accurately giving $g(121)/g(123)=1.79$ as compared with the experimental value 1.80. This agreement is due, however, to a numerical error present in this table and in the corresponding table of Landé. For Sb^{123} one cannot use $l_p=3$ because $i=7/2$ was used to obtain $g=0.60$ and for g (proton spin) $=g_{sp}=4$ one would have $g(123)=10/7=1.43$ as compared with the observed 0.60. On the other hand, using $l_p=4$, one gets $g(123)=0.67$. In order to obtain reasonable agreement with the observed $g(121)$ one has to use $l_p=4$ in Sb^{121} coupled to s_p to give $j_p=7/2$ which is then coupled to $j_n=1$ to give $i=5/2$. One obtains a theoretical $g=1.00$ and a theoretical $g(121)/g(123)=1.50$ which is in poor agreement with the observed 1.80. For Ga the table of Tamm and Altschuler gives for $g(71)/g(69)$ the values 1.50 theoretically which compares poorly with the experimental 1.28. Kallmann and Schueler obtain satisfactory ratios for Rb and Sb but for Ga the theoretical 1.36 is too large. Even if this discrepency were removed the value $g_{sp}=4$ used by K. S. is in definite contradiction with S. E. F. and R. K. Z. as well as with the g factor for Li^7.

It should be emphasized that in the above comparison the uncertain features of theoretical calculations have been eliminated. Thus the data available at present appear to indicate a variable g_s according to all the schemes proposed. None of the above values are in agreement with $g=2.2$ for Li^7 which leads to either $g_s=4.6$ or $g_s=-5.0$. Either of these values agrees with the measurements of S. E. F. and of R. K. Z. since the sign of g_s is left undetermined by them. On the other hand, adjusting $g(Li^7)$ to be 2 as is desired by Landé, implies an accuracy of only 10 percent in the theoretical calculations. The relative simplicity of the electronic configurations dealt with suggests a much higher accuracy.

(b) The attempt at a conclusion that the neutron is not an elementary particle from the sign of its g factor appears to be premature. It is well known that interaction terms of Pauli's type can describe a particle with an arbitrary magnetic moment so that either sign of the g factor is in agreement with the view that the neutron is an elementary particle. Further, either sign can be explained by supposing that the neutron is composite: a negative value can be explained by saying neutron = proton + electron, a positive value one could explain by saying neutron = neutron' + electron + positron.

The sense in which electrons or positrons may be said to exist in a nucleus is very obscure. We doubt whether much meaning may be ascribed to theories making detailed pictures of the composition of the neutron or proton.

(c) According to the usual ideas of nuclear structure the constitution of a nucleus resembles that of a polyatomic molecule or else of a liquid. It is questionable whether there is much meaning to a central field which one must necessarily assume in order to assign an orbital quantum number to a particle under these conditions. Even if the central field picture applies it is questionable whether the core may be considered as having a constant g factor as is done by Kallmann and Schueler. It is also questionable whether the coupling order $p(nn)$ used by Tamm and Altschuler is consistent with the generally supposed importance of the pn bond. One would rather suppose that $(pn)n$ is a more probable coupling possibility.

In the table of Landé for nuclei with odd Z and odd M some nuclei have $l_p>j_p$ and others $l_p<j_p$. Presumably one of these possibilities corresponds to a lower energy level than the other. The energy difference between $j_p=l_p+\frac{1}{2}$ and $j_p=l_p-\frac{1}{2}$ may be supposed to be of the order of the magnetic interaction energy of two nuclear magnetons located at a distance of 10^{-13} from each other. Its order of magnitude is several hundred volts. The probability of magnetic dipole radiation from the higher to the lower of these levels is such that the mean life would be $\sim 1/50$ sec. if $\Delta W=200$ volts. It is thus difficult to reconcile the known stability of a number of nuclei with the above theories of nuclear moments.

G. Breit
New York University
I. I. Rabi
Columbia University

July 21, 1934.

Theory of the Heat Treatment of Magnetic Materials

The magnetic permeabilities of certain alloys have been increased enormously by heat treating them in a magnetic field.[1] A permeability of over 600,000 has been attained in permalloy containing about 65 percent nickel. The purpose of this note is to discuss the nature of the changes that occur in these materials during the heat treatment in the field and more generally to discuss those structural changes, peculiar to ferromagnetic materials, which occur during heat treatment.

As a ferromagnetic specimen cools through the Curie point in the absence of an applied field, modern magnetic theory postulates[2] that small regions or domains become magnetized to saturation in a definite crystallographic direction, one of the <100> directions (cube edges) in the case of 65 permalloy.[3] As this magnetization develops, magnetostrictive stresses arise which tend to change the shapes of the domains, in the case of this alloy to increase the dimension in the direction of the local magnetization and decrease those at right angles. This process is illustrated in Fig. 1, where (a) represents a part of the material, above the Curie point, which is to become part of a single domain when cooled. A spherical form is assumed merely for convenience. As the specimen cools through the Curie point and becomes ferromagnetic, the domain becomes saturated in some direction as shown in (b) and also tends to change its shape because of its magnetostriction, as indicated in an exaggerated way by the dotted ellipse. If the domain were free in space it would assume the latter shape immediately, but actually it is surrounded by other domains which constrain it, preventing its change in shape. However, if the specimen is held for sufficient time at a high enough temperature (below the Curie point), the sphere will actually assume the shape shown in (c) by plastic flow of the surrounding domains. It is the latter idea, of plastic flow on account of the magnetostriction in the domains, that is fundamental to the theory of heat treatment here presented. The direction of magnetization in each domain is parallel to a crystallographic axis <100>, but the various domains will be oriented in equal numbers in all directions. When a field is applied for measurement at room temperature, the magnetization of the specimen as a whole will be changed in three ways: (1) reversal of the magnetization (180° change) in some of the domains; (2) change in the direction of magnetization in other domains by 90°, to a different <100> direction; and (3) rotation of the magnetization vector out of a <100> direction. The last process occurs to a considerable extent only in relatively high fields, and does not concern us here. Process (1), represented in Fig. 1 as a change from (c) to (d), takes place with a minimum of energy loss, because magnetostrictive strain is independent of the sign of the magnetization and the shape of the domain is the same before and after the change. Process (2), (c) to (e), requires work to be done against elastic forces. This additional energy involved in Process (2) as compared with Process (1) seems to be the reason for the more frequent occurrence of the latter process, as determined by Heaps[4] and more directly by McKeehan and Clash.[5]

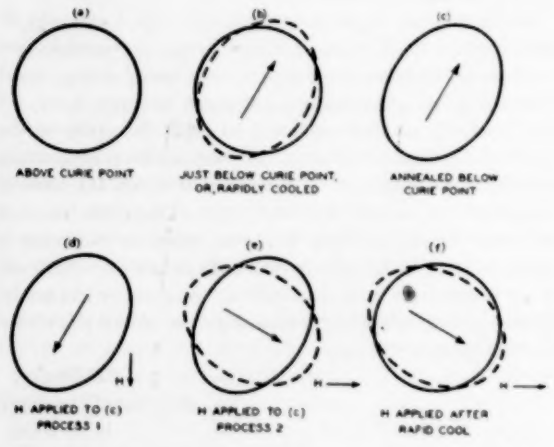

FIG. 1. The shapes of domains as influenced by heat treatment.

Obviously, the greater the proportion of changes of kind (1) the less the energy loss attending magnetization to technical saturation, and the greater the maximum permeability. An increase in the proportion of changes of kind (1) relative to kind (2) is just the result one attains when the material is heat treated in a magnetic field, for then the domains are *all* magnetized in the <100> direction nearest to that of the field and are stabilized in those positions by plastic flow. When the material is demagnetized at room temperature, half of the domains reverse (Process 1), and when the specimen is magnetized in the same or opposite direction to that in which the field acted during heat treatment, reversals again occur with a minimum of energy loss. On the other hand, if the field applied for measurement is perpendicular to that applied during heat treatment, one expects relatively large strains to be set up in the material (Fig. 1 (e)) and consequently much lower permeability. The experimental results are in accord with these views: the ratio of permeabilities in the two directions has been found to be as large as 200 to 1.

If the material is *cooled rapidly* enough from some temperature above the Curie point to a temperature below the recrystallization temperature, there will not be time for the domain to change its shape as shown in Fig. 1 (a) to (c), and the magnetostrictive stress will persist at room temperature as indicated by (b). When a field is then applied and the direction of magnetization changes by 90°, Fig. 1 (f), the elastic strains set up will have a different direction from that which they had before the field was applied, but will be of the same magnitude. Consequently, the energy loss will be less than that attending the change from (c) to (e) for the slowly cooled material. As a result,

[1] R. M. Bozorth, J. F. Dillinger and G. A. Kelsall, Phys. Rev. **45**, 742 (1934).
[2] See various papers by W. L. Webster, W. Heisenberg, R. Becker, F. Bitter, R. M. Bozorth.
[3] F. Lichtenberger, Ann. d. Physik **15**, 45 (1932).
[4] C. W. Heaps, Phys. Rev. **45**, 320 (1934).
[5] L. W. McKeehan and R. F. Clash, Jr., Phys. Rev. **45**, 839 (1934).
[6] Curve (a) from G. W. Elmen, J. Frank. Inst. **207**, 583 (1929); curve (b), from his unpublished data, is for a cooling rate of 20° to 40°C per second.

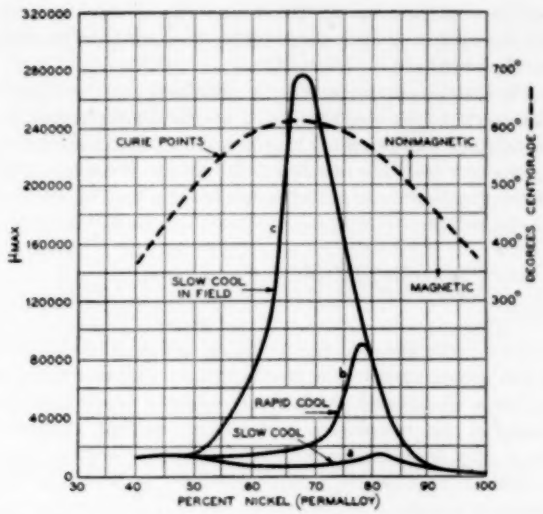

FIG. 2. The maximum permeabilities of Fe-Ni alloys as influenced by heat treatment. The dotted line shows the Curie points.

the maximum permeability will be higher for rapidly cooled material than for that slowly cooled in the absence of applied field; but the highest permeability of all will be attained in the material heat treated in a field. The maximum permeabilities[6] of the iron-nickel alloys are shown in Fig. 2 as a function of composition, for the three kinds of heat treatment discussed in relation to this theory.

One may consider whether the magnitude of the magnetostrictive strain, $\Delta l/l$, is adequate to change the magnetic properties as much as various heat treatments are observed to change them. Using the saturation value of $\Delta l/l$ for 65 permalloy, 2×10^{-5}, and Young's modulus, 2×10^{4} kg/mm^2, we find that a tension of about 0.4 kg/mm^2 will produce the same strain as magnetization to saturation. Measurement shows that the application of this stress to a specimen slowly cooled without applied field, increases the maximum permeability from 7000 to 25,000, the latter value being larger than that characteristic of the rapidly cooled unstrained material. This similarity in the effect of applied tension and magnetostrictive stress gives strong support to the fundamental idea of the theory.

According to the theory described, it is not to be expected that different magnetic behavior will result from different heat treatments of annealed material if the Curie point or a phase transformation point lies between room temperature and the temperature at which a slightly strained crystal relieves itself of strain. That this expectation is correct for the iron-nickel alloys is shown plainly in Fig. 2 where the Curie points,[7] shown by the dotted curve, lie above the strain-relief temperature for these alloys (400 to 500°C) for compositions between 50 and 85 percent nickel. It has been found also that heat treatment in a field has a negligible effect upon nickel, which has a low Curie point, and only a small effect upon iron, which has complicated magnetostriction. This heat treatment has also been found ineffective in certain iron-cobalt-nickel alloys which have low Curie points or low phase transformation temperatures.

R. M. BOZORTH

Bell Telephone Laboratories,
New York, N. Y.,
July 12, 1934.

[7] F. Hegg, Arch. d. Sci. Phys. et Nat. **3**, 15–45 (1910). The alloys actually used in obtaining curves (a), (b) and (c) of Fig. 2 contain 0.5 to 1.0 percent Mn and other impurities, and their Curie points are somewhat lower (perhaps by 50°C) than those reported by Hegg.

The Nuclear Spin of Columbium

In a preliminary report[1] the value of the quantum number of nuclear spin for columbium[93] was given as $I\geq7/2$. A more detailed study has been made of the hyperfine structure of the columbium spectrum. The discharge in a liquid air-cooled Schüler tube was used as a light source. The instrument of high resolving power used was a Fabry-Perot etalon. A three prism flint glass spectrograph was used as the instrument of auxiliary dispersion. The columbium spectrum has been photographed from λ4000 to λ7000 with etalon separators ranging in width from 2.5 mm to 15 mm. The results of the investigation may be summarized as follows: Measurements of the intervals between the hyperfine structure components of λλ4059, 4080 and 4649 indicate definitely a value $I=9/2$ for columbium. Relative intensity measurements on the hyperfine structure components of λ4117 and λ4649 also indicate a value $I=9/2$. The hyperfine structure patterns of the prominent unclassified lines λλ4672, 4675, 5344 and 6661 can be satisfactorily explained if 9/2 is accepted as the value of I for columbium. A detailed description of this investigation will be submitted for publication soon.

STANLEY S. BALLARD

University of California,
Berkeley, California,
July 3, 1934.

[1] N. S. Grace and S. S. Ballard, Phys. Rev. **44**, 128 (1933).

Fundamental Frequencies of Acetylene

Six frequencies were found in liquid acetylene by Raman scattering by using 4358 Hg and 4046 Hg: 382(5), 618(2), 631(5), 1762(1), 1959(10), 3338(5) cm^{-1}. The last two had been obtained before by Daure[1] and Daure and Kastler.[2] These new frequencies will be used to interpret the infrared bands of acetylene. This last point will be presented at the forthcoming American Chemical Society meeting in Cleveland.

GEORGE GLOCKLER
CHARLES MORRELL

University of Minnesota,
July 11, 1934.

[1] Daure, Trans. Faraday Soc. **25**, 825 (1929).
[2] Daure and Kastler, Comptes Rendus **192**, 1721 (1931).

Neutron Collisions and the Beta-Ray Theory of Fermi

The theory recently proposed by Fermi[1] for β-ray disintegration offers a precise theoretical method for treating the interaction of the neutron with charged particles. In calculations of simple interactions of this kind, three points become immediately apparent: The calculated effects are many orders of magnitude too small to have any bearing on the experimental behavior of free neutrons or on the exchange forces between nuclear neutrons and protons. This is a direct consequence of Fermi's introduction of the small dimensionless number

$$G=g(h/2\pi mc)^{-3}(mc^2)^{-1}\leqq 9\times 10^{-13}$$

to fit the empirical slowness of β-ray decay. Secondly, the field of force of the neutron for charged particles is appreciable out to a radius of some 10^{-10} cm, and this is traceable to the fact that the only characteristic length appearing in the formalism is $h/2\pi mc$. Finally, one occasionally finds divergent integrals of the same type as are met with in the quantum theory of the radiation field and of the positron. We have treated two simple cases of neutron interaction with charged particles—the inelastic scattering of a neutron by a heavy charged particle and the elastic scattering of a neutron by a proton—in the first of which the divergence difficulty does not occur, while in the second it can be obviated in a plausible manner.

According to the theory, any charged particle may interact with the neutron by polarizing the charge cloud produced by oscillation ($N\rightleftarrows P+e^-+n$) between the two states postulated for heavy particles by Fermi. In the case that the interacting particle is a proton, there is the additional possibility that this proton itself make a transition of the Fermi type, thus giving rise to an exchange force of the kind postulated by Heisenberg.

The simplest case considered is that of the inelastic scattering of a neutron by a heavy particle: $X+N\rightarrow X+P+e^-+n$. This is to be thought of in the formalism as a transition of the neutron into a proton with the emission of the two light particles, electron and neutrino, followed by a deflection of the created proton by the stationary particle through their Coulomb interaction. The effective cross section of the heavy particle for this type of collision is found to be

$$\sigma_{\text{inelastic}}=G^2Z^2(e^4/m^2c^4)f(v)\leqq 10^{-49}Z^2\ \text{cm}^2.$$

Here G is the small constant mentioned above, eZ is the charge of the heavy particle, $e^4/m^2c^4\leqq 10^{-25}$ cm^2 is approximately the area necessary to give observable scattering, and $f(v)$ is a function of the velocity of the incident neutron which vanishes unless the energy of the neutron is larger than the threshold value $(2+2\Delta)mc^2\leqq 2\times 10^6$ volts if the heavy particle is a proton, $m\Delta$ being the mass defect of the neutron with regard to the proton. With an available energy less than this threshold energy the process cannot occur because energy and momentum cannot simultaneously be conserved. If the heavy particle has infinite mass, the threshold is at $(1+\Delta)mc^2\leqq 10^6$ volts. For energies above the threshold $f(v)$ is roughly of the order of magnitude unity. The formula should be applicable to neutron energies up to 10^7 volts. The inverse process $N+P\rightarrow 2N+e^++n$ is describable by the same formula with the threshold at $(2-2\Delta)mc^2\leqq 0$.

The elastic scattering may be visualized as an exchange phenomenon: An electron and a neutrino are emitted by the neutron and absorbed by the proton, thus transferring momentum from the one heavy particle to the other. The effective cross section of the proton for this kind of collision may be written

$$\sigma_{\text{elastic}}=G^4\alpha^{-2}\left(\frac{M}{m}\right)^2\frac{e^4}{m^2c^4}\varphi(v)\leqq 10^{-61}\ \text{cm}^2,$$

where α is the fine structure constant and M/m is the ratio of the proton mass to the electron mass. $\varphi(v)$ contains the square of an integral which diverges like $\int^{\infty}dp/p$ for large values of the momentum p of one of the light particles. Since the contributions to the integral decrease with increasing p, it seems perhaps justified, at least for momentum transfers between the heavy particles not exceeding mc/α, to replace the upper limit by mc/α. This contributes a factor $(\log(1/\alpha))^2\leqq 24$; for the rest, $\varphi(v)$ is then a function of the velocity of the incident neutron which is roughly of the order unity.

One may further attempt to calculate the mutual potential energy (exchange energy) $\Phi(R)$ of the neutron and proton as a function of the distance $R\times h/2\pi mc$ between them. One would then expect the σ_{elastic} given above to be obtainable from this Φ by the methods of quantum-mechanical collision theory. The expression to which one is led is:

$$\Phi(R)=\frac{G^2mc^2}{64\pi^6}\int\int d\mathbf{k}d\mathbf{k}'\frac{\epsilon k'+(\mathbf{k}\cdot\mathbf{k}')}{\epsilon k'(\epsilon+k')}e^{\mathbf{k}\cdot\mathbf{R}+\mathbf{k}'\cdot\mathbf{R}},$$

where $d\mathbf{k}$ and $d\mathbf{k}'$ are the volume elements in the k and k'-spaces, $\epsilon=(1+k^2)^{\frac{1}{2}}$, and R is the relative distance in units $h/2\pi mc$. The double integral diverges, being of the form of an infinite sum of increasing terms of alternating sign. One may arbitrarily give a meaning to the expression by inserting factors e^{-ak} and $e^{-ak'}$, performing the integration, and taking the limit of the resulting expression as $a\rightarrow 0$. This gives a finite answer for all non-zero values of R; the force is attractive and the potential decreases like R^{-6} for distances small compared to $h/2\pi mc$ and exponentially for distances large compared to $h/2\pi mc$. This procedure is, however, quite arbitrary and does not lead to the formula given above for elastic collisions, but to one containing a more seriously divergent integral, so that little significance can be attached to Φ thus calculated. One may alternatively calculate the elastic scattering with the expression for Φ written above without first carrying out the integrations indicated, breaking off the resulting logarithmically divergent integral again at momenta mc/α. This gives just the cross section found directly, and corresponds roughly to inserting into the integral for $\Phi(R)$ the factor $e^{-a|\mathbf{k}'-\mathbf{k}|}$. With this definition of $\Phi(R)$, to which perhaps more significance can be attached, the explicit dependence on R is not readily calculable.

[1] Fermi, Zeits. f. Physik **88**, 161 (1934).

The elastic cross section and the exchange force have been calculated on the hypothesis that only the processes $N \rightleftarrows P+e^-+n$ with the electron in a positive energy state can occur. If one admits in addition the symmetrical and perhaps plausible possibilities $P \rightleftarrows N+e^++n$, the exchange energy is increased by a factor of 2 and the elastic cross section by a factor of 4.

The writer wishes to acknowledge suggestion and valuable discussion of these considerations on the part of Professor J. R. Oppenheimer.

ARNOLD NORDSIECK

University of Michigan,
Ann Arbor, Michigan,
July 11, 1934.

Ionization by Positive Alkali Ions as Measured by a Balanced Space-Charge Method

The minimum speeds at which ionization occurs when gas atoms are struck by accelerated positive alkali ions has been investigated for several gases and ions. By allowing the ionization to take place in a region containing a space-charge limited current of electrons, it has been possible to observe with great accuracy the formation of new positive ions because of the strong effect of positive ions on the electron current.[1] This method has the great advantage of being highly or completely insensitive to secondary electrons liberated from the walls and thus surmounts the greatest difficulty encountered in other methods.[2]

The electron space-charge was produced inside a cylindrical anode having an axially placed hot filament cathode. By using two such cylinders and filaments balanced against each other in a bridge circuit, with the filaments connected in parallel, and by allowing the ionization to take place in only one cylinder, all undesirable fluctuations in the space-charge current were eliminated. Extremely small changes in the electron current could thus be measured accurately.

Table I shows the results obtained (the numbers are the ion speeds in volts at which ionization was observed to start with the indicated ion and gas).

TABLE I.

TABLE I. *Ion energies in electron-volts at which ionization was observed to start.* (The dash indicates that no ionization was observed when ion speeds up to 530 volts were used.)

	Na^+	K^+	Rb^+	Cs^+
Ne	130±2	86±2	232±4 ?	—
A	105±3	82±2	135±3	340±2
N_2	88±2	79±2	260 ?	—
CO_2	95 ?	75±2		—

The manner of taking readings was to raise the speed of the beam and to observe the resulting deflection of the galvanometer measuring the difference of electron currents in the two cylinders. As the voltage was raised, the galvanometer showed no change in deflection (or very slight change) until the critical ionizing speed (see table) was reached. At this point the galvanometer started deflecting strongly, the deflection rising linearly with the voltage. The case of Cs^+ in A was the only exception. In this case the deflection started rather gradually, the range from 340 to 370 volts being covered before a linear deflection was reached.

The accuracies given are only approximate. They cover principally the errors that may arise from voltage gradients whose effect on the positive ion beam is unknown. Such gradients never spread over a range greater than five volts in the course of the measurements. Results could always be reproduced well within the errors given. A few results, as indicated, are doubtful because of the weakness of the ionization.

The results tend to be lower than those obtained by Beeck and Mouzon,[3] roughly by about the same multiplying factor. It is suggested that their results may have been higher because of space-charge retarding of the positive ion beam. The principal evidence for this is that at the higher speeds such as are necessary for Cs^+ in A the difference disappears. The higher voltages would naturally tend to eliminate space-charge effects.

If energy and momentum are to be conserved in a collision, the maximum energy available for outside work such as ionization or excitation is easily calculated to be the initial energy of the positive ion beam multiplied by the factor $m_2/(m_1+m_2)$, where m_2 is the mass of the gas atom and m_1 is the mass of the colliding ion. The application of this factor to the values in the table above gives the results in Table II.

TABLE II. *Reduced voltages available for ionisation.*

	Na^+	K^+	Rb^+	Cs^+
Ne	60.8	29.3	44.7	—
A	66.8	41.9	43.0	78.5
N_2	48.3	33.0	64.2	—
CO_2	62.4	38.8		—

This reduction factor still does not bring the ionizing energies down to the true ionization potentials of the gases involved. There is no apparent correlation among the reduced voltages; the chief point of interest is that they are all fairly low (under 100 volts).

The writer wishes to express his gratitude to Professor L. B. Loeb for his suggestions and continual guidance throughout the work. The writer wishes also to thank Doctor C. H. Kunsman for his kindness in providing the catalysts used as alkali ion sources.

ROBERT N. VARNEY

Department of Physics,
University of California,
Berkeley, California,
July 14, 1934.

[1] K. H. Kingdon, Phys. Rev. **21**, 408 (1923).
[2] See, for example, R. M. Sutton and J. C. Mouzon, Phys. Rev. **35**, 695 (1930); T. J. Câmpan, Phys. Zeits. **30**, 858 (1929); O. Beeck, Ann. d. Physik [5] **6**, 1001 (1930); and others.
[3] O. Beeck, and J. C. Mouzon, Ann. d. Physik [5] **11**, 858 (1931).

On the Photographic Infrared Absorption Spectrum of Mono-Deutero Acetylene

In an investigation of the vibration rotation spectrum of the heavy acetylenes several items have arisen which seem of sufficient interest to report briefly at this time.

The "heavy" acetylene was prepared from water containing 95 percent D_2O. By using absorbing columns up to 20 feet in length at atmospheric pressure, one band was found in the region 6000–11,000A. This band, with origin at λ10,302, has the same simple structure as the known C_2H_2 bands, namely a single R and a single P branch. Although we cannot account for the presence of enough protium to form sufficient C_2HD, we ascribe the band to this molecule.

Considerable work has been done on infrared absorption in acetylene[1] and Randall and Barker[2] in a preliminary report of a study of the far infrared bands of the "heavy" acetylenes have given values of ν_4 and ν_5 (using Sutherland's notation) for these molecules. However, the vibrational transitions giving rise to the λ10,302 band cannot be determined since of the five fundamental vibration frequencies, all of which are active in C_2HD, only two are known at present.[3]

Twenty lines in the R branch and twenty-two lines in the P branch of the band were measured on each of two plates. Results of the measurements permit the evaluation of the moment of inertia of the C_2HD molecule in the initial and final states involved. From the term differences we obtain $B_0=1.0097$ and $B=0.9951$ giving $I_0=27.39\times10^{-40}$ g cm² and $I=27.80\times10^{-40}$ g cm² for the moments of inertia in the normal and excited states, respectively. Assuming the internuclear distances given by Hedfeld and Mecke[1] for C_2H_2 (namely, $r_{CH}=1.08\times10^{-8}$ cm and $r_{CC}=1.19\times10^{-8}$ cm) to hold for C_2D_2 and C_2HD, we calculate I_0 for the normal state of C_2D_2 to be 32.75×10^{-40} and for C_2HD to be 28.55×10^{-40}. This would indicate that the carrier of the band is mono-deutero acetylene. The r_{CH} given by Mecke was computed from the Raman data on CH_4 obtained by Dickinson, Dillon and Rasetti.[3]

The above given values for r_{CH} and r_{CC} in acetylene are based on the assumption that r_{CH} is the same for acetylene as for methane. It seems much more direct and reasonable to use only the present data on C_2HD in conjunction with the data on C_2H_2. Employing the moments of inertia of acetylene and mono-deutero acetylene in the normal states together with the postulate that the internuclear distances are the same for C_2H_2 and C_2HD, we calculate the distances as $r_{CC}=1.24\times10^{-8}$ and $r_{CH}=r_{CD}=0.94\times10^{-8}$ cm. The postulate of unchanged distances is a basic assumption in the theory of the isotope effect in band spectra and is therefore substantiated by the proven validity of this theory. The value r_{CH} here given is somewhat smaller than previous figures but the assumptions involved in its calculation are considered less liable to error than those previously used. From experiments on electron diffraction in acetylene, Wierl[4] obtains a value of r_{CC} 1.22±0.08A. This is seen to be in good agreement with the present as well as the former determinations.

It is of interest to add that in preparing the acetylene no difference[5] was observed under identical conditions in the reaction rates between H_2O and CaC_2 and between D_2O and CaC_2. Both appeared to be very rapid. The speed of the reaction would tend to prevent observation of a difference in reaction rates if it should be present.

The spectrum is being further studied and the results together with the complete data of the present work will be reported shortly.

C. A. Bradley*
Andrew McKellar*
George Eastman Laboratory of Physics,
Massachusetts Institute of Technology,
June 20, 1934.

[1] Levin and Meyer, J.O.S.A. and R.S.I. **16**, 137 (1928); Hedfeld and Mecke, Zeits. f. Physik **64**, 151 (1930); Childs and Mecke, ibid. **64**, 162 (1930); Mecke, ibid. **64**, 173 (1930); Hedfeld and Lueg, ibid. **77**, 446 (1932); Lochte-Holtgreven and Eastwood, Zeits. f. Physik **79**, 450 (1932); Mecke, Zeits. f. physik. Chemie **17**, 1 (1932); Sutherland, Phys. Rev. **43**, 883 (1933).
[2] Randall and Barker, Phys. Rev. **45**, 124 (1934).
[3] Dickinson, Dillon and Rasetti, Phys. Rev. **34**, 582 (1929).
[4] Wierl, Ann. d. Physik **13**, 453 (1932).
[5] Urey and Price, J. Chem. Phys. **2**, 300 (1934).
* National Research Fellow.

Anomalous Rotation of HgH Molecules

This is a preliminary report of some results which have been obtained in an extensive study of the mercury-sensitized fluorescence of HgH. (It was discovered by Gaviola and Wood[1] that HgH molecules can be excited with abnormally high rotation by this method.) Various gases are introduced into the fluorescence tube for the purpose of finding their effect on the intensity distribution within an individual band. In this way it is possible to gain information about conditions which govern intermolecular transfers of energy.

Quantitative measurements have shown that the rotational temperatures are considerably higher than the previous estimates of Beutler and Rabinowitsch[2]: when the fluorescence tube contains a few mm of N_2 and a trace of H_2 (along with the usual 1/1000 mm of Hg vapor) the rotational temperature of the 4017 band is about 10,000° (instead of 3000°).

Addition of 80 mm of He to the above mixture results in reduction of the rotational temperature to approximately the normal value. This effect is similar to that of He on the OH bands in the electric discharge,[3] and is to be similarly interpreted. According to classical mechanics, the rather small difference between the masses of the He atom and the H atom permits a rather large exchange of kinetic energy. In collisions which occur during the lifetime of the excited state, kinetic energy of rotation of the H atom of the HgH molecule is converted into translational energy of the He atom. Because of its considerably greater atomic weight, argon would be expected to be less effective than He in a process of this kind, and it is actually found that A is less efficient in quenching the excess rotation.

N_2 might be expected to resemble A rather than He in its effect on the rotation of HgH. However, its behavior is

[1] E. Gaviola and R. W. Wood, Phil. Mag. **6**, 1191 (1928).
[2] H. Beutler and E. Rabinowitsch, Zeits. f. physik. Chemie **8**, 420 (1930).
[3] O. Oldenberg, Phys. Rev. **46**, 210 (1934).

entirely different from either. When the pressure of N_2 is raised to 80 or 160 mm, the high rotation lines are strikingly enhanced.

There is no doubt about the temperature of the gas in the fluorescence tube—it is room temperature. The energy of the HgH molecules emitting the spectrum discussed above is most certainly derived from excited Hg atoms. The occurrence of high rotational temperatures contrasts strongly with the behavior of N_2^+ and CO^+ excited by collisions of the second kind. Duffendack, Revans and Roy[4] have found that under these conditions the rotational temperatures were probably close to the real temperature of the gas.

There is a significant difference in the conditions of excitation of N_2^+ and CO^+ on one hand, and HgH on the other. In the first case, the resonance condition is obeyed within a few tenths of a volt. In the case of HgH, bands appear with high intensity even though their excitation energy is more than a volt lower than that of the metastable Hg atom. In addition, the total pressures in the fluorescence experiments are higher, resulting in a greater probability of collisions during the lifetime of the excited molecules. Discussion of the elementary processes leading to the excess rotation observed will be postponed until a more thorough investigation has been completed.

F. F. RIEKE

Harvard University,
Cambridge, Massachusetts,
July 7, 1934.

[4] O. S. Duffendack, R. W. Revans and A. S. Roy, Phys. Rev. **45**, 812 (1934).

Spontaneous Disintegration of Proton or Neutron According to the Fermi Theory

According to the Fermi[1] theory of β-decay, a β-emission is described as a process in which a neutron in the nucleus is transformed into a proton and an electron and a neutrino are emitted.

$$N \rightarrow P + e^- + n. \tag{1}$$

The mathematical description of the process is quite analogous to the description in the radiation theory of the transition between two states of an atom together with the emission of a light quantum. For the coupling between the heavy particle and the electron-neutrino field, Fermi takes the simplest form which assures that with every transition of the heavy particle from neutron state to proton state there will appear in the electron-neutrino field one electron and one neutrino. In the theory there enters the arbitrary constant g, of dimensions erg cm^3, which describes the strength of the coupling. To explain the slowness of β-decay, Fermi has to take for g the very small value $4 \cdot 10^{-50}$ erg cm^3. The theory accounts for the general shape of the continuous β-ray spectrum and for the relation already found empirically by Sargent[2] between the lifetime and the upper limit of the continuous β-ray spectrum.

Anderson and Neddermeyer[3] have shown that Sargent's law holds also for the artificial radioactive elements which emit positrons. This seems to justify the application of the Fermi theory with the same constant g to the transition

$$P \rightarrow N + e^+ + n. \tag{2}$$

(We should perhaps speak here of an anti-neutrino.)

It may be of interest to remark that since there are two light particles emitted, the presence of a nucleus is not required for conservation of momentum. If the mass difference of proton and neutron is larger than the sum of the masses of electron and neutrino, then the Fermi theory predicts the spontaneous occurrence for the free particle of either the transition (1) or the transition (2), depending on the sign of the mass difference.

For the rate of transition one finds

$$(G^2/4\pi^3)(mc^3/h)[(1+\eta_0^2)^{\frac{1}{2}} \operatorname{arc\,sinh} \eta_0 - \eta_0 - \eta_0^3/3 + 2\eta_0^5/15]. \tag{3}$$

Here G is the dimensionless constant $g(2\pi mc/h)^3(mc^2)^{-1} = 9 \times 10^{-13}$ and η_0 is $(\Delta^2-1)^{\frac{1}{2}}$, where $m\Delta$ is the mass difference of proton and neutron. Following Fermi we have taken the neutrino mass to be zero. We have supposed that Δ is small compared to M/m so that we are justified in neglecting the kinetic energy taken up by the heavy particle.

One can convince himself that if the kinetic energy of the heavy particle is negligible, the calculation given by Fermi becomes applicable in the present case when we put $Z=0$ and

$$|\int u^* U d\tau|^2 = 1. \tag{4}$$

In fact, one may obtain (3) by putting (4) into Fermi's expression and integrating between the limits $\eta=0$ and $\eta=\eta_0$.

For small values of $\Delta-1$, (3) gives for the lifetime

$$\tau = 5 \times 10^5 (\Delta-1)^{-\frac{5}{2}}.$$

It is clear that the transitions can occur only if $\Delta > 1$. Thus both proton and neutron will be stable if the neutron mass lies in the range $1.0067 - 1.0077$.

For $\Delta = 1.1$ one finds $\tau \sim 50$ years, and for $\Delta = 1.4$, $\tau \sim 0.4$ year. This means that according to this theory one should expect hydrogen to be observably radioactive if the neutron mass were lower than Chadwick's value 1.0067 by even so small an amount as 0.00005. Of course if one assigns a mass to the neutrino, the lower limit of the neutron mass is pushed down by just that much.

As to the upper limit for the mass of the neutron, one cannot be so definite, since the free neutron may really be unstable. If we take the Curie-Joliot mass, 1.010, for the neutron, then the lifetime of the neutron according to (3) is 10^3 sec. This seems improbably small, but there is no experimental evidence to the contrary.

HUGH C. WOLFE
G. E. UHLENBECK

Department of Physics,
University of Michigan,
July 11, 1934.

[1] Fermi, Zeits. f. Physik **88**, 161 (1934).
[2] Sargent, Proc. Roy. Soc. **A139**, 659 (1933).
[3] Anderson and Neddermeyer, Phys. Rev. **45**, 653 (1934).

Energy of Removal of Neutrons and Alpha-Particles from Nuclei and Alpha-Instability Below the Radio-Elements

Gamow,[1] arguing from the existence of a minimum at about atomic number 50 in his plot of nuclear energy (negative mass defect in formation from alpha-particles, protons and electrons) against number of constituent alpha-particles, discusses the possibility that elements above this point in the periodic system are unstable with respect to alpha-emission. This possibility results as a more definite conclusion from quite different considerations,[2] based upon the approximate theory of Heisenberg, involving more varied and more numerous data. Since the preparation of the paper embodying these ideas, interesting articles by Gapon[3] and Landé[4] which bear upon the point in question have been brought to my attention. The following comments are intended to assist in bringing the various lines of approach into relation, and to emphasize that all indicate the alpha-instability in about the same region of relatively low atomic number.

Gapon and Landé treat the nucleus as composed of alpha-particles, neutrons, and zero or one proton. Gapon deals with quantities which may best be described as mean "apparent" mass defects of the particles within the nucleus. He concludes that for the neutron this quantity is constant in any series of isotopes of a single element, and that it has nearly the same value in the various elements for which data are available. The first of these conclusions can be roughly substantiated, as far as the form of the relation is concerned, by the methods of the previous paper.[2] Thus, the condition for constancy of the binding energy of the neutron to a nucleus (which is approximately equivalent to Gapon's quantity) can be shown to be $Z^2/M^{4/3}=\text{const.}$, where Z is the atomic number and M the mass number. This condition is roughly fulfilled within any series of isotopes. The variation in number of neutrons within such a series is, however, small compared to the total number, and a considerable variation in binding energy is still possible if the entire number is taken into account. The second of Gapon's conclusions is pretty definitely contradicted by the general considerations and numerical results of the former paper. Heisenberg's assumption of a dependence of binding energy on the neutron-proton ratio seems to be well supported as far as the general trend throughout the system of elements is concerned. The numerical results which suggested this conclusion to Gapon are of insufficient accuracy to support it as a close approximation. This affects to some extent the validity of some of Landé's extrapolations.

In his curve of (negative) mass defect of the alpha-particle against number of particles, Gapon finds a minimum in the general region of Gamow's. Insofar as such "apparent" quantities have significance, it is again that the emission of single particles from elements to the right of the minimum is energetically favored, in agreement with the deductions first mentioned. Gapon considers the point at which his mean defects reach zero as the region of "instability" of elements. This type of instability, however, would concern only the explosion of his "alpha-aggregate" into its separate particles. There is no conclusive evidence favoring the idea that such an explosion is energetically possible in any of the known elements.

Landé points out that if the "constituents" of the nucleus be taken as previously stated that the mass defect curve shows no maximum within the range of low atomic number. (The same is true, incidentally, if the constituents be taken as neutrons and protons, or protons and electrons.) Such a maximum may be approached at the largest values of Z, though the error of the measurements is too large to permit this conclusion. This is again not relevant to the question as to alpha-instability. The quantity necessary here is, of course, $(\Delta E/\Delta n_\alpha)_{n_1, n_2 \cdots}$, where E is the energy of formation of a nucleus synthesizable from n_α alpha-particles and n_1, n_2, $\cdots$, particles of any other arbitrarily selected kinds. Gamow discusses schematically curves of a type which exhibit this quantity. Landé in his second article gives a plot of actual data, in part extrapolated (compare above), of the requisite type, and here recognizes instability in the region of atomic number 50, in agreement with the conclusion referred to above.

Because of the importance of this question of stability it is desirable to show exactly what pertinent direct data exist, uninfluenced by extrapolations, and with the attendant error clearly indicated. This is difficult in a small scale plot. The table of reactions (Table I), however, presents them in simple form. This comprises all the data pertaining to reactions involving the removal of alpha-particles alone, in the region of atomic number between 40 and 60. If the value of $(\Delta E/\Delta n_\alpha)$ is negative the reaction indicated is energetically possible. For those reactions involving more than one alpha-particle only mean values may be inferred. In the last column is given the probable error in $(\Delta E/\Delta n_\alpha)$. In the reactions Xe→Sn and Te→Sn the mass defect is favorable to the emission of alpha-particles and of the same order as the error. In all other cases the probable error is at least twice as great as the indicated effect. No more positive statement than that $(\Delta E/\Delta n_\alpha)$ is zero within the error is therefore possible from the table or from the treatments in references 1, 3 and 4. In this respect it is thought that the calculations cited above[2] represent a

TABLE I. *Energy changes in emission of alpha-particles.*

Parent nucleus	Products	Energy change per alpha-particle (g per g at. $O^{16}=16$)	Probable error
$_{54}Xe^{126}$	$_{42}Mo^{100}+6\alpha$	0.0042	0.009
$_{54}Xe^{128}$	$_{50}Sn^{116}+2\alpha$	− .0073	.009
$_{54}Xe^{128}$	$_{50}Sn^{116}+2\alpha$	− .0073	.009
$_{54}Xe^{128}$	$_{50}Sn^{120}+2\alpha$	− .0083	.009
$_{54}Xe^{130}$	$_{50}Sn^{122}+2\alpha$	− .0078	.009
$_{54}Xe^{130}$	$_{52}Te^{126}+\alpha$	.0081	.029
$_{54}Xe^{132}$	$_{50}Sn^{124}+2\alpha$	− .0083	.009
$_{54}Xe^{132}$	$_{52}Te^{128}+\alpha$	.0102	.029
$_{50}Sn^{114}$	$_{42}Mo^{94}+4\alpha$	.0094	.013
$_{50}Sn^{116}$	$_{42}Mo^{100}+4\alpha$	.0099	.013
$_{52}Te^{126}$	$_{50}Sn^{122}+\alpha$	− .0238	.029
$_{52}Te^{128}$	$_{50}Sn^{124}+\alpha$	− .0269	.029
$_{56}Ba^{138}$	$_{54}Xe^{134}+\alpha$	.0152	.030

[1] Gamow, Der Bau der Atomkerns u. die Radioaktivität, Leipzig, 1932, pp. 15–24.
[2] Eastman, Phys. Rev. **46**, 1 (1934).
[3] Gapon, Zeits. f. Physik **79**, 676 (1932).
[4] Landé, Phys. Rev. **43**, 620, 624 (1933).

considerable improvement over the data on masses, and constitute the best present evidence that nuclei in this region are actually unstable. Exceptions, in the nature of fluctuations from the general trend, are of course to be anticipated.

The adoption of this view raises the question of the probability of the alpha-emission. Except in cases of extremely small energy changes, this must be very low to account for the failure of direct detection in these elements. This may, of course, be due sometimes to the necessity for multiple emission. Landé, however, suggests that the mechanism of ejection may require that the residual nucleus be left with a considerable excitation. Emission would then be probable only when the total energy of the change exceeds the necessary residual excitation. As pointed out independently in another connection in the former[2] paper there is some indication that the residual nucleus in many of the known alpha-changes is excited, even in cases where no gamma-rays are found. This perhaps offers support to Landé's suggestion.

E. D EASTMAN

Department of Chemistry,
University of California,
Berkeley, California,
June 13, 1934.

Energy States of Doubly Excited Helium

In a letter in the July 1st issue of the *Physical Review*, Fender and Vinti gave the result of their calculation of the lower states of doubly excited helium. They compared their result with the assignments of the two lines in the extreme ultraviolet by Kruger and of the corona lines by Rosenthal.[1] Dr. Goudsmit and the writer, in an attempt to examine the possible relation of the spectrum of doubly excited helium and the corona spectra, have also undertaken similar calculations of the approximate positions of the levels of doubly excited helium. A modified form of the variational method[2] was employed; hydrogenic wave functions were used and two "screening constants," one for each electron, introduced as variational parameters with respect to which the energy integral is to be minimized. As the finding of the exact minimum in some cases requires a considerable amount of numerical computations, we are content at present with approximate values of the minima. The preliminary result of such calculations is given in Table I. The energies in column (1) are in units of R, measured from the state of the naked nucleus, those in column (2) are in wave numbers above the first ionization limit of helium. For comparison, the values obtained by Fender and Vinti are given in column (3).

The relative positions of these levels show some unexpected features. The level $2s2p\ ^3P$ is lower than $2s^2\ ^1S$, whereas a superficial comparison with the normal helium spectrum might falsely suggest the opposite is the case. That this can be so is easily understood without any detailed calculations. The electrostatic repulsion between two electrons both in the $2s$ state will be greater than for the $2s2p$ configuration and as the energy of a single $2s$ or $2p$ electron in He^+ is practically the same, the $2s^2\ ^1S$ will be higher than $2s2p$. The exchange energy complicates these considerations somewhat and the calculations show that the $2s2p\ ^1P$ state is considerably higher than the ^3P of this configuration, and that the $2s^2\ ^1S$ lies between these two multiplets. Another result is that the levels of the $2p^2$ configuration have low positions.

TABLE I.

State	Energy (1)	Energy (2)	Energy (3)
$2s4d\ ^1D$	$-1.062\ R$	322,000 cm^{-1}	
$2s4s\ ^1S$	-1.090	319,200	
$2s4s\ ^3S$	-1.102	318,000	
$2s3d\ ^1D$	-1.110	317,000	
$\ \ ^3D$	-1.112	316,800	
$2s3p\ ^1P$	-1.126	315,000	
$\ \ ^3P$	-1.146	313,000	
$2s3s\ ^1S$	-1.175	310,000	
$2s3s\ ^3S$	-1.222	304,600	
$2s2p\ ^1P$	-1.308	295,000	296,118
$\ \ 2p^2\ ^1D$	-1.320	294,000	
$\ \ 2s^2\ ^1S$	-1.445	280,000	275,000
$2s2p\ ^3P$	-1.504	274,000	274,526
$\ \ 2p^2\ ^3P$	-1.662	256,000	

The spectrum of doubly excited helium calculated from the states in Table I is given in Table II.

TABLE II.

Possible transition	Wave number
$2s^2\ ^1S-2s3s\ ^1P$	35,000 cm^{-1}
$2s2p\ ^1P-2s4d\ ^1D$	27,000
$2s2p\ ^3P-2s3s\ ^3S$	30,000
$2s2p\ ^1P-2s4s\ ^1S$	24,000
$2p^2\ ^1D-2s3p\ ^1P$	21,000
$2s2p\ ^1P-2s3d\ ^1D$	22,000
$2p^2\ ^3P-2s2p\ ^3P$	18,000
$2s^2\ ^1S-2s2p\ ^1P$	15,000
$2s2p\ ^1P-2s3s\ ^1S$	15,000

These energy levels and wave numbers of possible transition are, on account of the nature of the calculation, only rough approximations. A partial support, however, is given by the two lines observed by Kruger and Paschen in the far ultraviolet spectrum of He (λ320.4 and λ357.5). Using the energy levels calculated above, we find,[3]

$1s2s\ ^3S-2s2p\ ^3P$	314,000 cm^{-1}	observed lines
$1s2p\ ^1P-\ \ 2s^2\ ^1S$	311,000 "	312,117 cm^{-1}
$1s2p\ ^3P-\ \ 2p^2\ ^3P$	289,000 "	279,715 "

In a separate paper[4] the possible relation of the spectrum of doubly excited He with the solar coroner spectrum is discussed.

TA-YOU WU

Department of Physics,
University of Michigan,
July 16, 1934.

[1] Rosenthal, Zeits. f. Astrophysik 1, 115 (1930).
[2] C. Eckart, Phys. Rev. 36, 878 (1930).
[3] This agreement, however, should not be stressed upon too much, for the energy involved in these transitions is in the main part the excitation of an electron from $1s$ to $2s$ or $2p$ state. Furthermore, the numerical error in the calculation of states can easily be 0.005 R corresponding to about 500 cm^{-1}, not to say the inaccuracy inherent in such *methods* of calculation.
[4] Goudsmit and Ta-You Wu, to appear presently in the Astrophys. J.

Concerning the Carbon Dioxide Content of the Atmosphere of the Planet Venus

Recent work at the Mount Wilson Observatory on the infrared spectrum of Venus[1] disclosed three absorption bands with centers at 11,496.5 cm^{-1}, 12,672.4 cm^{-1}, and 12,774.7 cm^{-1}. From the major interval between neighboring fine-structure lines the moment of inertia of the absorbing molecule was computed to be 70.5×10^{-40} gram cm^2, and the atmospheric constituent responsible for the spectrum was therefore assumed to be carbon dioxide. This claim was fully substantiated by subsequent theoretical work[2] in which it was shown that the carbon dioxide molecule does indeed possess three rotation-vibration bands precisely coincident with the planetary ones both in position and detailed structure. In the latter investigation, the bands were identified in terms of the fundamental frequencies of the molecule as

$$5\nu_3 = 11{,}496.5 + 0.769N - 0.0153N^2$$

$$5\nu_3 + \left\{\begin{matrix}\nu_1\\ 2\nu_2\end{matrix}\right\} = \left\{\begin{matrix}12{,}672.5 + 0.769N - 0.0153N^2\\ 12{,}774.7 + 0.769N - 0.0156N^2,\end{matrix}\right.$$

where the two combination bands form a group because of the resonance degeneracy $[\nu_1 \cong 2\nu_2]$ inherent in the molecule.[3]

It is evidently of considerable importance to ascertain the quantity of carbon dioxide present in the absorbing layers of the Venus atmosphere. The most satisfactory method by which to achieve this end is to determine the quantity of the gas required for the detection of the bands $5\nu_3$ and $5\nu_3+\binom{\nu_1}{2\nu_2}$ in the laboratory. Adams and Dunham were unable to detect these bands in the solar spectrum shortly before sunset, at which time it is estimated there exists in the earth's atmosphere a CO_2 path length of at least thirty meter-atmospheres. Nor were the bands found to be present in a spectrum taken with forty meters of CO_2 gas at three atmospheres pressure.[1]

We have recently succeeded in photographing the band $5\nu_3$ by using an absorption cell forty-five meters in length charged with forty-seven atmospheres of gas. The spectra were taken with a glass prism Hilger E–I; and although they show a well-defined envelope structure for $5\nu_3$ at 11,496 cm^{-1}, they evince no trace of the bands $5\nu_3+\binom{\nu_1}{2\nu_2}$. This is entirely in accord with the experiments[4] on ν_3 and $\nu_3+\binom{\nu_1}{2\nu_2}$ which show that the path length necessary for the detection of $(2n+1)\nu_3$ is of a lower order of magnitude than that required for the observation of $(2n+1)\nu_3+\binom{\nu_1}{2\nu_2}$.

The lower limit of an estimate on the CO_2 content of the absorbing strata of Venus is apparently two mile—atmospheres whereas the amount actually present in these layers is very probably several times greater. Accordingly there is more than 10^{15} tons of CO_2 present in the upper strata; and this is, presumably, just a very small fraction of the total CO_2 content of the entire atmosphere.

In the upper strata alone, Venus possesses 10^4 times as much CO_2 as is present in the entire atmosphere of the earth.

ARTHUR ADEL
V. M. SLIPHER

University of Michigan
and Lowell Observatory,
July 23, 1934.

[1] Adams and Dunham, Pub. A.S.P. **44**, 243 (1932).
[2] Adel and Dennison, Phys. Rev. **43**, 716; **44**, 99 (1933).
[3] Due to the fact that the oxygen nucleus has zero spin, half the fine-structure lines of CO_2 are missing in these bands. The above formulae represent the observed positions of the lines when N takes on the values 1, 3, 5, ... R-branch; and -2, -4, -6, ... P-branch.
[4] Martin and Barker, Phys. Rev. **41**, 291 (1932).

On the Identification of the Methane Bands in the Solar Spectra of the Major Planets

Recent analysis of the absorption spectra of the major planets (Jupiter, Saturn, Uranus and Neptune) has shown that they consist almost wholly of rotation-vibration bands of methane. The classification of thirty-four of these planetary CH_4 bands in terms of the four fundamental frequencies of vibration of the molecule (inactive: $\nu_1=2915$ cm^{-1}, $\nu_2=1520$ cm^{-1}) (active: $\nu_3=3014$ cm^{-1}, $\nu_4=1304$ cm^{-1}) is tabulated in Table I.

TABLE I.

Location ($\mu\mu$)	Identification	Planets in whose spectra the bands have thus far been located			
		J	*S*	*U*	*N*
886	$4\,\nu_3$	*			
725	$5\,\nu_3$	*	*		
619	$6\,\nu_3$	*	*	*	*
543	$7\,\nu_3$	*	*	*	*
486	$8\,\nu_3$			*	*
441	$9\,\nu_3$				*
980	$8\,\nu_4$	*			
874	$9\,\nu_4$	*			
788	$10\,\nu_4$	*			
720	$11\,\nu_4$	*	*		
662	$12\,\nu_4$			*	*
614	$13\,\nu_4$			*	*
566	$14\,\nu_4$			*	*
534	$15\,\nu_4$				*
502	$16\,\nu_4$				*
861	$3\,\nu_3+\nu_1$	*			
702	$4\,\nu_3+\nu_1$	*	*	*	*
595	$5\,\nu_3+\nu_1$		*	*	*
521	$6\,\nu_3+\nu_1$				*
987	$3\,\nu_3+\nu_2$	*			
782	$4\,\nu_3+\nu_2$	*	*		
656	$5\,\nu_3+\nu_2$			*	*
568	$6\,\nu_3+\nu_2$			*	*
504	$7\,\nu_3+\nu_2$				*
1009	$3\,\nu_3+\nu_4$	*			
798	$4\,\nu_3+\nu_4$	*			
668	$5\,\nu_3+\nu_4$	*	*	*	*
576	$6\,\nu_3+\nu_4$	*	*	*	*
509	$7\,\nu_3+\nu_4$			*	*
(459–560)	$8\,\nu_3+\nu_4$				*
643	$10\,\nu_4+\nu_2$			*	*
597	$11\,\nu_4+\nu_2$			*	*
557	$12\,\nu_4+\nu_2$			*	*
523	$13\,\nu_4+\nu_2$				*

The spectra of ethane, ethylene and acetylene have been carefully examined. There appears to be no detectable amount of these low boiling point hydrocarbons in the upper strata of the giant planets.

Complete details of the investigation will appear in the future.

ARTHUR ADEL
V. M. SLIPHER

University of Michigan
and Lowell Observatory,
July 23, 1934.

The Chemistry of Element 93 and Fermi's Discovery

E. Fermi's[1] interesting experiments on the bombardment of uranium by neutrons have led him to conclude that elements with an atomic number above 92 are formed. He specifically assumes that his product, with a period of 13 minutes, which is precipitated from a highly oxidizing and acid solution together with manganese, is the highest homologue of the latter or element 93.

However, we would predict according to Mendelejeff's periodic law, other properties[2] for element 93 or eka-rhenium (En); its highest oxide En_2O_7 will surely be stable under the conditions of Fermi's experiment and form the acid soluble pereka-rhenic acid $HEnO_4$ (or its derivatives) similarly to Re_2O_7 and $HReO_4$. Element 94, if it is an eka-osmium (Eo), will also give the acid soluble and volatile EoO_4.

These considerations have led us to repeat some of Fermi's experiments using protactinium as an indicator. We found that element 91 gives identical reactions as Fermi's 93. Element 91 is practically quantitatively precipitated by manganese from a highly acid uranyl nitrate solution on adding sodium chlorate, exactly like Fermi's 93.[2] On making the same experiment with rhenium we found that it all remained in solution, and as stated above we have to expect the same analytical behavior for eka-rhenium. We expect that Fermi's 13-minute product will show also other reactions of element 91, of which the most characteristic[3] is the precipitation, together with zirconium, by phosphoric acid from a strongly acid (20–30 percent HCl or HNO_3) solution.[3]

Fermi's statement that the 13-minute product is not identical with element 91 is based on experiments with its isotope brevium (UX_2) which unfortunately, because of its very short life ($T = 68$ sec.), introduces some difficulties into the chemical operations.

We are forced to conclude (unless evidence to the contrary is provided) that the product of uranium with a half period of 13 minutes is a new isotope of element 91; it can be called, according to the nomenclature recently introduced by Curie and Joliot,[4] radio-brevium (Rm), provided it meets the approval of its discoverer.

The production of 91 out of 92 is in agreement with the other results of Fermi,[1] since he showed, that in most cases of neutron bombardment, the Z of an element is changed into $Z-1$ (or $Z-2$, see reaction (2) and he has never observed an increase in atomic number.

The nuclear reaction, leading to the formation of Rm is either:

$$U_{92}^{238} + n_0^1 \rightarrow Rm_{91}^{238} + H_1^1 \quad \text{and} \quad Rm_{91}^{238} \xrightarrow{\beta} U_{92}^{238} \qquad (1)$$

or

$$U_{92}^{238} + n_0^1 \rightarrow Th_{90}^{235} + He_2^4$$

and

$$Th_{90}^{235} \xrightarrow{\beta} Rm_{91}^{235} \xrightarrow{\beta} U_{92}^{235} \text{ (actinouranium?)}. \qquad (2)$$

If Eq. (2) is correct it might be possible to separate Th_{90}^{235} with ordinary thorium.

In conclusion, we would like to emphasize that we have no doubt in future successful synthesis of artificial and radioactive new elements by nuclear bombardment; in fact, one of us definitely expressed this opinion even before the discovery of artificial radioactivity.[5]

A. v. GROSSE
M. AGRUSS

Kent Chemical Laboratory,
University of Chicago,
July 7, 1934.

[1] E. Fermi, Nature **133**, 898 (1934).
[2] Details will be published in chemical journals.
[3] A. v. Grosse, Berichte Deutsch. Chem. Ges. **61**, 237 (1928).
[4] I. Curie and F. Joliot, Comptes Rendus **198**, 559 (1934).
[5] A. v. Grosse, Chem. Bulletin of the Chicago Section of Am. Chem. Soc. **20**, 15 (1933).